ELECTROCHEMICAL PREPARATION AND APPLICATION OF THE FERRATE (VI) ION FOR WASTEWATER TREATMENT.

by

Adrian James Denvir

A thesis submitted for the degree of

DOCTOR OF PHILOSOPHY

November 1995

Department of Chemistry

University of Southampton

UNIVERSITY OF SOUTHAMPTON

ABSTRACT

FACULTY OF SCIENCE

CHEMISTRY

Doctor of Philosophy

ELECTROCHEMICAL PREPARATION AND APPLICATION OF THE FERRATE (VI) ION FOR WASTEWATER TREATMENT

by Adrian James Denvir

The electrochemical preparation of ferrate by the anodic dissolution of iron and its alloys in concentrated sodium hydroxide has been reinvestigated. It has been shown that the current efficiency for ferrate formation can be improved significantly by (a) the use of a three dimensional iron anode and (b) the choice of an iron alloy with a high carbon content. Ferrate (VI) was produced by anodic dissolution of an iron wool anode in 10 M NaOH in a membrane flow cell. It was shown that using a current density of 18 mA cm^{-2}, the current efficiency could be as high as 60 % but it usually dropped to ≈ 25 % during an extended electrolysis. The reason for this change in current efficiency was investigated using voltammetric techniques and it is proposed that the ratio of oxygen evolution/ferrate production is sensitive to the composition, structure or thickness of the iron oxide/hydroxide layer on the anode surface. Periodic current reversal overcomes this loss in current efficiency to some extent. The influence of sodium hydroxide concentration and temperature on the electrolyses were also investigated. Voltammetric methods have also been used to define the influence of the composition of the anode on the transpassive dissolution of the iron and its alloys. It was concluded that the carbon content of the steel was critical and this was also demonstrated by preparative electrolyses at flat plate anodes.

Ferrate may have applications as a water treatment chemical and experiments were carried out to define the ways in which it could be employed. Hence, the kinetics of the reaction of ferrate (VI) with water, aliphatic alcohols and phenol have been investigated. It has been shown that the ferrate (VI) ion exhibits good stability at 298 K in aqueous 10 M NaOH solution, having a half life of approximately one month. The stability of the ion was found to be strongly dependent on temperature with the decomposition occurring 1000 times faster when the temperature was raised to 333 K. The NaOH concentration also determines the life time of the ion in solution; in 1 M NaOH, the half life of the ion was only 7 minutes and the mechanism of decomposition had changed. Ferrate can, however, be added as a solid to polluted water whereupon it will react selectively with the organics. The kinetics of the reactions of ferrate (VI) were also studied in 10 M NaOH; commonly, the reactions are very fast compared to that with water. Moreover, with it was shown that some organics (methanol, ethanediol and phenol) undergo complete oxidation to CO_2 and H_2O. Other organics appear to undergo only partial oxidation although these results may be distorted by adsorption of the organics on the $Fe(OH)_3$ precipitate formed during the reaction.

To my wife.

List of symbols.

Symbol	Definition.	Typical units.
A	Electrode area	cm^2
A_E	Electroactive area per unit electrode volume	cm^{-1}
c^∞	Concentration of electroactive species in the bulk solution	mol dm^{-3}
c	Concentration	mol dm^{-3}
D	Diffusion coefficient	cm^2 s^{-1}
E_e	Equilibrium electrode potential	V
$E_{1/2}$	Half wave potential	V
E_e^C	Equilibrium cathode potential	V
E_e^A	Equilibrium anode potential	V
E_e^o	Standard electrode potential	V
E_{cell}	Cell potential	V
E_A	Anode potential	V
E_C	Cathode potential	V
F	Faraday constant	A s mol^{-1}
ΔG	Gibbs free energy change	J mol^{-1}
i	Current	mA
i_L	Limiting current	mA
j_P	Peak current density	mA cm^{-2}
j_L	Limiting current density	mA cm^{-2}
k	Rate constant for a first order chemical process	s^{-1}
k_m	Mass transport coefficient	cm s^{-1}
m	Number of moles of electroactive species	mol
M	Molar mass	g mol^{-1}
n	Number of electrons	Dimensionless
q	Total electrical charge	A s
R	Electrical resistance	Ω
R_{CELL}	Cell resistance	Ω

$R_{CIRCUIT}$	Resistance of electrical circuit	Ω
t	Time	s
T	Temperature	K
V	Volume	cm^3
V_E	Electrode volume	cm^3
x	Distance, thickness or penetration	cm

Greek

η	Overpotential	V
η_C	Overpotential at cathode	V
η_A	Overpotential at anode	V
η	Viscosity	$g\ cm^{-1}\ s^{-1}$
η_0	Absolute viscosity	Dimensionless
ν	Kinematic viscosity	$cm^2\ s^{-1}$
ϕ	Current efficiency	Dimensionless
ϕ_M	Absolute potential at electrode surface	V
ϕ_S	Absolute potential of bulk solution phase	V
ω	Angular rotation rate of disc	s^{-1}

Contents.

Chapter 1. Introduction.

1.1 Treatment of industrial wastewater effluent. 1

1.2 Chemical disinfectants used in wastewater treatment. 2

1.2a Chlorine. 2

1.2b Chlorine dioxide. 5

1.2c Ozone. 6

1.3 Treatment of industrial effluent. 8

1.3a Biological effluent treatment. 8

1.3b Supercritical water. 9

1.3c Electrochemical technology for effluent treatment. 9

(I) Direct oxidation. 10

(II) Indirect oxidation. 14

1.4 Cell design for environmental electrochemistry. 20

1.4a General considerations. 20

1.5 Three dimensional electrodes. 24

1.6 Ferrate (VI) ion. 28

1.6a Chemical data on ferrate (VI). 28

1.6b The chemistry of ferrate (VI). 29

1.6c Ferrate (VI) and its potential for wastewater treatment. 30

(I) Inactivation of water borne viruses. 30

(II) Oxidation of organic compounds. 32

1.6d Electrochemical generation of ferrate (VI). 33

(I) Metal dissolution. 33

(II) Electrochemical synthesis of ferrate (VI). 34

Chapter 2. Experimental.

2.1 Chemicals and materials. 38

2.2 Electrode preparations. 39

(I) Stationary disc electrodes. 39

(II) Flat plate electrodes. 40

(II) Three dimensional electrodes. 40

2.3 Analytical and electrochemical equipment. 40

2.4 Cells. 41

(I) Cyclic voltammetry cell. 41

(II) Rotating disc cell. 42

(III) Microelectrode cell. 43

(IV) H cell. 44

(V) Pipe cell. 45

(VI) Flow cell. 46

2.5 Analysis of ferrate (VI) solutions. 49

Chapter 3. Preliminary investigation into the feasibility of using ferrate (VI) ion in wastewater treatment.

3.1 Introduction. 50

3.2 Determination of ferrate (VI) concentration. 50

3.3 Stability of ferrate (VI) in sodium hydroxide solutions. 53

3.3a Effect of temperature. 53

(I) Decomposition at room temperature. 53

(II) Decomposition at elevated temperatures. 56

3.3b Decreasing the NaOH concentration. 59

3.4 Reactions with organics. 62
3.4a Reactions of ferrate (VI) with concentrated organic solution. 62
(I) Reaction with ethanol. 62
(II) Reactions with other alcohols. 64
3.4b Reaction of ferrate (VI) with dilute organic solutions. 65
(I) Aliphatic alcohols. 65
(II) Reactions with phenol. 69
3.5 Electrochemistry of ferrate (VI) solutions.
(I) Electrochemistry of ferrate (VI) on a platinum disc. 73
(II) Electrochemistry of ferrate (VI) on a platinum microelectrode. 74
(III) Reduction of ferrate (VI) on a rotating glassy carbon disc. 76
(IV) Electrochemistry of ferrate (VI) on iron. 78
(V) Electrosynthesis of ferrate (VI). 80
3.6 Summary of conclusions. 81

Chapter 4 The electrochemical generation of ferrate (VI) on iron wool anodes.

4.1 Introduction. 83
4.2 Electrosynthesis of ferrate (VI) in a flow cell at room temperature. 83
(I) Effect of applied current. 83
(II) Effect of changing the applied current. 85
(III) Ferrate (VI) formation at 0.2 A. 88
4.3 Effect of temperature on current efficiency. 92
(I) Electrolysis at 333 K. 92
(II) Effect of changing the temperature. 94
4.4 Methods of oxide removal. 95
(I) Acid washing. 95
(II) Addition of chloride ions. 97

(III) Current reversal. 99
4.5 Ferrate (VI) synthesis in low alkali electrolyte. 102
4.6 Summary of conclusions. 104

Chapter 5 Effect of anode composition on ferrate (VI) synthesis.

5.1 Introduction. 106
5.2 Voltammetry of different steels. 106
5.3 Effect of alloy composition on ferrate (VI) formation. 108
5.4 Electrosynthesis of ferrate (VI) on flat plate anodes. 111
(I) Alloy E. 111
(II) Other alloys. 114
5.5 Effect of conditioning time on ferrate (VI) formation. 117
(I) Alloy E. 117
(II) Other alloys. 120
5.6 Effect of temperature on ferrate (VI) formation on iron alloy anodes. 121
5.7 Summary of conclusions. 127

Chapter 6. Conclusions. 129

References. 132

Acknowledgements

First I would like to thank my supervisor Prof. Derek Pletcher for all his help and encouragement throughout my three and a bit years in Southampton. Also I am grateful to Dr. A. M. Couper at ICI Chemicals and Polymers for the financial support throughout the project.

To me oul ma, da and brother Colly, for all the words of encouragement which helped me get along when I was far away from my native home and needing a wee bit of Northern Ireland crack.

A big thanks goes out to all my friends in the Department, you know who you are. However, there a few who deserve a mention. Emma for helping me out with my proof reading and Neil for being there right from the start ready to lend a hand. I would like to acknowledge all my other colleagues, both past and present, for all their support.

I am very grateful to Ian and, even though it goes against everything I have said for the last two years I must give a mention to Thierry, for letting me stay in the house for two months.

Finally I want to say thanks to my dear wife who had to put up with me in my bad moods for the past five years.

Adrian Denvir

Chapter 1

Introduction.

1.1 Treatment of industrial wastewater effluent.

Over the last decade there has been an ever increasing public demand for greater protection of the environment. This has prompted the government to bring into effect strict legislation governing the discharge of waste into the environment. High fines and bad publicity have placed the chemical and other related industries in the position where they face the dilemma of trying to maintain a growth in productivity while adhering to the strict government guidelines. Being continually responsible for their waste, most of which is placed back into the environment, (waste water into the sea, rivers or lakes and solids in landfill sites), has caused many industries to search for better and more cost effective methods of waste disposal. Indeed a long term aim must be to recycle all water and chemicals back into the process streams, but this also requires treatment of such streams to prevent the build-up of impurities.

Wastewater generally undergoes several physical processes (see figure 1.1) before it can be discharged. The first step is to allow large particles to settle out in tanks before the microstraining process can commence. Microstraining uses filters made of stainless steel with pore size of between 60 and 70 μm and as the larger particles are collected so the pore size is reduced to around 10μm allowing the removal of the smaller matter such as bacterial cells.[1]

The next step is the flash mixing process where a coagulant is added to the effluent. The most common coagulant used in this process is still alum although, as aluminium is toxic to fish life, there has been some trend towards using less toxic ferric salts instead.[2] During the flash mixing process lime is added to alter the pH to between 10.5 and 11.5 This will precipitate out metal ions especially calcium and magnesium as the insoluble hydroxide species. The removal of calcium and magnesium is important if

the water is to be recycled back into the plant as the mineral deposits coat the surface of hot water systems, blocking pipes and reducing heating efficiency.

After the flash mixing, the water is transferred to a clarifier where flocculation takes place. The flocculation process causes the coagulation agent to coalesce absorbing dissolved organic species on its surface.[2, 3, 4 5] Alum has been shown to be 20% more efficient at removing organics than the ferric oxy-hydroxide,[3] although the ferric oxy-hydroxide can remove phosphorous compounds with up to 90% efficiency. Break point chlorination at this stage is used to oxidise any soluble heavy metal ions causing them to precipitate out and be trapped in the colloidal suspension. The sludge is then collected and the water is passed through a series of activated carbon filters where it is neutralised by passing CO_2. The used carbon is then recycled and the water passes to the final stage where disinfection takes place.

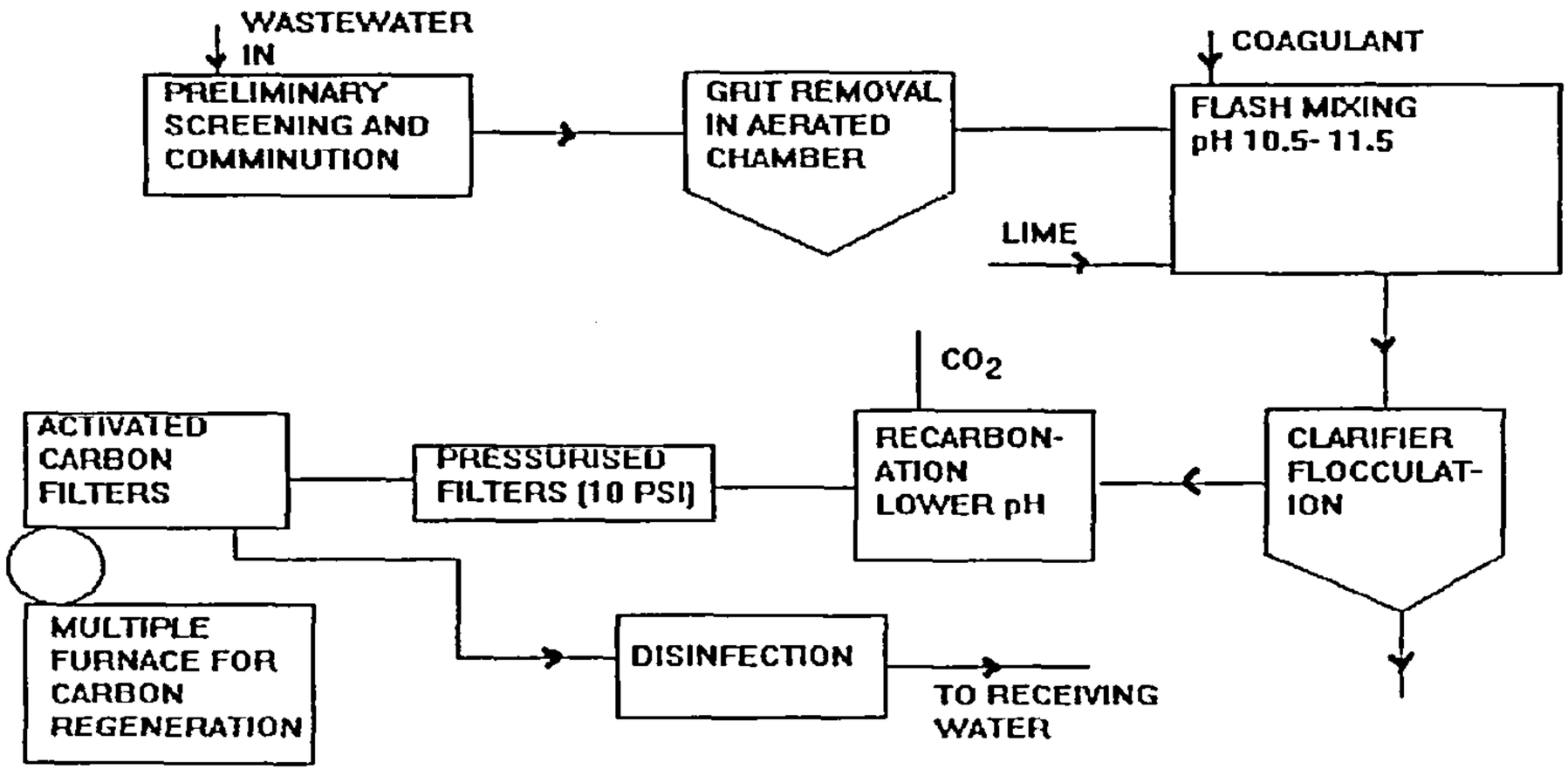

Figure 1.1

Schematic diagram showing the physical processes involved in the treatment of industrial waste.

1.2 Chemical disinfectants used for wastewater treatment.

1.2a Chlorine.

Chlorine is the most commonly used disinfectant employed for killing bacteria in water. When added to water chlorine is rapidly hydrolysed to give hypochlorous acid. This weak acid also dissociates to give hypochlorite.[6,7]

$$Cl_2 + H_2O \rightarrow H^+ + Cl^- + HOCl$$

$$HOCl \leftrightharpoons H^+ + OCl^-$$

Both the HOCl and the OCl^- species (known as the free available chlorine) are involved in the disinfection process. Due to the risks involved in the transport of chlorine gas it is becoming more common for water treatment facilities to generate the chlorine on site electrochemically by oxidisation of NaCl or HCl[7,8] solutions using transition metal oxide anodes.[9-12]

Anode reaction.

$$2Cl^- - 2e^- \rightarrow Cl_2$$

Cathode reaction.

$$2H_2O + 4e^- \rightarrow 2OH^- + H_2 \quad \text{(Brine electrolysis)}$$

This method makes use of membrane cell technology, which has been the major development making the small modular processes economically viable. In the case of brine electrolysis, the electrolyte is made by addition of commercial NaCl [6] as the presence of Ca^{2+} and Mg^{2+} ions, for example present in sea water, damage the membrane and therefore need to be removed before the electrolysis. There is a range of low tonnage chlorine electrolysers available on the market and depending on the demand they can produce from 30 grams to a few kilograms per hour. [6-8]

When the membrane is removed from these systems, hypochlorite is formed *in situ* by the reaction of the chlorine and the OH^- generated at the cathode.

$$Cl_2 + 2OH^- \rightarrow OCl^- + H_2O + Cl^-$$

Though hypochlorite is safer to handle than chlorine gas it contains less than 15 % by weight of active chlorine. There are, however, problems inherent in these systems which lowers the current efficiency for the process. At high flow rates or under turbulent flow the mass transport of the hypochlorite to the electrodes becomes an important factor which may result in its reduction at the cathode,

$$OCl^- + H_2O + 2e^- \rightarrow Cl^- + 2OH^-$$

or oxidation at the anode.

$$6OCl^- + 3H_2O - 6e^- \rightarrow 2ClO_3^- + 4Cl^- + 6H^+ + 3/2O_2$$

At low concentration of NaCl, the current efficiency drops as oxygen evolution becomes the prevalent reaction.

Transition metal oxides may also be used as anodes for the electrolysis of hydrochloric acic, although graphite is used in most commercial cells.[8] These cells use industrial grade HCl which is a cheap source of electrolyte,[7] (more than 90 % is produced as a by-product from chemical manufacture) in 18 to 27 % concentrations.

Though there are advantages in using chlorine in the disinfection process there are also major disadvantages which have resulted in the fall of chlorine production for wastewater treatment. The main problem is the formation of toxic trihalomethanes from nontoxic organic waste.[13, 14, 15] This has given the incentive to find a more environmentally acceptable alternative to chlorine. This has resulted in developing new technologies, although they remain a long way from being able to replace chlorine completely.

1.2b Chlorine dioxide.

Chlorine dioxide is as effective a disinfectant as chlorine[1, 16, - 19] but it has the advantage that it does not form harmful trihalomethane, hypobromates or react with NH_3 to give chlorinated amines. It is formed by the reaction of chlorine gas with solid sodium chlorate.

$$2NaClO_3 + Cl_2 \rightarrow 2ClO_2 + 2NaCl$$

The reduction of chlorate can also be carried out in strong acid solution where the chlorate is converted to chloric acid. Suitable reducing agents include NaCl, HCl, SO_2 and methanol. Chlorine dioxide can also be generated electrochemically by the electroreduction of chlorate.[16] The reaction is as follows.

$$ClO_3^- + e^- + 2\,H^+ \rightarrow ClO_2 + H_2O \qquad E_e^\circ = 1.15\ V$$

Its reactions as an oxidant are as follows.

$$ClO_2 + 4H^+ + 5e^- \rightarrow Cl^- + 2H_2O$$

or,

$$ClO_2 + e^- \rightarrow ClO_2^-$$

The production of chlorine dioxide must be carried out on site as it is an explosive gas with the initiation and termination reactions occurring [17] on the walls of the container.

The other problem with using chlorine dioxide is the formation of chlorate ions which can get back into the water supply. When chlorine and chlorine dioxide are mixed in equal amounts the chlorite ions are reoxidised to give chlorine dioxide [17] making the process more cost effective. It was hoped that the chlorine dioxide would oxidise any

organic species in solution before the chlorine, thus, helping to reduce the amount of harmful chlorinated by-products. However, it has been shown that the chlorine reacts more rapidly. Another problem is that chlorine dioxide fails to remove some micro-organisms present in the suspended floc and thus they require removal by coagulation, sedimentation and filtration before the disinfection process.

1.2c Ozone

In Europe ozone is beginning to emerge as an alternative to chlorine as a disinfectant especially as it is more destructive to viruses.[1] In most applications ozone is made in the gas phase. However, ozone can be generated on site electrochemically by the oxidation of water with a fluoroboric acid electrolyte; (see figure 1.2). The anode is a usually a fluorocarbon impregnated glassy carbon tube. The reaction is given below.[6, 20]

$$3H_2O \rightarrow O_3 + 6H^+ + 6e^- \qquad E_e^\circ = 2.07\ V$$

The competing reaction is the evolution of oxygen; to maintain suitable current efficiencies the process is run at low temperature and high current densities. An air cathode of the type used in fuel cells is used to reduce atmospheric oxygen and operates at around 220 mA cm^{-2}.

The cathode reaction is

$$O_2 + 4H^+ + 4e^- \rightarrow 2H_2O.$$

Another electrochemical method for the production of ozone is the use of solid polymer electrolyte technology. Pure water is passed along the back of a porous three dimensional anode, (see later), in contact with a solid polymer electrolyte, where the oxidation of the water takes place. This method has the advantage that there are no ionic contaminants in the stream but management of the hydrogen formed by the cathode reaction becomes a problem.

The half-life of ozone in water is about 20 minutes (though there is still some controversy over the actual kinetics of ozone inactivation [21]). This is important as there are some applications where it is undesirable to have residual ozone present in the supply. Using ozone in conjunction with ultraviolet radiation it is possible to decompose the trace ozone as well as any residual bacteria.[23]

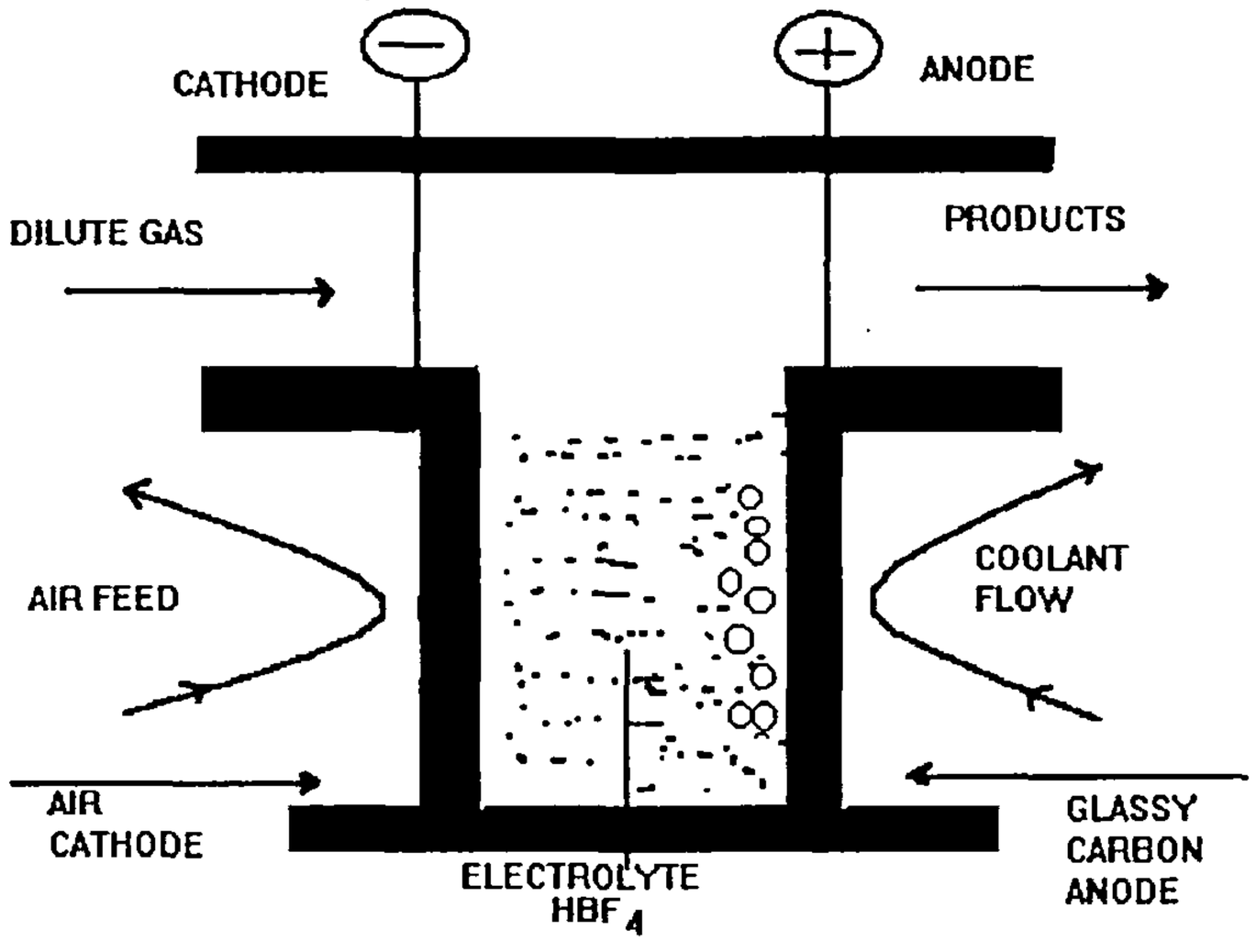

Figure 2.2

A schematic representation of the I.C.I " ECHO " ozone generator.

Ozone is a highly effective and competitive species for decolourising dyes by oxidising the nitrogen in the azo groups to give nitrogen gas as well as forming nitrate from nitro groups[23 - 25]. It has however recently been found that the reaction of ozone with bromide ions results in the formation of bromate ions and hypobromate [26 - 28] by the reactions.

$$O_3 + Br^- \rightarrow O_2 + OBr^-$$

and

$$2O_3 + OBr^- \rightarrow 2O_2 + BrO_3^-$$

Bromate is a carcinogen and the World Health Organisation has set a limit of 3µg/l for drinking water. This is an alarming discovery because if the natural water contains any bromide ions the bromate concentration will build up with time. This problem becomes particularly acute in the treatment of seawater aquaria.

1.3 Treatment of industrial effluent.

1.3a Biological effluent treatment.

With growing industrialisation, the need for puirification of moderate and highly loaded industrial wastewater has resulted in the develpoment of high performance aerobic biological reactors. The plants that have been developed for this pourpose are a marked improvement on conventional plants [29, 30] (described in section 1.1). The latest development in this technology is the impinging loop system which shows a marked increase in biomass degradation as well as exhibiting compact construction. The system uses a membrane filtration unit to concentrate the biomass leaving the water free of solid matter and infectious organsims. In this system the wastewater is mixed with the aerobic bacteria and fed into the system in a loop where it is fed with a flow of air. After the aerobic bacteria digest the biomass material the wastewater is passed through a membrane system. The pore size of the membrane is not large enough to let the bacteria cells pass and they collect with the sludge. These systems have a disadvantage over the conventional methods of effluent treatment as the set up costs are higher and the cost of the sludge removal higher.

1.3b Supercritical water.

Supercritical water has properties which are markedly different from normal water.[31 - 34] The dielectric constant of the water drops from 87.7 at 0°C to 6, at the critical point (t_c = 374°C and P = 22.1 MPa) and as the temperature increases the dielectric constant falls further, therefore, the water ia able to dissolve organic compounds that are normally hydrophobic.[31] Oxygen gas is partially miscible in supercritical water. [32- 36] This results in the oxidation of dissolved organic species with up to 99.9 % efficiency.

The problem with this procedure is that the system cannot handle inorganic materials. The solubility of NaCl drops to 100 ppm at 450°C and that of $CdCl_2$ to 10 ppm. This has made the treatment of halogenated organic compounds difficult as they form sticky solids which can block the system.

1.3c Electrochemical technology for effluent treatment.

The electrochemical treatment of industrial effluent is a more costly process than the traditional method described in section 1.1 and 1.3a with the oxidation of organic material requiring 4 electrons per carbon in the molecule. However, if the waste contains pesticides or toxic material which may prove to be poisonous to the bacteria at work in the sewage treatment plant, then electrochemical technology can be used to pretreat the waste streams. Hence the common aim of an electrochemical process is to convert toxic organic materials to biodegradable materials with the minimum electricity. These electrochemical techniques have definite advantages over the traditional methods as they are able to convert heavy aromatic petroleum residues to humic acid and carboxylic acid as well as reclaiming hydrochloric acid from chlorinated organics. Metals can be removed from effluent streams and deposited on the cathode while at the anode harmful organic materials may be oxidised. Toxic substances can also be concentrated by electrochemical methods before being treated. Oxidation of organic species in solution

can be achieved by either direct oxidation at the anode or by using a powerful oxidising agent generated at the electrode surface.

(I) Direct oxidation.

In principle, fuel cell type anodes with preicous metal catalysts could be used for direct oxidation of organics. Although there is a substantial amount of literature [35, 36] on the oxidation of organics on platinum metals and there is evidence that the reaction occours by a predissociation mechanism. The use of such technology is impossible because there are two major problems that arise during the oxidation of small organic molecules to CO_2.

1) The direct removal of an electron from an organic molecule in solution occurs at high positive potentials. For the oxidation to occur close to the reversible potential there must be a predissociation of the molecule giving rise to smaller fragments which are more easily oxidised. In the example of methanol:

$$CH_3OH \rightarrow H_{ADS} + (CH_2OH)_{ADS}$$

which is followed by further such reactions resulting in CHOH, CHO and CO being adsorbed on the electrode surface. These reactions are found to be slow and limit the current density on all the anode materials tried.

2) Due to the nature of the anodic reaction some of the organic species can be strongly adsorbed on the anode surface and act as poisons by reducing the number of catalytic sites needed to carry out the desired reaction. For the oxidation of formic acid on platinum there is a rapid decrease in activity due to the reaction:

$$Pt—COOH + HCOOH + 2Pt \rightarrow Pt_3—CHO + CO_2 + H_2O$$

The CHO acts as the poison. This is confirmed by the fact that if the surface is covered with a sub-monolayer of lead;[35] (which breaks up the platinum surface, greatly reducing

the number of three adjacent platinum sites required to form the poison), the anode then becomes an efficient catalyst for the oxidation of formate. Piersma and Gileadi[37] showed that on platinum anodes the oxidation of many organic species in aqueous solution occurred between 0.4 and 0.9 V vs NHE. When working within this potential range the electrode quickly became passivated and increasing the potential only resulted in a decrease in the rate of oxidation until oxygen evolution occoured. Even though the cell current increased at very positive potentials there was no evidence that any organic oxidation was occurring under these conditions. It is now widely accepted that the oxidation reaction occurs via adsorbed oxygen species.

Though the oxidation of small organic molecules in fuel cells has been extensively studied, there is an ever increasing amount of research describing oxidation of organic species in wastewater effluent. Unlike the fuel cell reactions, these oxidation reactions occoured at high positive potentials and initially it was thought that electrogenerated oxygen was responsible for the oxidation reaction. The rate determining step for this process is the anodic discharge of water to give hydroxide radicals close to or adsorbed at the electrode surface. The mechanism can be represented as follows where AS[ ] is the active site for the adsorption of the hydroxide radicals.[42]

$$AS[\,] + H_2O \rightarrow AS[OH^{\cdot}] + H^{+} + e^{-}$$

$$AS[OH^{\cdot}] + R \rightarrow AS[\,] + RO + H^{+} + e^{-}$$

There are several criteria that must be met if an electrode material is to be used successfully as an anode for the direct oxidation of organic waste in effluent streams. It must have high chemical and electrochemical stability, high electrical conductivity and a high oxygen overpotential. Though electrode materials such as platinum and other noble metals exhibit all of these properties, but, they are very expensive and thus there is considerable research into finding more efficient and cheaper alternatives.

There is extensive literature on the use of lead dioxide [7, 38] electrodes in electrochemical incineration reactions. Lead dioxide electrodes used for the destruction

of organic waste are prepared by electrolytic deposition of thin Pb (IV)[7] films from acidic solution. These thin film electrodes exhibit different properties from bulk lead dioxide electrodes. The films are highly conductive with high oxygen overpotentials and an extensively defective structure allowing the incorporation of foreign ionic or neutrals species into the lattice. Chettiar and Watkinson[38] studied the oxidation of several organic molecules found in coal residues at low concentration (1g/l) on lead dioxide deposited on a graphite substrate. They found that the ease of oxidation under constant current conditions was phenol > 2,3-xylenol > resorcinol > p-cresol > 3,4-xylenol > o-cresol. Although the phenolic species were destroyed the by-products from the reaction were quinones and hydroquinones. A mixture of five monohydric phenols showed 96% destruction under the same conditions but there was only a 50% decrease in the biological oxygen demand (BOD) and only 22% total organic carbon.

Johnson *et al.*[7] found that the efficiency of the thin film lead dioxide anodes was greatly enhanced by doping with bismuth. They proposed that the bismuth sites on the electrode surface are in the +5 state because of their existence within a high positive electric field. Because the oxygen stoichiometry for pure Bi_2O_5 is greater than that for PbO_2 they speculated that the Bi (V) sites in the Bi-PbO_2 surface adsorb the OH radicals generated by the discharge of water. These radicals are not stabilised on the electrode surface by the formation of bridging metal oxygen metal bonds and thus there are more sites available for the oxygen transfer reaction. Yeo and his co workers[39] reported that there was a direct link between the rate of Mn (II) oxidation (a reaction which does not occur readily on bulk lead dioxide electrodes) and the ratio of Bi:Pb in the anode. Johnson[7] also showed that the rate of phenol oxidation varied from almost no reaction to one where the rate was virtually mass transport limited. In another experiment using a rotating disc thin film lead dioxide electrode they showed that, for a solution containing 10 mM DMSO no anodic wave observed when the potential was swept form +1.3 V vs SCE to + 1.9 V vs SCE. However, on the addition of 8.3 μM Bi (III) to the solution, the potential sweep showed an oxidation wave for the oxidation of the DMSO that was mass transport controlled.

Another anode material which has received considerable attention is tin dioxide. Pure tin dioxide is an n-type semiconductor with a direct band gap of 3.5 eV and it can be used as an electrode material with good conductivity at high temperature or when doped. Like the lead dioxide anodes, the doped tin dioxide electrodes have a high chemical and electrochemical stability as well as a large oxygen overpotential which makes them suitable electrodes for electrochemical incineration. Kotz *et al.*[40, 41] produced a comprehensive study of the use of tin dioxide for wastewater treatment. In their papers they described a method of preparing thin films of doped tin dioxide on a titanium substrate. Several dopants were studied and antimony was found to perform the best. The dopant concentration did not seem to have an effect on the oxygen evolution potential or Tafel slope. However, results showed that the potential for oxygen evolution was 0.3 V higher on a doped tin dioxide anode than on an anode prepared by deposition of a thin film of lead dioxide on a titanium substrate (at a reference constant current density of 0.1 mA cm^{-2}). Under the same conditions there was a 0.45 V difference in oxygen overpotential when compared to a platinum anode and at higher current densities this difference increased to 0.65 V. The dopant concentration is important when considering the oxidation of Ce (III) to Ce (IV). Increasing the concentration of antimony incorporated in the tin dioxide anode resulted in an increase in the exchange current density for the couple

The study also compared the efficiency of lead, tin dioxide and platinum in the anodic oxidation of organic waste. It was reported that, on tin dioxide, the oxidation of phenol in 0.5 M Na_2SO_4 was complete after 1 hour but it required 8 hours to eliminate the total organic carbon. Though the removal of the phenol was good on the lead dioxide anode, the removal of the total organic carbon was poor and on platinum the reaction stopped with the formation of maleic and oxalic acid. Comninellis [43] obtained similar results. For the oxidation of aromatics, simple aliphatic compounds and carboxylic acids, the tin dioxide anodes performed 5-7 times better than platinum. The most significant difference was observed for the oxidation of benzoic acid where the concentration, (along with the total organic carbon), disappeared rapidly to zero on the tin dioxide anode, considerably faster than the other two anode materials. This reaction was found

to be independent of pH (which effects the degree of dissociation of the molecule and hence the charge).

The problem with this type of effluent treatment is the presence of chloride ions or chlorinated species in solution which may be oxidised at the anode to form chlorine or chlorinated organic compounds. Both Kotz [41] and Comninellis [42 43] found that, unlike platinum, tin dioxide did not catalyse the formation of chlorine and that any chlorinated organic species formed were further oxidised to volatile trichloromethane.

The applications in this area of electrochemical technology is limitless.[44 - 50] A recent paper [44] has proposed an electrochemical water treatment system to be used as a means of water reclamation for controlled ecological life support systems for future lunar/Mars habitats. It uses and recycles spacecraft water by removing organic species from 100 ppm to less than 500 ppb total organic carbon. Another more down to earth application is the destruction of cyanide from electroplating baths.[37] The cell use alternating stainless steel anodes and cathodes. The cell operates at a current density of 4 A cm^{-2} with an initial CN^- concentration of 100,000 ppm and a final concentration of between 0.4 - 0.1 ppm. As the CN^- ion concentration decreases, the current efficiency decreases although this can be rectified by clever engineering. For example, an ion selective electrode can follow the decrease in CN^- concentration and adjust the current density accordingly. Along with better cell design and anode materials, this is a large step towards zero effluent technology.

When seeking to remove organics present in low concentration, the rate of oxidation is limited by mass transport.

(II) Indirect oxidation.

As mentioned above in section (I), directly oxidising organic species at an electrode surface has several disadvantages: Products and by products of the direct oxidation reaction may foul the electrode surface and, prolonged reaction times lead to the passivation of the surface. One way to avoid this is to use electrochemically generated redox species to act as an intermediate which shuttles between the electrode

surface and the reactants in the bulk solution. The scheme is represented in figure 1.3 below

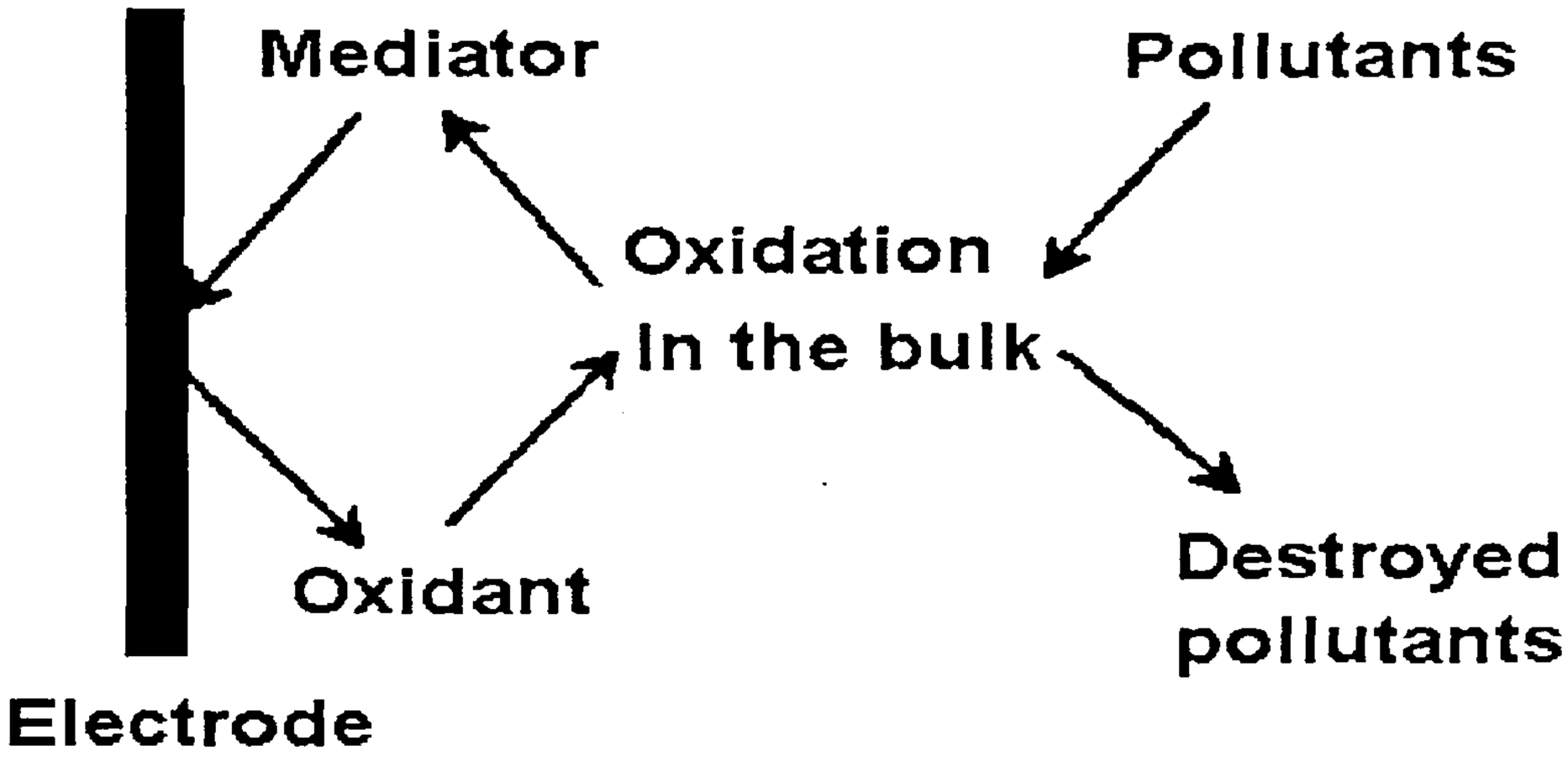

Figure 1.3

A schematic diagram showing the pollutant removal pathway for an indirect electrochemical oxidation process.

When dissolved in mineral acids, Fe (III) is an efficient reagent for oxidising organic material. Iron is an environmentally benign species and may also be beneficial as well as being relatively inexpensive. Its use as an oxidising agent in an electrolytic cell was first proposed by Bockris.[51] They studied the oxidation of coal slurries, which contain high amounts of phenolic residues, in 4 M sulphuric acid on platinum electrodes. They noted that at 0.6 V vs NHE the current increased sharply until a steady state at 0.8 V vs NHE was reached. It was proposed that Fe (III) in the coal was leaching out and oxidising the surface of the coal forming Fe (II) which in turn was being reoxidised at the electrode surface. These results were supported by the findings of Dhooge *et al.*[52] who

reported that by maintaining a constant potential in the mass transport region, (for Fe (II) oxidation), it was possible to maintain a constant current for over 100 hours.

The applications of this technology have been reviewed in an excellent article by Clarke *et al.* [7]. They found that the rate of oxidation of coal and coke slurries, in 4 M sulphuric acid, at iridium oxide coated titanium anodes, was increased by the addition of iron sulphate into the solution. However, its solubility was low and the process became mass transport limited at current densities above 200 $mAcm^{-2}$. It was found that by running the cell at 150°C, (and hence elevated pressure), in 4 M sulphuric acid, the Fe (III) was capable of oxidising vitreous carbon as well as many polyaromatics to carbon dioxide. An interesting advantage of this process is that the reaction can be stopped at the point where the surface of the carbon waste is covered in oxygen containing functional groups; these can be stripped off by digestion in sodium hydroxide and precipitated as humic acid. Humic acid is beneficial to soil acting as a natural exchange resin for phosphates, nitrates potassium and other essential metals. Thus there is an economic advantage of providing humic acid for a fraction of the price for complete combustion to CO_2.

The cell used in these experiments employed narrow gap cell technology. The Fe (III) was mixed with the organic species in a separate digestion chamber and the Fe (II) formed is then recycled by flowing through the cell back into the digester. Under the conditions described above, soluble organic materials such as sugars, alochols and esters were completely combusted. Larger more substantial carbonaceous waste such as corn husks saw dust and samples of raw sewage were also completely digested. Higher temperatures were required to completely oxidise coal and coke. On the treatment of sludge obtained from refinery run off at 150°C in 4 M sulphuric acid, molecules such as PCB were also completely oxidised. Treatment of the waste sludge with adsorbent material allowed the organic species to be concentrated before being oxidised. Based on the findings of this work, Clarke *et al.*[7] have proposed interesting solutions to several problems in the treatment of refinery sludge and supertoxic materials. The disadvantage of the system is the high temperatures needed for the oxidation to occur at a satisfactory

rate. This necessitates high pressure cells and the materials needed for construction must be capable of withstanding the harsh conditions.

Another redox couple that is proving to be of great interest is the Ag (I) / Ag (II) system. Interest in this couple was stimulated by reports that anodically generated Ag (II) could be used for the oxidation and dissolution of plutonium oxide to the soluble PuO_2^{2+} ion in nitric acid at room temperature.[7] Ag (II) is a strong oxidising agent with a standard potential of E_e° = 1.98 V vs SHE. It is a reasonably stable ion at room temperature in acid solution. However, it does undergo a slow reaction with water.

$$2Ag^{2+} + H_2O \rightarrow 2Ag^{+} + 2H^{+} + 1/2\ O_2$$

The Ag (II) exists as $AgNO_3^+$ in nitric acid solution and reacts with water via a number of reactive intermediates including $OH^{\cdot}$ and $NO_3^{\cdot}$.

Fleischmann *et al.*[53] found that, on a platinum anode in 3 M nitric acid, the rate of oxidation of Ag (I) became mass transport controlled, and this, coupled with the fact that the silver nitrate has good solubility in nitric acid allowed efficient generation of the Ag (II) at high current densities. They also reported that at high potentials, (ie greater than + 2.0 V vs NHE), the Ag (II) species will deposit on the electrode surface as the oxide AgO, while below this potential only solution free Ag (II) is produced by the electrode reaction. The concentration of the Ag (I) in solution was also found to be important with concentrations above 1 M causing the adsorption of Ag (I) onto the platinum surface. Using the Ag (II) ions generated *in situ* they were able to oxidise benzene to p-quinone with a current yield of 33% and toluene to benzaldehyde with a current yield of 90%. The oxidation of toluene on platinum proceeds slowly and is diffusion limited at all but the lowest current densities. The direct oxidation also forms a number of by products and tars which block the anode surface. They noted in the paper that the Ag (II) ion was a useful intermediate in electrode reactions and allowed oxidation of organic and inorganic species that were not directly oxidised at a platinum surface. Goodridge *et al.*[54] have also looked into the use of Ag (II) oxidation of benzene to form the quinone on an industrial scale and although the economics of using

silver would be acceptable, there were a number of engineering problems that would need addressing before a process could be designed.

Steele *et al.*[7] described a method to prepare Ag (II) to be used in the treatment of waste from the nuclear industry. At temperatures above 50° C, cellulose tissues contaminated with plutonium were completely oxidised and the waste plutonium dissolved. Tri-butyl phosphate and kerosene were also efficiently oxidised. Platinum was chosen as the anode material for these experiments because of its high oxygen overpotentials and stability, (tin dioxide anodes have also been used although they did not prove to be an efficient material for the oxidation of Ag (I)), in a 4 M nitric acid electrolyte at 50°C. The cell itself was divided with a cationic membrane to prevent mixing of the powerful oxidising agent produced at the anode and the reduced species in the catholyte. The cathode reaction was the reduction of the nitric acid to nitrous acid on a titanium electrode and the electrolyte contained excess silver ions to prevent diffusion through the membrane. The cell could be run at a current density of 1 A cm^{-2}, but, it was most generally run at 0.5 A cm^{-2} so as not to exceed the limiting current density of the membrane. In the case of chlorinated compounds a small amount of silver chloride is formed and although it reduces the amount of silver ion in the electrolyte it has the beneficial effect of acting as a chloride buffer.

In a comparative study of the Ag (II) mediated oxidation with direct oxidation on carbon anodes Almon *et al.*[7] showed that the destruction of organic species proceeded at an enhanced rate in the presence of silver ions than by direct oxidation. For benzene the rate of oxidation was 0.32 ml/Amp-Hour in the presence of silver compared to 0.24 ml/Amp-Hour without and cyclohexane was 0.31 ml/Amp-Hour compared to 0.20 ml/Amp-Hour. The study also showed that the rate of oxidation of the organic species dropped dramatically at temperatures above 50°C. This was probably due to the increasing rate of the parasitic reaction of the Ag (II) with water. Almon *et al.*[7] also found that concentration of the Ag (I) as well as applied potential also had an effect on the reaction with these results following the findings of Fleishmann *et al.* [61]

A large number of other metals have been used as charge carriers in systems similar to the ones described above. In most of the cases, the oxidation reaction is carried

out in concentrated sulphuric or nitric acid and the anode material is usually a noble metal or a noble metal oxide such as platinum or iridium oxide. These systems are usually run at elevated temperatures, and pressure is also used to enhance the rate of oxidation. Bockris [51] has used ultrasound to enhance the rate of oxidation of Ce (IV) with the organic material which constitutes human waste biomass. This improvement allowed removal of 95% total organic carbon from the solution and only producing 0.1% chlorine gas from the electrolysis of urine biomass. Zawodzinski[55] used the Co (III)/Co (II) couple in concentrated nitric acid to react with cellulose materials used to clean up low level radioactive materials in glovebox environments.

So far these discussions have concentrated mainly on anodic reactions.However, in a recent publication, Pletcher and Ponce de Lyon [56] showed that formaldehyde could be oxidised *in situ* by hydrogen peroxide generated by the reduction of oxygen in solution at an RVC cathode. Oxygen reduction in both acid and basic mediums [57, 58] has been extensively reported in the literature. The reaction can occour on a number of different cathode materials, for example in is thought to be a possible by product in the corrosion of iron.[59] Otsuka *et al.*[58] showed that hydrogen peroxide could be generated in acid solution in a fuel cell type reaction using catalytically inactive electrode materials such as graphite (on platinum and palladium the reduction of oxygen went completely to water). In acid solution the half cell reaction is:[6]

$$O_2 + 2H^+ + 2e^- \rightarrow H_2O_2$$

and in basic media:

$$O_2 + H_2O + 2e^- \rightarrow OH^- + HO_2^-$$

Hydrogen peroxide, when generated at the site of use, offers particular advantages in the paper and pulp industries as a bleaching agent to replace the use of chlorine. The use of hydrogen peroxide in conjunction with UV light or ozone it has shown promise in the treatment of industrial effluent. The electrochemical method for the production can be

cost effective for small scale operations. Dow Chemical Company [6] have designed a system which works at ambient temperature and pressure using a trickle bed cell. The cathode material used is a composite PTFE-carbon chip manufactured with a PTFE latex to surface coat carbon black onto the graphite particles. At the anode oxygen is evolved and slowly seeps into the catholyte compartment. The flow of the catholyte through the cell is carefully controlled so the desired amount of hydrogen peroxide is produced. Greater knowledge of the conditions necessary for successful synthesis of hydrogen peroxide could result in an increasing number of applications in the future. It has been reported that for successful synthesis, an alkaline electrolyte is preferred, as are carbon based electrodes with high surface areas. The electrolyte itself must be free of any transition metal impurities which may cause the decomposition of the hydrogen peroxide and hence lower the current efficiency of the process. The kinetics of the reaction are quite slow; operating at higher overpotentials leads to a reduction in the current efficiency for the reaction, due to the reduction of hydrogen peroxide at the cathode.

As mentioned in section 1.2a hypochlorite solutions can be prepared electrochemically in an undivided cell by the reaction of chlorine and OH^- ions generated at the cathode. Hypochlorite solutions oxidise numerous inorganic species [13] and since it exists as either HClO or ClO^- depending on the pH only one of the species is active in the reaction. The oxidation of CN^- is an important reaction in wastewater treatment. The reaction occurs via a ClCN intermediate, which is further oxidised to nitrogen and bicarbonate. Hypochlorite undergoes a viriety of reactions with organic compounds, most of which involve the chlorination of the functional groups which is still an environmental problem.

1.4 Cell design for environmental electrochemistry.

1.4a General considerations

The design of the cell is probably the most important factor when considering the scale up of any electrolysis. As it has been shown in the previous sections that there are

many technologies available for the treatment of effluent and a wide varity of cell can be used for this purpose. For example, the cell designed for the direct electrolysis of phenol using lead dioxide anodes is different to that used in the electrochemical generation of ozone. There are, however, several general factors that govern the design of any electrochemical cell for effluent treatment.

a) Mass Transport

No reaction can occur more rapidly than the rate at which the electroactive species arrive at the electrode surface. Thus the design of electrochemical cells must take into account mass transport which is often rate limiting when dealing with dilute solutions. There are three types of mass transport:

1) Diffusion. This is movement resulting from concentration gradients and is defined by Ficks first and second law.

2) Convection. Movement due to an external mechanical force.

3) Migration. This is movement of a charged species due to a potential gradient.

These three forms of mass transport are well documented in the literature [35] In the treatment of wastewater/effluent, the solution is flowed through or by the electrode and convective diffusion becomes the dominant form of mass transport. For a process under mass transport control the limiting current is given by the expression:

$$i_L = k_m AnFc^{\infty}$$

Therefore, the mass transport coefficient is given by:

$$k_m = \frac{i_L}{(AnFc^{\infty})}$$

(All symbols are defined in list of symbols).

The limiting current for a reaction is strongly determined by the mass transport coefficient and the electrode area. In the case of metal deposition, near the limiting current a rough deposit will not only increase the electrode area but, turbulent flow over the roughened surface will increase the mass transport. Mass transport to the electrode may also be increased by placing non conducting plastic mesh in front of the electrode to produce turbulent flow.

b) Current Efficiency.

The current efficiency for the desired reaction is given by:

$$\phi = \frac{mnF}{q}$$

c) Cell Voltage E_{cell}

In order to reduce the electrolytic power consumption of a reaction it is necessary to operate at the lowest possible cell voltage. The cell voltage is a complex term made up of a number of components and it is difficult to determine analytically. The cell voltage can be defined by the following equation:

$$E_{cell} = E_e^C - E_e^A - |\eta_C| - |\eta_A| - |iR|_{cell} - |iR|_{circuit}$$

Where E_e^A and E_e^C are the equilibrium potentials for the anodic and cathodic reactions respectively. The free energy change for the overall chemical change in the cell is given by:

$$\Delta G = - nF(E_e^C - E_e^A)$$

In the case of fuel cell reactions ($E_e^C - E_e^A$) is positive and the free energy change for the reaction is negative. In most cases ($E_e^C - E_e^A$) is negative and thus the potential must be increased until the free energy change becomes negative. These overpotentials and iR

terms represent inefficiencies in the system and, although they cannot be avoided, they may be minimised.

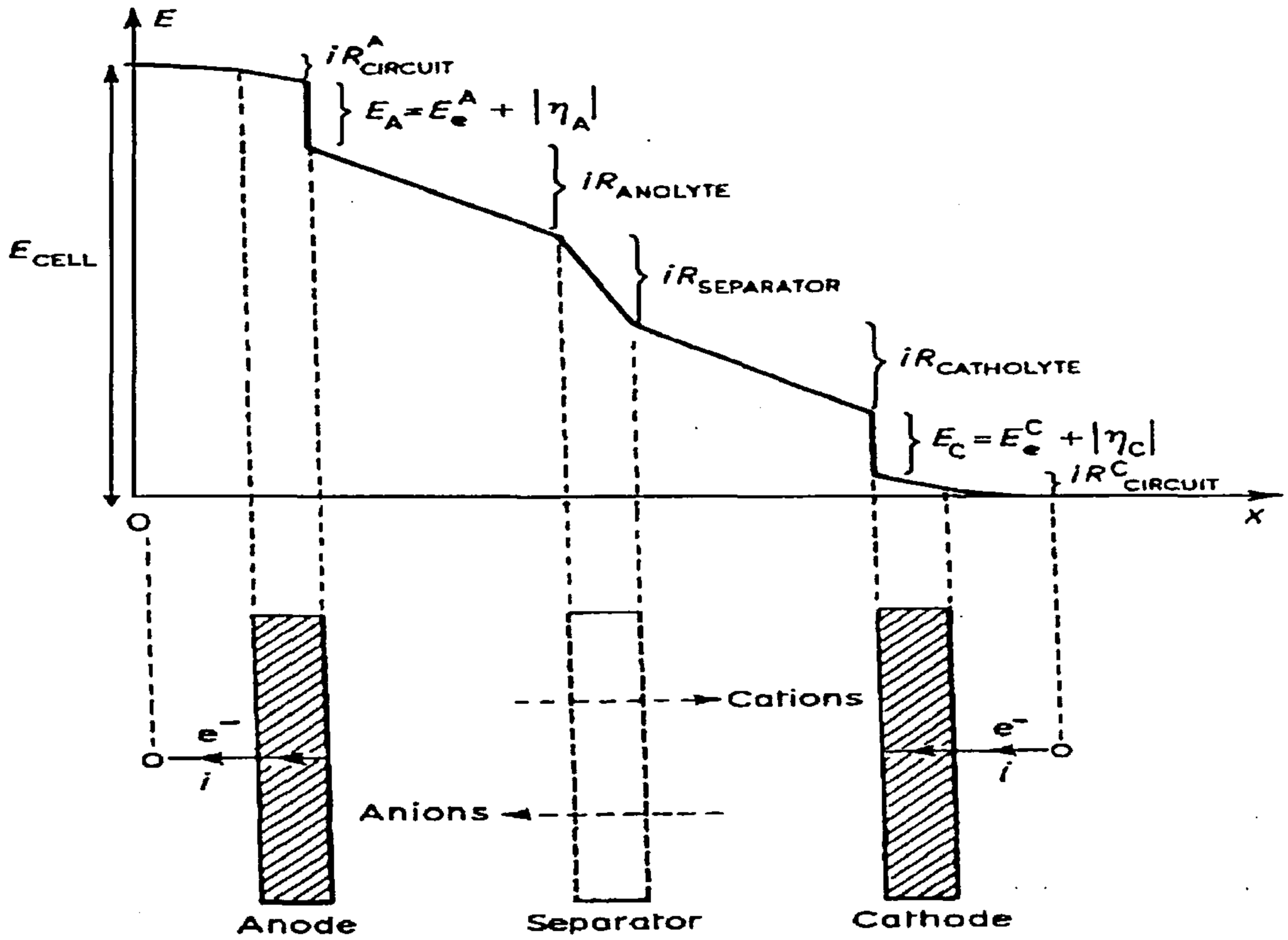

Figure 1.4

Schematic diagram showing the overpotentials responsible for the potential drop within a cell.

Minimising the interelectrode gap will reduce the internal cell resistance and hence the cell voltage. Removal of separators will also reduce the cell resistance although this stratagy may result in a reduction of the product yield or unnecessary damage to the electrodes.

Figure 1.4 shows the various iR terms associated with a divided cell configuration and how these terms contribute to the overall cell voltage. This is however, a simplified representation and does not take into account the formation of gas bubbles or the formation of oxides or polymers on the working electrode surface.

1.5 Three dimensional electrodes.

Experimental evidence has shown that the limiting current for a mass transport controlled reaction can be 1000 times greater on a three dimensional electrode than on a two dimensional electrode.

STATIC ELECTRODES	MOVING ELECTRODES
Porous electrodes	Active fluidised bed electrodes
perforated stacks	microspheres
stacked meshes	spherioids
cloths	
felts	Moving bed electrodes
foams	
	slurries
Packed bed electrodes	inclined beds
	tumbled beds
granules/flakes	vibrated beds
microspheres	beds with pulsed flow
sphereoids	
fibres	
rods	
Rasching rings	

Table 1.1

A list of some three dimensional electrodes used in effluent treatment.

The limiting current at a porous three dimensional electrode is given by:

$$i_L = nFA_EV_Ek_mc$$

The porous structure gives rise to turbulent flow which results in improved mass transport as well as high values of A_EV_E. The combination of these factors enable three dimensional electrodes to be used successfully in the treatment of effluent with low concentrations of metal ions or organic species. Indeed they are useful whenever reactions can proceed only at low current densities.

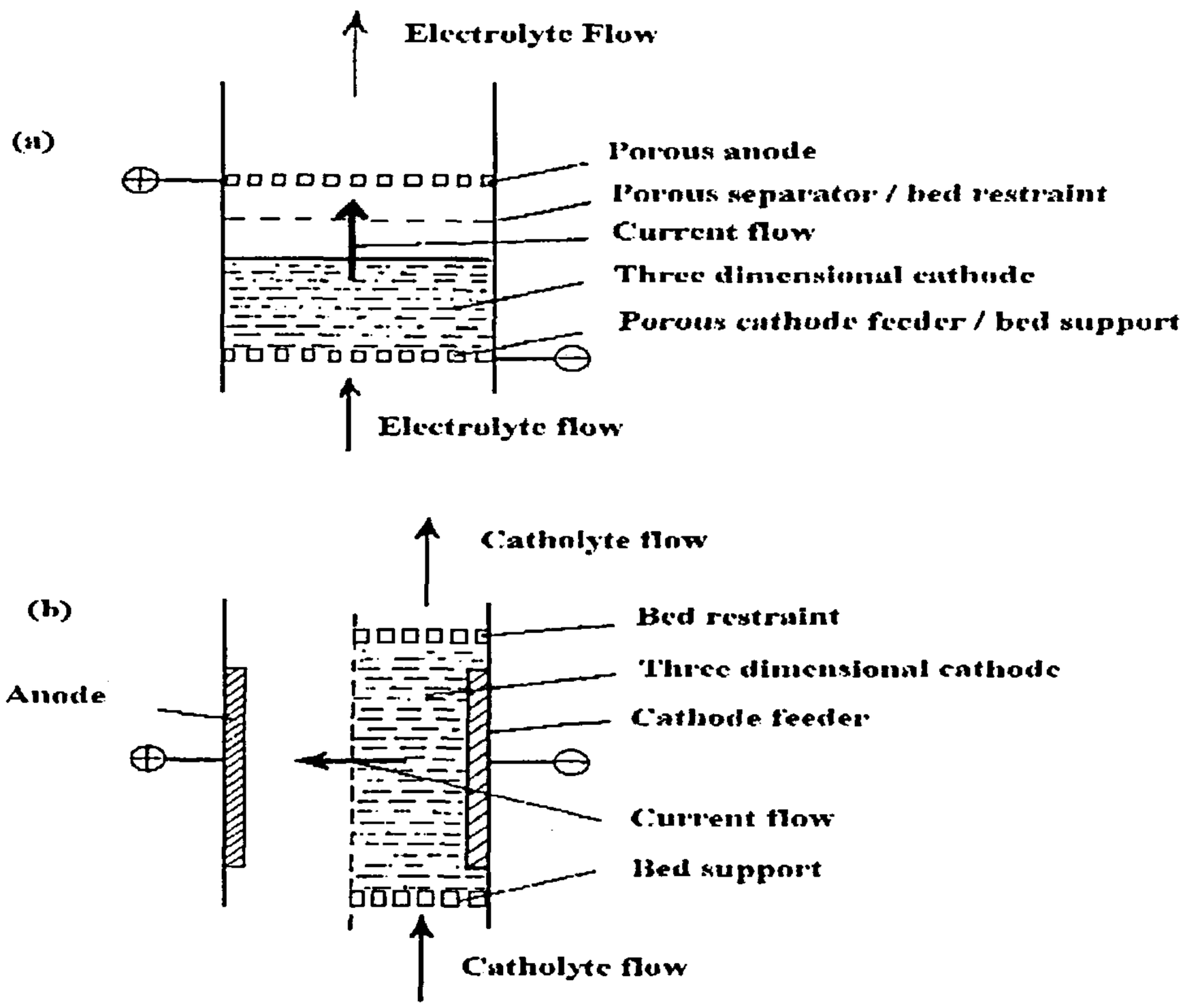

Figure 1.5

Representation of the two configurations in which a three dimentional electrode may be used.

a) Represents the flow through configuration

b) Represents the flow by configuration.

Table 1.1 shows a range of three dimensional electrodes available for effluent treatment. Three dimensional electrode cells are operated in either the flow though or the flow by configuration see figure 1.5.

In the case of the flow through configuration, the current flow is parallel to the flow of the electrolyte, while with the flow by configuration the current flow is perpendicular to the flow of the electrolyte. The fluid flow through the cell is an important parameter as it controls the mass transport coefficient, and may affect chemical reactions as well as help in the removal of gas bubbles thus lowering the cell potential. The hydrodynamics are complex but well reviewed in the literature.[60, 61]

Potential distribution across the electrode will depend on the relative positions of the anode and cathode as well as their surface profiles. As mentioned before to obtain a high space time yield the whole electrode must operate in the limiting current region, with a current efficiency of 100% for the reaction.

Therefore the overall behaviour of a three dimensional electrode depends on obtaining a uniform potential distribution and thus a uniform current distribution. If the bed is thin then the absolute potential at the electrode surface ϕ_M will drop slowly with distance from the separator due to a small iR drop within the electrode. The solution phase potential ϕ_S will also vary with distance due to iR drop in solution. This results in a reduction in electron transfer near the feeder electrode. As the bed thickness increases the potential for electron transfer (ϕ_M - ϕ_S) falls until the bed reaches a thickness where the rate of electron transfer is negligible. The thickness is known as the effective depth, above this depth the current is also negligible. The distributions of electrode potential and normalised current is shown in figure 1.6.

The discussion so far has been based on static three dimentional electrodes. However if the potential range for the limiting current is not small, a fluidised bed can be used as the potential distribution is more uniform. The fluisied electrode will require a higher cell voltage than a packed bed electrode for a given current density. The main use of three dimentional electrodes is the removal of low concentration of metal ions. However, there are some examples in the literature where they have been used to

detoxify effluent streams containing polyaromatics or to carry out low current density syntheses.

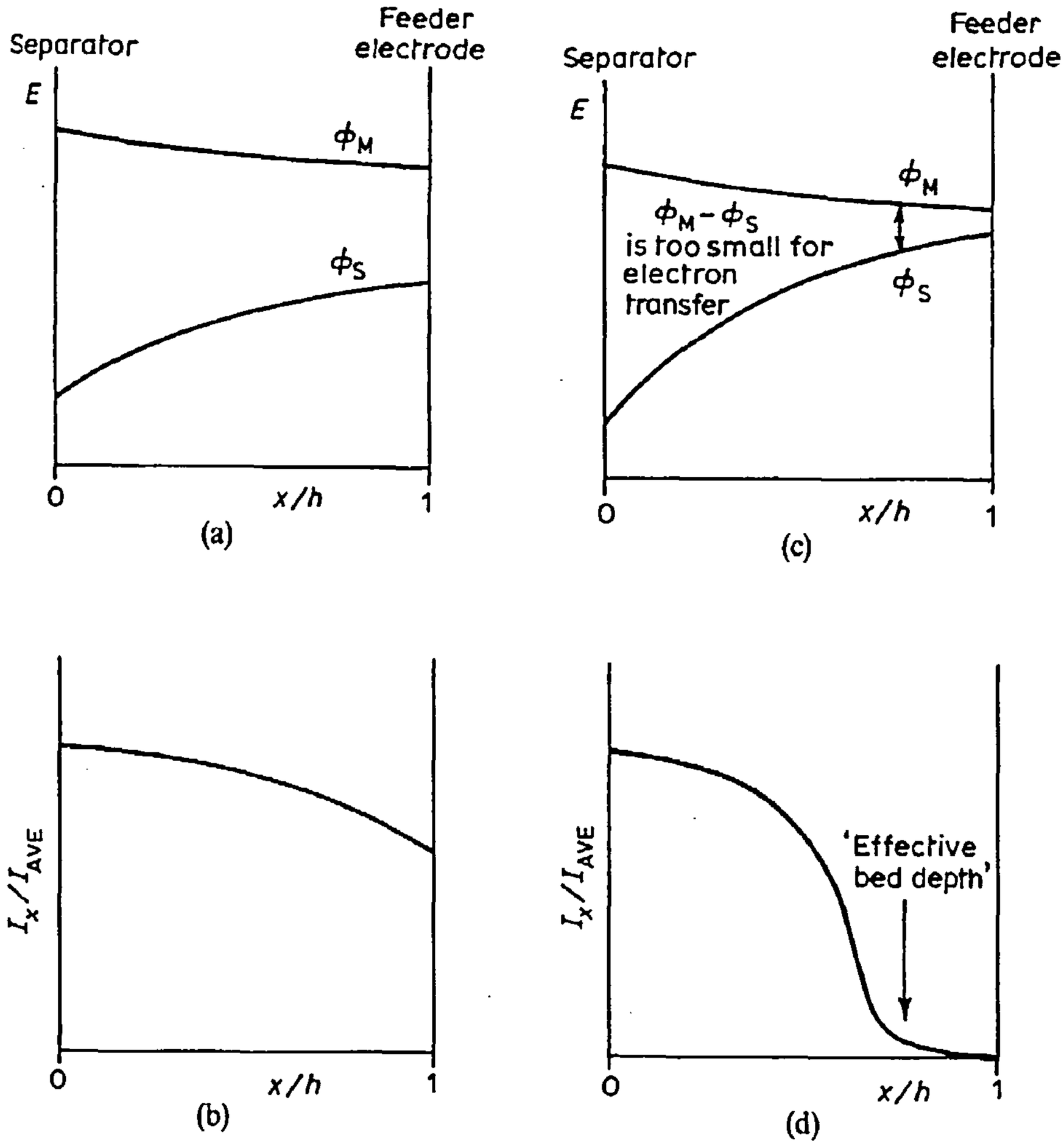

Figure 1.6

Diagram showing the electrode potential distribution and the normalised current distribution for a thin packed bed electrode (a and b) and a thick packed bed electrode (c and d). I_X = local current density at point x; I_{AVE} = average current density over all x; x = distance from the separator to the feeder electrode; h = depth of bed parallel to the direction of current flow; ϕ_M = electrode potential and ϕ_S = solution potential. ϕ_M - ϕ_S = driving force for electron transfer.

1.6 Ferrate (VI) ion.

1.6a Chemical data on ferrates (VI).

Alkali metal ferrates are salts with the formula M_2FeO_4 where M is usually Na or K. The existence of alkali metal ferrates has been known for some time with the first reported synthesis of potassium ferrate, by mixing iron filings with fused potassium nitrate, being reported by Fremy in 1832.[62] The iron has an oxidation state of (VI) and magnetic moment calculations by Hrostowski and Scott [63] suggested that the structure of the ion was tetrahedral. Murman and co-workers [64] confirmed that the structure was tetrahedral using x-ray diffraction. There are three independent Fe-O bond lengths in the FeO_4^{2-} ion which range from 1.66Å to 1.671Å. Solid K_2FeO_4 is isomorphic with K_2CrO_4 and K_2MnO_4 and is orthorhombic in shape though the oxygen metal bond is longer in the iron salt than in the others. The cell parameters are given in the table 1.2 below.

Cell Parameters	Ratio
a	7.690
b	10.328
c	5.855

Table 1.2

Table showing the cell parameters for K_2FeO_4 determined using Mo $K\alpha_1$ radiation, $\lambda = 0.70926$ Å

Like the other transition metal oxyanions alkali metal ferrates have a strong visible absorption spectrum, and these were reported by Carrington *et al.* [65, 66] The ferrate (VI) ion is characterised by a strong broad asymmetrical peak at 505 nm, a shoulder at 570 nm and a smaller peak at 780 nm. (Several other workers have also compiled data on the absorption spectrum of the ferrate (VI) ion and these studies were summarised in a paper by Levason and McAuliffe [67]). Thermodynamic information on

potassium ferrate was compiled by Wood *et al.* [68]; they reported the free energy of formation and the enthalpy of formation.

1.6b The chemistry of ferrate (VI).

The ferrate (VI) ion acts as a strong oxidising agent, and is always reduced to the (III) oxidation state. However Bielski and Thomas [69] reported the formation of Fe (V) and Fe (IV) during the reaction of Fe (VI) with CO_2^- radicals generated *in situ* from the radiolysis of formate. Kalecinski [70] also reported the formation of $HFeO_4^{2-}$ from direct gamma radiolysis of alkaline solutions containing ferrate (VI) ions. The species formed in these reactions were unstable and the final decomposition product was ferric hydroxide.

The stability of the ferrate (VI) ion is strongly dependant on pH as is the mechanism for the decomposition reaction. Ernst and co-workers [71] suggested that in acidic and neutral media the decomposition reaction followed second order kinetics and is almost instantaneous with the rate equation being given as:

$$d[\,Fe^{(III)}\,]/dt = k[\,FeO_4^{2-}\,]^2$$

Increasing the pH to 8.9 caused the kinetics of decomposition to change. The reaction order became zero order and this was attributed to inhibition effects of the OH^- ions. In more concentrated alkali solutions the decomposition reaction followed pseudo first order kinetics. In all these studies, the ferric hydroxide product was removed by complexing with the phosphate buffer to give soluble Fe (III) phosphate species.

Murman [72] followed these reactions using oxygen - 18 enriched water. They found that there was oxygen exchange between the water and the four kinetically equivalent oxygens on the ferrate (VI) ion. By monitoring the rate that the oxygen on ferrate (VI) ion exchanged with the labelled oxygen they were able to detect the labelled oxygen released from the decomposition which allowed the calculation of the rate and order of reaction. The results from this study showed strong agreement with those previously presented which stated that the reaction was second order with an isotropic

equilibrium with ferrate (VI) and the solvent in acidic medium. However, in basic and neutral mediums (pH range between 7 and 9) the decomposition showed an order of reaction of 3/2 with respect to the [FeO_4^{2-}].

The ferrate (VI) ion has been exploited by organic chemists to perform selective synthesis not only for its strong oxidising ability but because it provided a more environmentally attractive alternative to using the more common oxidants such as chromate, permanganate and ruthenate. Audette and co workers [73] suggested that, under the proper conditions, ferrate (VI) ion could be used as a selective oxidising agent for primary alcohols, amines and secondary alcohols which would be converted to their corresponding aldehyde or ketone. However, double bonds as well as aldehyde, tertiary alcohol's and tertiary amine functional groups were resistant to oxidation under the conditions employed. The mechanism proposed for the reaction was a 2+2 metal-oxo double bond with a C-H or an O-H hydrogen bond which resulted in an organometallic intermediate, which when undergoing rearrangement would produce either free radical or a carbocation. In a study by Lee *et. al.*[74] this mechanism was also proposed with the 2+2 addition between the α-C-H and the Fe=O to give an organometallic species. BeMiller and Darling [75] found that the oxidation of carbohydrates by ferrate (VI) had a far greater specificity than using chromium (VI) in sulphuric acid or pyridine mixtures. The fact that the ferrate (VI) ion is a strong and environmentally safe oxidant has made it a perfect compound to be studied for the treatment of wastewater effluent.

1.6c Ferrate (VI) and its potential for water treatment.

(I) Inactivation of bacteria and water borne viruses.

To compete with the traditional effluent treatment oxidants, the ferrate (VI) ion had to be shown to be as effective in the destruction of water borne viruses. The evidence that the ferrate (VI) ion was an effective disinfectant was first reported by Murman and Robinson. [76] However, the first detailed studied was carried out by Gilbert and co workers [77, 78] who reacted ferrate (VI) with *Escherichia coli* in buffered

distilled water and found that below pH 8 there was a marked increase in the disinfection ability. They also found that a 5-fold excess in ferrate (VI) was required to disinfect secondary effluent containing the same concentration of *E. coli.* virus to the same degree. Waite *et al.*[79, 80] tested several gram negative organisms from the *Enterobacteriaceae* family with ferrate (VI) ion all of which were rapidly and effectively inactivated in buffer solution. Their research did show that with gram positive organisms *Strepococcus faecalis, Streptococcus bovis, Staphyloccous aureus* and *Bacillus cereus* the organisms were more resistant to treatment and required at least one order of magnitude greater concentration of ferrate (VI) to achieve the same degree of disinfection. Fagen and Waite [81] observed the retardation of biofilm growth in model condenser systems by dosing the system twice a day for 5 minutes with a ferrate (VI) solution.

Viruses are among the most difficult of all species to remove from wastewater and the viruses of greatest concern in wastewater treatment are the enteric viruses. These viruses are associated with a number of diseases, hepatitis being one of many which can survive for long periods of time in clean and polluted water as well as being able to reproduce in some of these. Schink and Waite [82] used the f 2 virus as a model (as it resembles both hepatitis and poliovirus II in reactions with chlorine and iodine) virus to test the efficiency of ferrate (VI) ion as a disinfection. In all cases the ferrate (VI) proved to be more efficient than chlorine, bromine and iodine by requiring lesser concentration of starting material as well as reacting faster. Experiments carried out on secondary effluent showed agreement with those of Gilbert.[77] Ferrate (VI) ion has been shown to be excellent in the inactivation of bacteria and viruses (99 % at pH 7 and 12 minutes reaction time). When used as a pretreatment to ozonation, this value increases to 99.99941 % and there is also a decrease in the turbidity of the solution even when raw sewage is added.[83]

(II) Oxidation of organic compounds.

When considering the oxidation of organic species in solution with ferrate (VI) ion it is important to determine the nature of the reaction by products, and how much of a threat they would impose. DeLuca *et al.*[84] used *Samonella typhimurium* to show that there were no mutagenic compounds formed by the action of ferrate (VI) ion and some common organic pollutants, as this special strain cannot grow in the absence of histidiene but upon contact with mutanogens can reproduce.. Bartzatt and Nagel [96] reacted aqueous potassium ferrate with N-nitroso compounds, these are potential carcinogens and widespread in the environment. They revealed that excess addition of the ferrate (VI) ion resulted in the complete removal of the N-nitroso group as well as oxidation of the functional groups on the nitroamine aliphatic chain. Carr *et al.*[97] found that there was a 50 fold difference in the oxidation rates for primary, secondary and tertiary amines when nitilotriacetic acid is reacted with ferrate (VI) resulting from the sequential oxidation of the N-C bond. In a study by Waite and Gilbert [87] it was shown that phenol was completely oxidised to CO_2.

DeLuca *et al.*[88] showed that the ferrate (VI) ion had the capability of being used as a wastewater treatment chemical. They studied the oxidation potential and flocculation ability with several Environmental Protection Agency, (EPA), priority pollutants. In the oxidation studies, it was found that the ferrate (VI) ion reacted at different rates depending on the pollutants structure and chemistry of the pollutant. Phenol, naphthalene and trichloroethylene were oxidised in a matter of minutes whereas nitrobenzene required several hours before any oxidation products could be identified, and bromodichlorobenzene and dichlorobenzene did not react at all. DeLuca proposed that this was the result of the different oxidising products formed from the decomposition of the ferrate (VI) ion with water. By comparing the results with data from the National Bureau of Standards, he identified several species such as oxygen, hydroxyl radicals and other intermediate oxidising agents which reacted at comparable rates with the organic species chosen.

The ability of the ferrate (VI) ion to form a $Fe(OH)_3$ flocculant [89, 90] and thus aid in the removal of organic species showed that, compared to alum, ferrate (VI) ion was more efficient at removal of some of the pollutants and just as efficient for the others. The study also showed that the best flocculation conditions were produced by bubbling gas through the system; this process was enhanced by the oxygen evolved during the decomposition process. The ability of the ferrate (VI) ion to act as both oxidising agent and coagulant was also studied by Murman [89] who looked at the use of ferrate (VI) ion in the removal of metal ions from Missouri river water, tap water and three types of deep well water. The concentration of metal ions such as lead (II), chromium (III), copper (II) and mercury (II) were reduced to accptable levels by the action of ferrate decomposition.

Though the ferrate (VI) ion may not be the complete shotgun cure for water treatment it does seem to have several important advantages over the traditional methods. The fact that that it can be made as a solid and thus shipped safely as well as providing an oxidant/coagulant reagent in one (reducing the amount of equipment needed) make it a good contender for use in small factories for on site effluent treatment [91] or for use in the pre chlorination stage [92] in larger wastewater treatment plants. The major drawback is that at the present time ferrate (VI) ion is relatively expensive and there is considerable waste in raw materials during the synthesis to make it viable at the present time.

1.6d Electrochemical generation of ferrate (VI)

(I) Metal dissolution.

The ferrate (VI) ion is generated electrochemically by either the direct oxidation of an iron species in solution [93, 94] or by the transpassive dissolution of an iron containing anode. Anodic dissolution has been widely used for the preparation of high purity metal salts which are difficult to produce by chemical or thermal methods [6]. When metal is electrorefined it is anodically dissolved to produce the metal ion in

solution. This can be deposited as pure metal[96 - 98] on the cathode, however, in some special cases the metal complex (in solution) may have a higher market value than the pure metal. For example a silver anode can be anodically disolved in nitric acid in a two compartment cell to produce the more expensive silver nitrate solution.[99] In the formation of potassium stannate,[100] the anode is a steel basket filled with pure tin bars or pellets which is immersed in a KOH electrolyte. Applying a suitable current the tin dissolves to form stannite.

$$Sn + 4KOH - 2e^- \rightarrow Sn(OH)_4^{2-} + 4K^+$$

By passing air through the system the stannite is oxidised further to stannate which is continually removed from the electrolyte. The steel cathode, which is seperated from the anolyte, reduces water to form H_2 and OH^- ions. These OH^- ions then react with the K^+ ions which traverse the seperator to reform KOH. However, there is a drawback with this system as the anode may passivate due to the formation of insoluble species on the surface.

(II) Electrochemical synthesis of ferrate (VI).

The electrochemistry of iron containing electrodes in alkali solution has been well documented in the literature [101 - 114] but, there is still some debate over the nature of the species formed in solution and on the electrode surface. Current potential curves show the regions where the electrode is active and passive. In a study by Armstrong [114] on iron disc electrodes in alkaline solution, it was found that that both Fe (II) and Fe (III) species could be found in solution when the potential was held at -1.1 V vs Hg/HgO. The nature of the passive layer has been studied using a number of spectroscopic techniques but it is still an area of controversy and debate. The general view is that the electrode surface is made up of a layer of $Fe(OH)_2$ which is covered with a thicker layer of FeOOH which exists as a porous gel. As time increases this gel is converted to Fe_2O_3 and Fe_3O_4. At aproximately +0.7 V vs Hg/HgO there is an increase in the anodic current

which is a result of the oxidation of water and the transpassive dissolution of the iron to form the FeO_4^{2-} ion.

The first report of the electrosynthesis of ferrate was by Poggendorf,[115] who was studying the use of iron electrodes in alkaline solutions for accumulators. He noted that the solution around the anode turned purple when oxygen was evolved at the anode and hence it became one of the earliest electrochemical preparations. This method of ferrate (VI) synthesis by transpassive dissolution of the anode is similar to methods for the production of MnO_4^{2-} [116 - 117] and CrO_4^{2-}. [118] Although the reaction has been studied at intervals over the last two hundred years there is not a very extensive literature on the subject. Haber [119] found that in the electrosynthesis of the ferrate (VI) ion, NaOH acted as a better electrolyte than KOH and cast iron was a more efficient anode material than either steel or wrought iron. The conditions used in the experiments (70°C and concentrated alkali electrolyte), 70% of the iron anode entered solution with between 2 and 14% being converted to the ferrate (VI) ion. This work was continued by Pick [120] who assuming that the only competing reaction was oxygen evolution, used this to determine the concentration of ferrate (VI) formed in the reaction by measuring the amount of oxygen evolved. From these experiments he also found a relationship between the anode material and the concentration of ferrate (VI) formed in the electrolysis.

Later Grube and Gmelin [121] found that during the electrosynthesis of ferrate (VI), the electrode passivated. It was assumed that this was due to a coating of an oxide layer, and the use of an alternating current density (5 mA cm^{-2}) helped remove the passivating film and an improvement of 160% was achieved over the use of the direct current method. They also suggested that a divided cell configuration was necessary to prevent reduction of the ferrate (VI) at the cathode. Tousek [122 123] also made a comprehensive study of the electrochemical generation of the ferrate (VI) ion in concentrated alkali solution. Again the concentration of the ferrate ion was determined by measuring the oxygen evolved in the reaction and assuming that this was the only competing reaction. The findings of his work showed that the best current density for the synthesis of ferrate (VI) was 1 mA/cm^2 at a temperature of 25°C. It was also noted that

the current efficiency for the reaction dropped with time. Up until this time, all the studies of ferrate (VI) synthesis were all carried out under constant current conditions. Venkatadri *et al.*[124] reported the synthesis of ferrate (VI) under potentiostatic control and found that there was a narrow potential range between 0.6 V and 0.65 V vs Hg/HgO where ferrate (VI) was formed with good current efficiency. From the results of the experiment it was concluded that at potentials more negative than those quoted, the only anode reaction was the formation of a ferric oxide. At more positive potentials, although some ferrate (VI) was being formed, oxygen evolution was the prefared reaction. It was also reported that Fe (III) formed during the electrolysis caused the ferrate to spontaneously decompose.

Deininger *et al.*[125 126] obtained two patents for cells designed for the synthesis of ferrate (VI) ion in concentrated NaOH and KOH using either an iron anode or a suspension of FeOOH particles. The technology makes use of membrane technology used in the chlor alkali industry. The ferrate (VI) is formed on flat plate anodes under an applied constant current of between 1 and 4 A. Both the anolyte and catholyte solutions where of a concentration 40% weight percent alkali and were separated from each other using a Nafion® membrane. It was also suggested that the addition of halide ion such as chloride or bromide ions into the electrolyte would aid in the formation of the ferrate (VI) ion. Ferrate (VI) produced by this method has been used to remove trans uranium waste from effluent streams with great success. There have been several other reports in the literature [93, 94, 95] on the synthesis of ferrate (VI) using suspended Fe (III) particles, although in all cases the yields were poor and the solutions difficult to handle. Bouzek and Rousar [127, 128] also studied the synthesis of ferrate in a divided cell. Again the current efficiency for the reaction was shown to be dependant on the applied current and potential. The application of an a.c. current was shown to improve the ferrate (VI) yield.

Venkatadri *et al.*[129] reported that the method of ferrate (VI) determination using the chromite method [130] gave results which were lower than those expected therefore, use of electrochemical methods for the determination of the ferrate (VI) concentration was considered. They found that on iron electrodes the ferrate (VI) was reduced to the ferric (III) at a potential of -0.25 V vs Hg/HgO. Using iron electrodes

held at a constant potential of +0.7 V vs Hg/HgO it was shown that the peak height for the reduction was increased by holding the potential for longer time periods. In a very comprehensive review Beck [131] looked at the reduction of ferrate (VI) on platinum electrodes using rotating disc and cyclic voltammetry. From the data obtained Beck was able to calculate the diffusion coefficient for the ferrate (VI) ion in concentrated NaOH solution using the Stokes-Einstein equation as 3.5×10^{-7} cm^2s^{-1} at 20°C. The transpassive dissolution of ferrate (VI) on iron electrodes was also studied and Beck suggested a reaction scheme for the electrochemical generation of ferrate (VI).

Chapter 2

Experimental.

2.1 Chemicals and materials.

All chemicals were used as supplied unless otherwise stated. The sources and qualities are shown in table 2.1.

Chemicals.

Chemical	Source	Grade
Sodium hydroxide	BDH	Analar
Sodium hypochlorite	Hogg Laboratory supplies	Reagent
Anhydrous ferric chloride	BDH	Reagent
Water	Millipore purification	Deionised
Methanol	Aldrich	Reagent
Ethanol	Aldrich	Reagent
Propanol	Aldrich	Reagent
Butan-2-ol	Aldrich	Reagent
2-Methyl-2-butanol	Aldrich	Reagent
Ethanediol	Aldrich	Reagent
Phenol	Aldrich	Reagent

Table 2.1

Sources and purity of chemicals.

The composition and suppliers of the iron alloys are reported in table 2.2.

Alloy	Electrode materials Composition	Alloy form	Supplier
Iron	Fe > 99.5 %, C 0.08 %	Plate	Goodfellow
Alloy A	Fe > 99.7 %, C 0.04 %, Mn 0.26 %, others, < 0.05 %	Plate	British Steel
Alloy B	Fe > 98 %, C 0.16 %, Mn 0.75 %, Si 0.21 %, others < 0.03%	Rod	British Steel
Alloy C	Fe > 98 %, C 0.20 %, Mn 0.94 %, Si 0.31 %, others < 0.03 %	Plate	British Steel
Alloy D	Fe 98 %, C 0.65 %, Mn 0.78 %, Si 0.22 %, Cr 0.35 %, others < 0.05 %	Plate	British Steel
Alloy E	Fe > 96.5 %, C 0.90 %, Mn 1,30 %, Cr 0.50 %, W 0.50 %, V 0.2 %, others 0.02 %	Rod + Plate	British Steel
Alloy F	Fe > 96.5 %, C 0.22 %, Mn 1.14 %, Si 0.97 %, others < 0.02 %	Plate	British Steel
Alloy G	Fe > 96.5 %, C 0.25 %	Plate	British Steel

Table 2.2

Composition of iron containing anode materials used.

2.2 Electrode preparation.

(I) Stationary disc electrodes.

Metal disc electrodes were prepared by either cutting a cross section of a 5 mm diameter bar, or cutting a 5 mm disc from a sheet. A nickel wire was spot welded onto one of the disc faces and the assembly was placed in a glass tube, (internal diameter 5.8 mm). The other disc face was held flush with the end of the tube and epoxy resin, (from RS Supplies), was poured in from the other end. The epoxy resin was allowed to set for 48 hours. The surface of the disc was polished successively on grades of emery paper descending in coarseness from 400 to 1600. In order to obtain a mirror finish the disc

was then polished sequentially with 1, 0.3 and 0.05 μm alumina powder on a felt pad, (both supplied by Buehler), and washed well in water.

(II) Flat plate anodes.

The flat plate disc anodes were prepared by cutting a 4 cm diameter disc from a sheet of the ferrous metals shown in table 2.2. A nickel wire was spot welded onto the back of the disc. A thick layer of epoxy resin was applied to the back and attached to a B 34 ground glass joint. This was allowed to set for 48 hours. The disc was polished using the same method as described in part (I).

(III) Three dimensional electrodes.

Iron wire, 36g, was cut into 20 cm lengths and divided into three equal portions, these were worked into a bundle 2 cm wide, 1 cm thick and 10 cm long. When the three separate bundles had been made the were worked together so the structure was as uniform as possible. The bundles were then secured by tying them together with single strands of iron wire.

2.3 Analytical and electrochemical equipment.

Constant current electrolyses were performed with a Powerline Labornezgerat regulated power supply type LAB 505. All other electrochemical experiments were controlled with a Hi-Tek potentiostat, type DT2101, and waveform generator, type PPR1, and the responses were recorded on a Bryans Instrument XYt chart recorder. The rotating disc electrode was controlled with a EG & G PARC model 616 rotating disc control unit. All potentials are quoted against a Radiometer type K401 saturated calomel reference electrode or a home made mercury/mercury oxide in 10 M NaOH reference electrode. The Hg/HgO electrode had a potential of -0.143 V vs. SCE.

2.4 Cells

(I) Cyclic voltammetry cell.

All cyclic voltammetry was carried out in a glass cell manufactured by the glassblowers in the Chemistry Department, Southampton University. The cell is shown in figure 2.1.

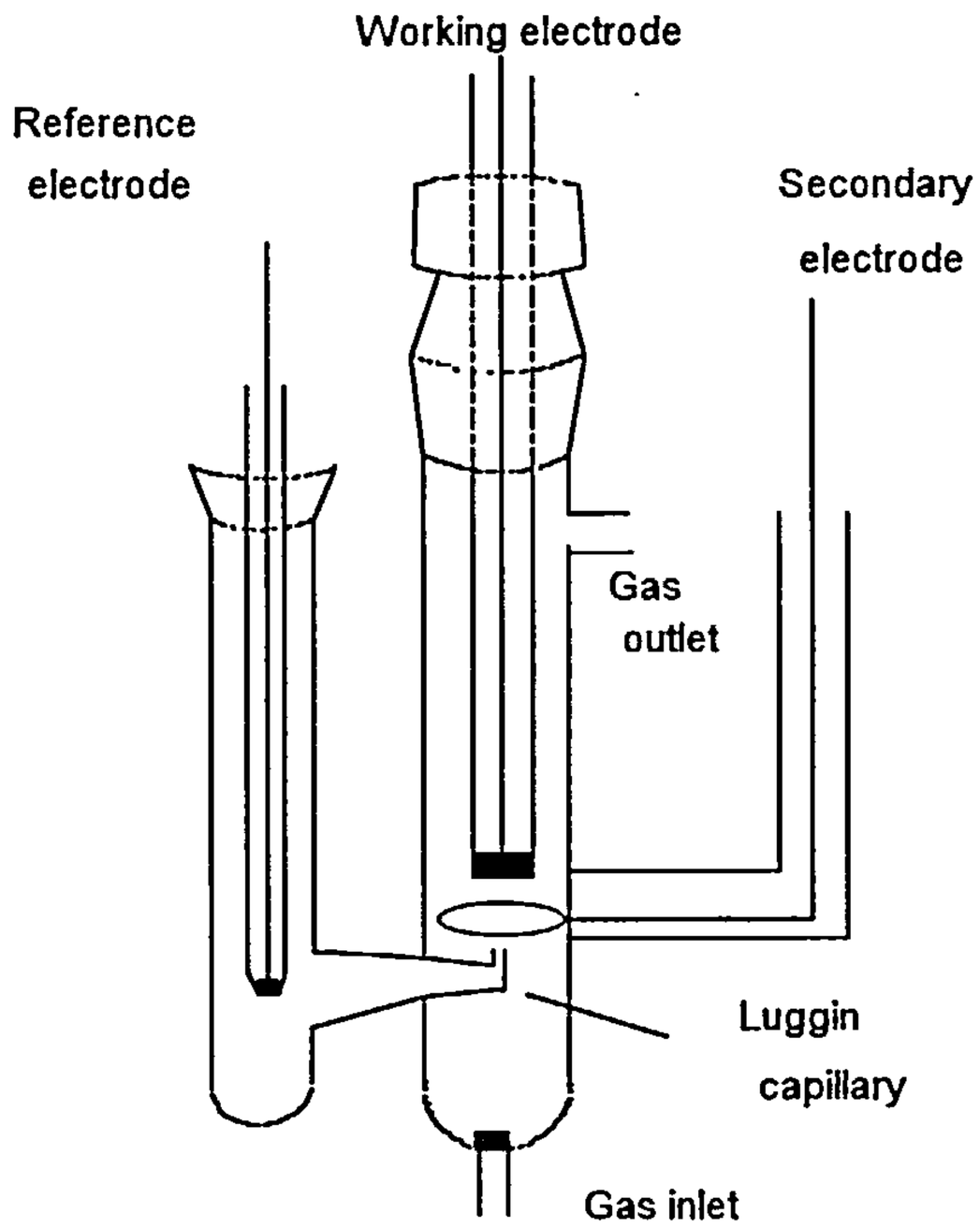

Figure 2.1

Electrochemical cell for cyclic voltammetry.

It consisted of a fixed platinum ring secondary electrode which surrounded the working electrode. The reference electrode compartment was fixed to the side of the cell with a Luggin capillary extension placed in a position directly underneath and in the center of the working electrode. A glass frit was incorporated at the bottom of the cell to act as a gas inlet, allowing the solution to be nitrogen purged. The cell had a volume of 30 cm^3.

(II) Rotating disc cell.

All rotating disc experiments were carried out in a cell made in the University. The cell, shown in figure 2.2, consisted of a central compartment with a volume large enough to accommodate 50 cm^3 of solution.

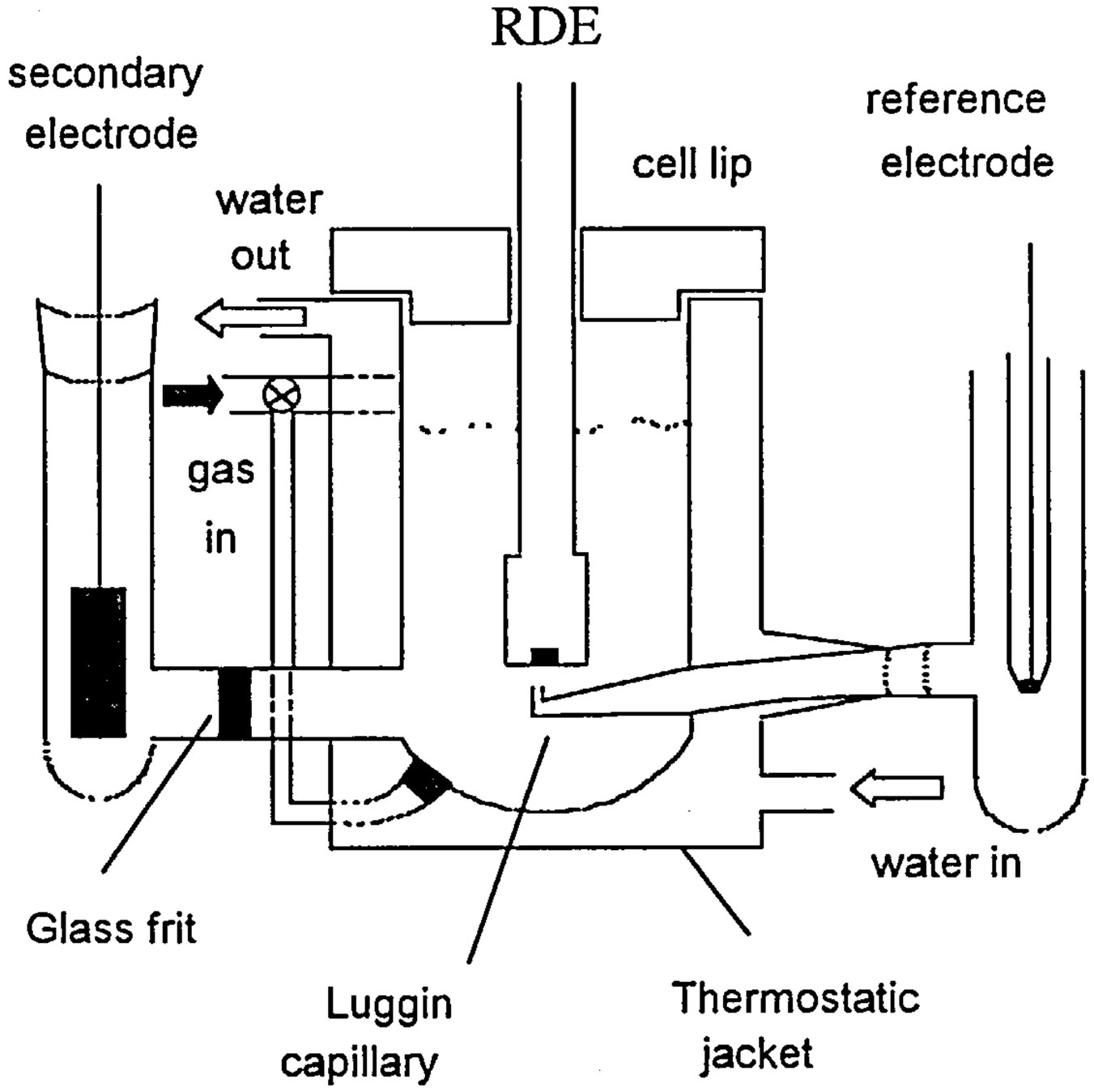

Figure 2.2

Electrochemical cell for rotating disc studies.

The reference electrode compartment incorporated a Luggin capillary which was inserted into the central body section so it was positioned directly under the carbon disc working electrode. The secondary electrode compartment was joined via a glass frit to the cell and a platinum spade electrode was used. The working electrode was a 4 mm diameter vitreous carbon disc in a PTFE sheath with an internal screw thread. The electrode was made by the Engineering Workshop in the University. The electrode, which was placed in the cell in a central position

above the Luggin capillary. A glass frit at the bottom of the main cell body was used to pass gas through the solution.

An external water jacket with an inlet and outlet for the passage of water if the cell needed to be thermostatted was also incorporated into the design. Two flanges at either side of the central section were used for the attachment of the reference and secondary electrode compartments.

(III) Microelectrode cell.

The microdisc electrodes were made by the glassblower in the University by sealing the appropriate microwire in glass. In order to get a flat smooth surface, the microdiscs were polished on polishing alumina of 5, 3, 1, 0.3 and 0.05 μm supported on a felt pad and lubricated with water. A two electrode cell, shown in figure 2.3, was used for the microelectrode studies.

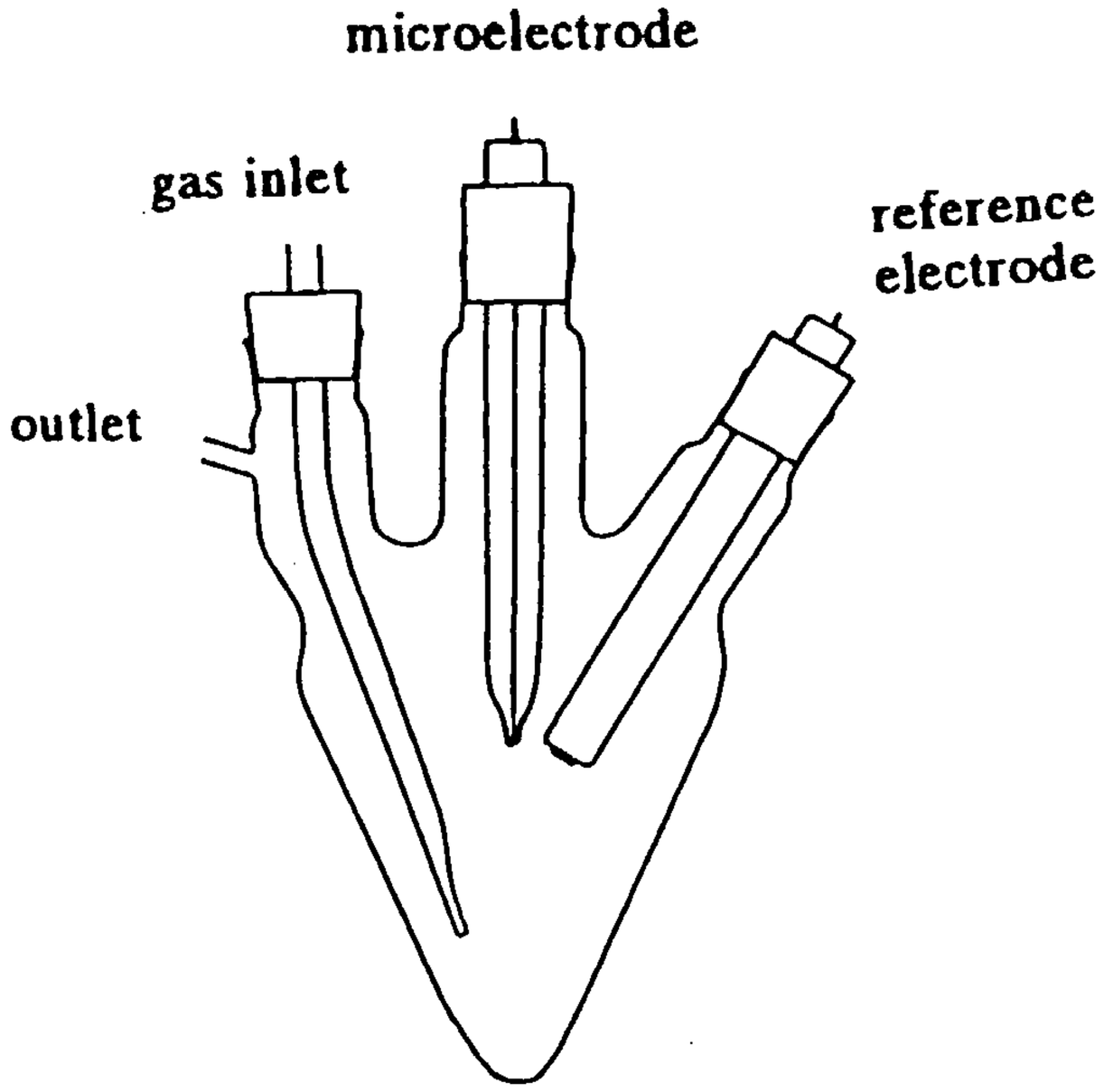

Figure 2.3

Two electrode cell for microelectrode studies.

The reference electrode, a saturated calomel electrode, also acted as the secondary electrode. The potential was controlled directly with a waveform generator, Hi-Tek PPR1. Cell currents were amplified using a home built current follower. The cell was placed in a Faraday cage to isolate the system from noise.

(IV) H cell

Figure 2.4 shows the typical set up employed for preliminary H cell electrolyses. The H cell was constructed from glass in the University. The anolyte and catholyte compartments were separated by a glass sinter, 20 mm in diameter. Both the anolyte and catholyte compartments had a volume of 30 cm^3. The anode and cathode, both iron wool bundles, were prepared from 10g of iron wire, their dimensions were 100 mm x 20 mm x 10 mm. Electrolyses were carried out galvanostatically.

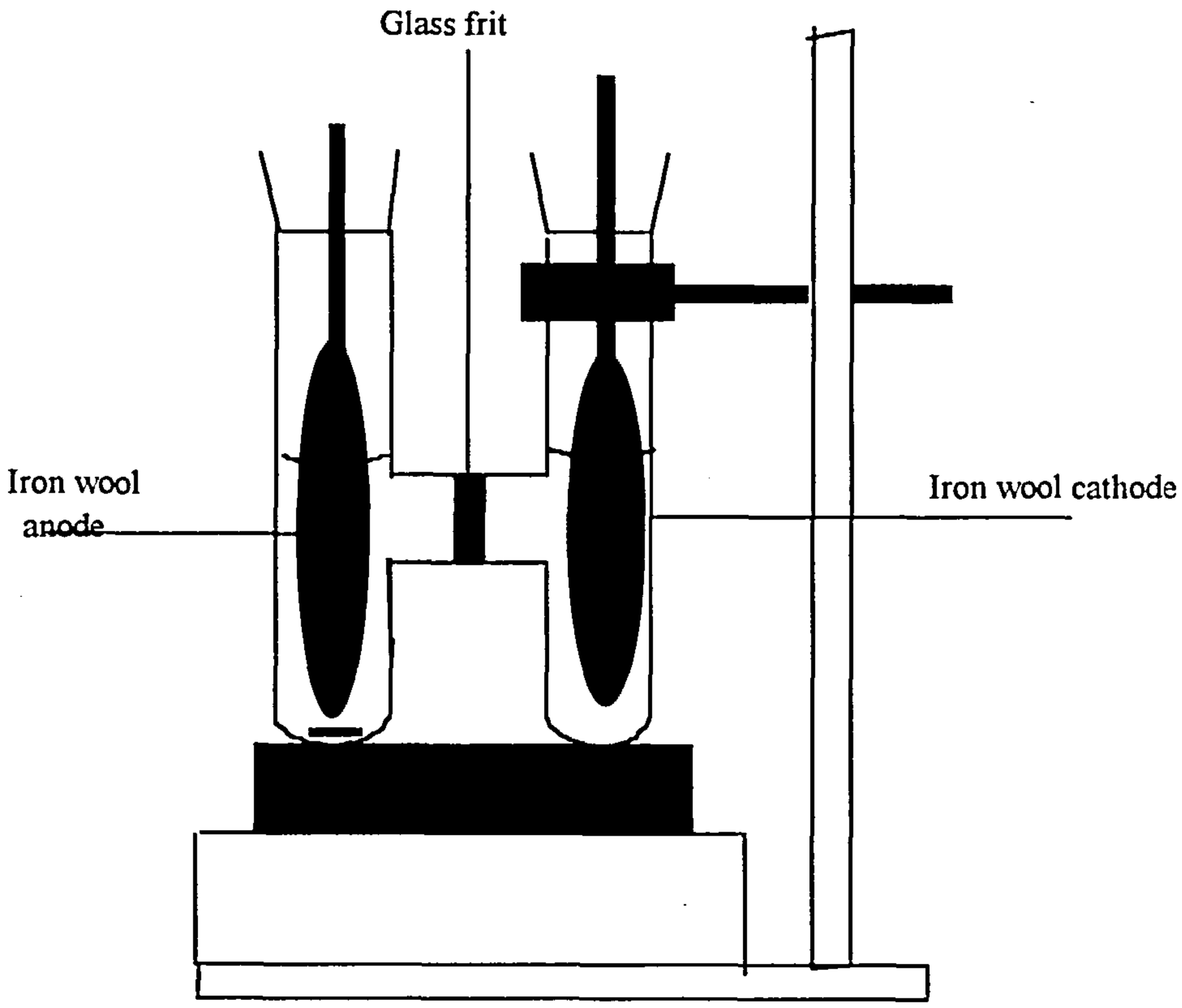

Figure 2.4

H cell used for the electrosyntheses of ferrate (VI).

(V) Pipe cell.

The pipe cell used for the electrosyntheses of ferrate (VI) was also built by the glassblowers in the University. The cell, shown in figure 2.5, consisted of an anolyte and catholyte compartments separated by a glass sinter of diameter 4 cm. The anode was a flat disc with a diameter of 4 cm. It was held in the cell via a B 36 ground glass joint and sealed with PTFE tape. The cathode consisted of a circular platinum gauze with a diameter of 4 cm. This was held in the cell in a similar manner to the anode. A glass inlet in the main body of the anolyte compartment allowed the passage of nitrogen through the solution. The anolyte and catholyte compartments had a volume of 25 cm^3 of electrolyte. There were outlets in the anolyte and catholyte compartments to allow gas to escape and to allow samples of the anolyte to be taken for analysis

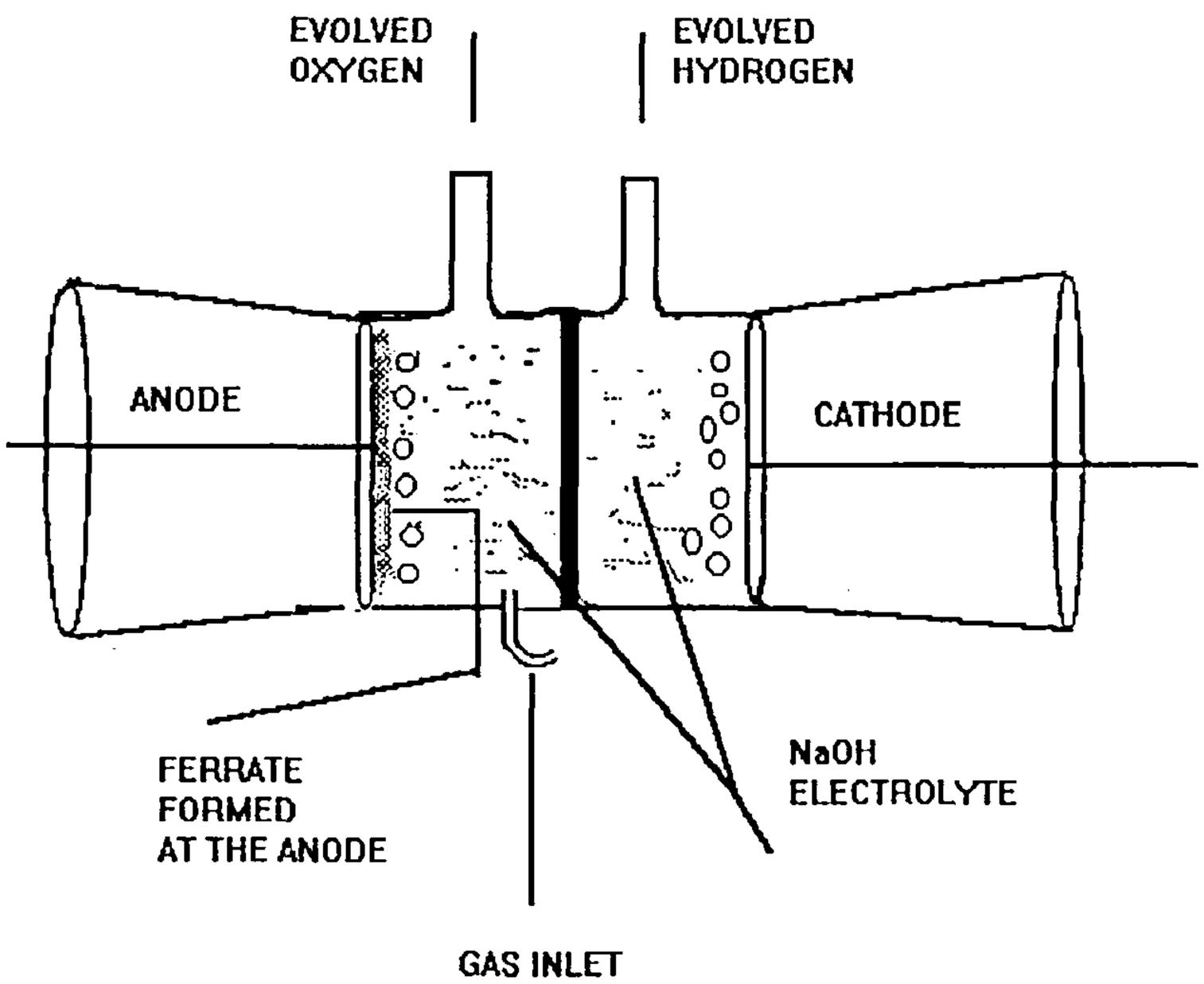

Figure 2.5

Pipe cell used for the electrosyntheses of ferrate (VI).

(VI) Flow cell.

The flow cell used for the preparative electrolyses, shown in figure 2.6, was constructed from polypropylene blocks 270 mm x 100 mm x 10 mm. The centre two formed the electrolyte compartments and were machined so that there were entry and exit zones where the channel broadened slowly. The current collectors were stainless steel plates, 100 mm x 60 mm, sunk into one of the outer blocks, with an electrical connection which was spot welded on the back. A Luggin capillary entered the anolyte compartment through a 2 mm hole drilled through the outer block and current collector. The cathode was an iron wool bundle pressed against the current collector. The separator was a Nafion 350 cation permeable membrane and the gaskets were cut from Vitron sheet. The cell was sealed via 16 bolts. The iron wool anode, (Fe > 99.5 %, C 0.08 %), with dimensions 100 mm x 60 mm x 10 mm, was fitted into the anolyte channel so that it was adjacent to the anode current collector plate. The membrane was protected from the iron wool with a sheet of coarse polymer mesh. The anolyte and catholyte used were 10 M NaOH unless stated otherwise.

The electrolyte was placed in a 1 l glass reservoir and was pumped around the external circuit, see figure 2.7, using a Totton pump type NDP 14/2, (2 l/min). The flow was controlled with a 0.2 - 1.5 l/min flow meter type GTF 2ASS from Flowbits. The electrolyses generally used 0.45 l of both anolyte and catholyte and the electrolyte flow rate was 0.8 l/min unless otherwise stated. The hydraulic circuit was made from PVC pipework. The pipes were connected to the cell with Soltube Quick-Disconnect fittings, type 6175, with 1/4 inch internal diameter and supplied by Nalgene.

Immediately prior to commencing a preparative electrolysis the anode was washed in concentrated H_2SO_4 to remove any oxide formed on the surface. When the surface was clean, the wool electrode was removed form the acid and placed under running water for a few minutes. This was followed by extensive washing in deionised water until all the acid had been removed. A cloth was used to remove the surplus water from the electrode, while a fast stream of N_2 was used to dry the interior of the electrode. The electrode was stored in a desiccator until needed.

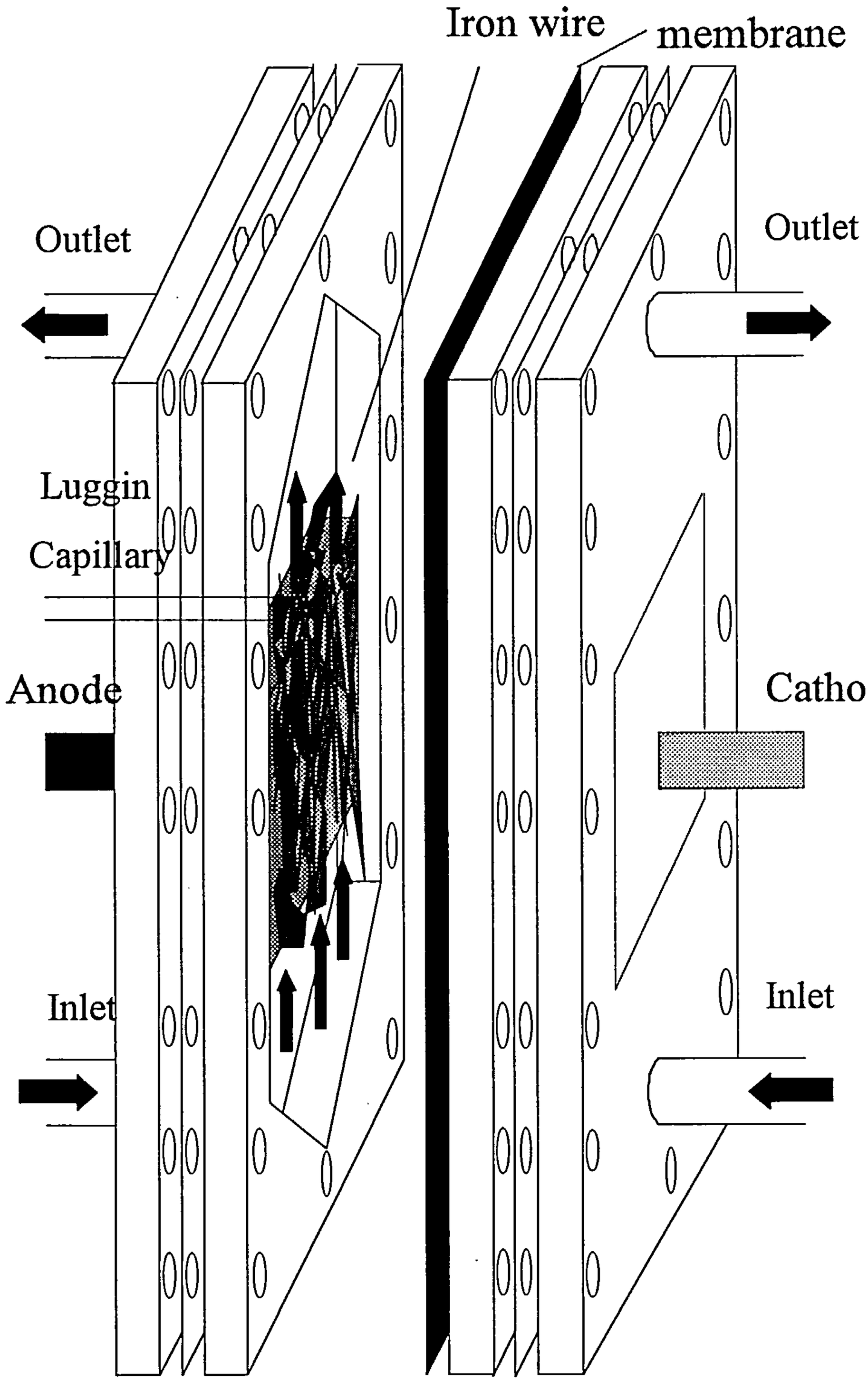

Figure 2.6

An expanded view of the flow cell used for the electrosyntheses of ferrate (VI).

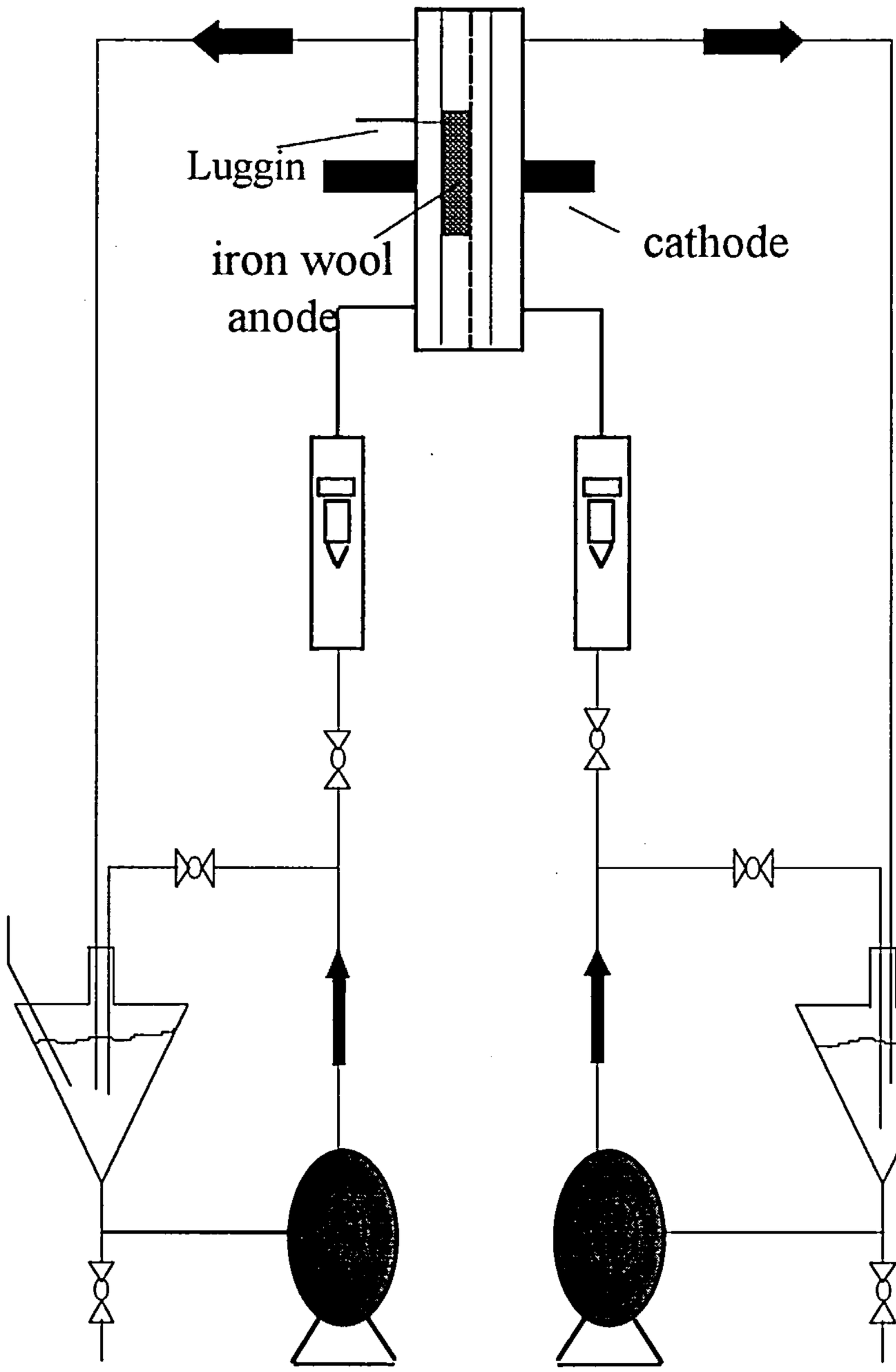

Figure 2.7

Hydraulic circuit used for electrolyses in the flow cell.

2.5 Analysis of ferrate (VI) solutions.

The analysis of ferrate (VI) solutions was carried out using a Philips PU8730 fixed bandwidth uv/vis spectrometer. The precision optical cells, supplied by Thermal Syndicate Ltd., were made from optical glass.

During an electrolysis, the increase in ferrate (VI) concentration in the electrolyte was monitored by removing a small volume of the anolyte from the reservoir, (approximately 1 cm^3). Aliquots of anolyte were transferred to a glass cuvette, (pathlength 2 mm). The cuvette was placed in an ultrasonic bath for a few seconds to remove any gas bubbles that may interfere with the absorbance measurements. A blank containing the electrolyte was used to calibrate the spectrometer which was pre-programmed to record the absorbance between 350 and 900 nm. Once the absorbance had been recorded the anolyte solution was returned to the reservoir or cell.

Visible spectroscopy was also used to follow the reactions of ferrate (VI) with water and organic compounds. The optical cell containing the reaction mixture was placed in the spectrometer, and the absorbance was measured between 350 and 900 nm. Ferric oxide/hydroxides formed during the reaction were removed by washing the cell in dilute acid, then in deionised water until all the acid was removed. For the reactions involving organic species a reference solution, containing no organics, was prepared and, run under similar conditions to compare the reaction of the ferrate (VI) and organic with ferrate (VI) with water.

Chapter 3.

Preliminary investigation into the feasibility of using ferrate (VI) ion in wastewater treatment.

3.1 Introduction.

In principle, there are several ways in which ferrate (VI) can be used to treat wastewater.

1) Prepare the ferrate as a solid and add it directly to the waste in the required quantity.

2) Generate the ferrate (VI) *in situ* in the wastewater.

3) Prepare a concentrated solution of ferrate (VI) and slowly bleed into the effluent stream.

To establish which of these methods are possible for use in wastewater treatment, the stability of ferrate (VI) in various media including solutions containing organics was determined.

3.2 Determination of ferrate (VI) concentration.

In order to determine the concentration of ferrate (VI) in solution, an analytical procedure had to be developed. It has been reported that ferrate (VI) is most stable in strong aqueous alkali;[69] therefore 10 M NaOH was chosen as a medium. A solution containing a known concentration of ferrate (VI) was prepared by oxidising a weighed sample of anhydrous $FeCl_3$, 1.622g (10 mmol), in a mixture prepared from 1000 cm^2 of 14 % NaClO (providing a very large excess of oxidising agent) solution made up to 10 M NaOH. The solution was stirred with a mechanical stirring device until almost all the Fe(III) had been completely oxidised. This took several hours. The solution was then filtered using a glass sintered filter which had been dried and weighed beforehand. The small quantity of the solid Fe (III) residue was collected in the filter, placed in an oven to dry and weighed.

When the reaction was completed the solution had turned a purple colour very similar to a permanganate solution. The residue in the filter (0.096g) was red/brown in colour. It was assumed that the filtered residue was Fe_2O_3. The amount of iron oxidised in the reaction was determined by subtracting the amount of iron in the solid form the amount of iron originally used. This gave a total iron concentration of 9.4 ± 0.5 mM in the solution.

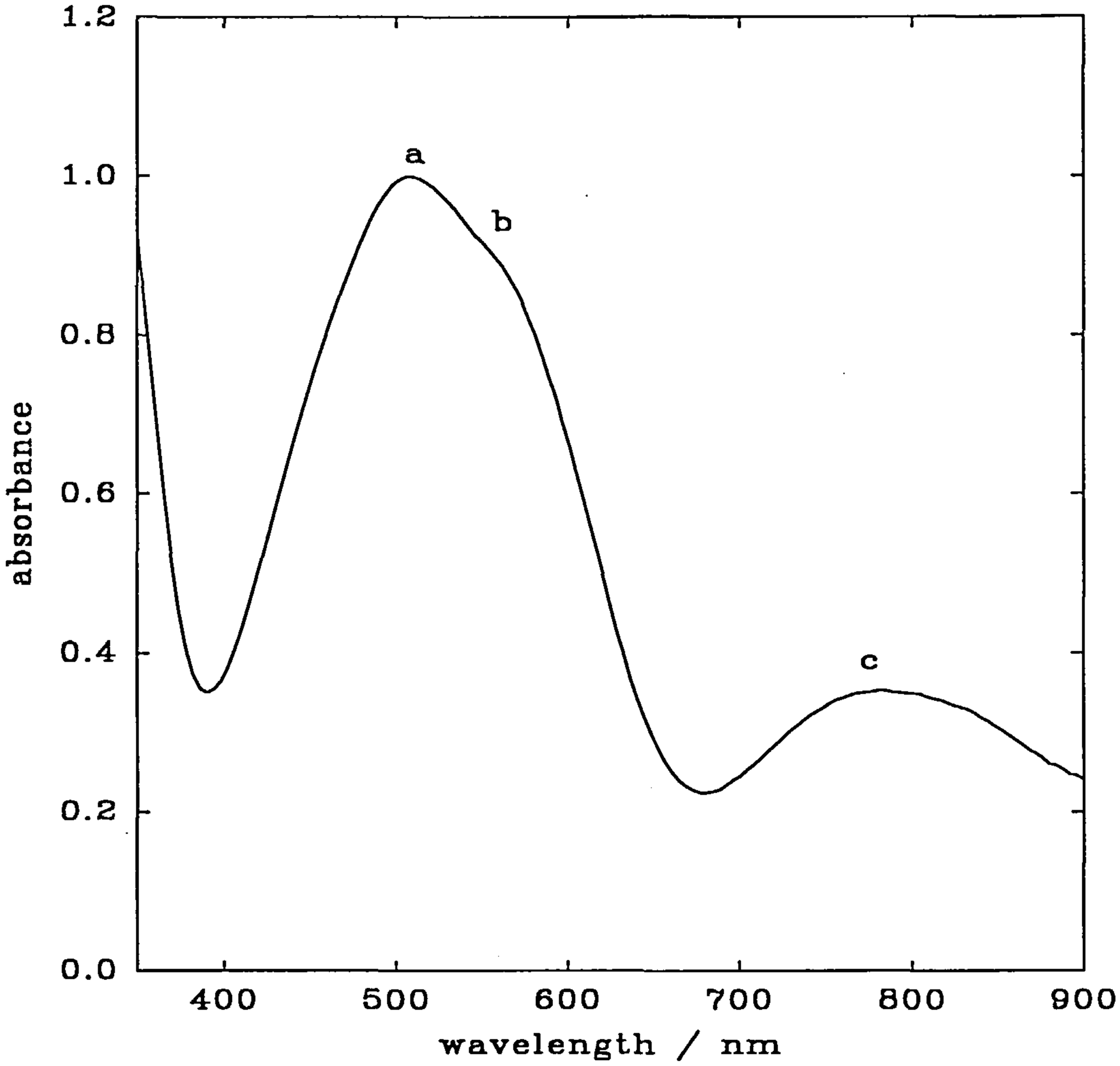

Figure 3.1

The visible spectrum of ferrate (VI) ion recorded between 350 and 900 nm in a 1 mm pathlength optical cell.

An aliquot of the filtered ferrate (VI) solution was placed in a 1 mm pathlength optical cell and the absorbance was recorded between 350 and 900 nm. The absorbance of the

NaClO + NaOH over this range was very low and was subtracted automatically by the spectrometer, the spectrum is shown in figure 3.1.

The spectrum has the three characteristic features reported earlier by Carrington [65, 66] and Ezhov [93, 94] for solutions containing ferrate (VI) ion. A large peak was observed at 505 nm (a) with a small shoulder at 580 nm (b) and a smaller peak at 780 nm (c). A spectrum recorded in 1 M NaOH has an identical form.

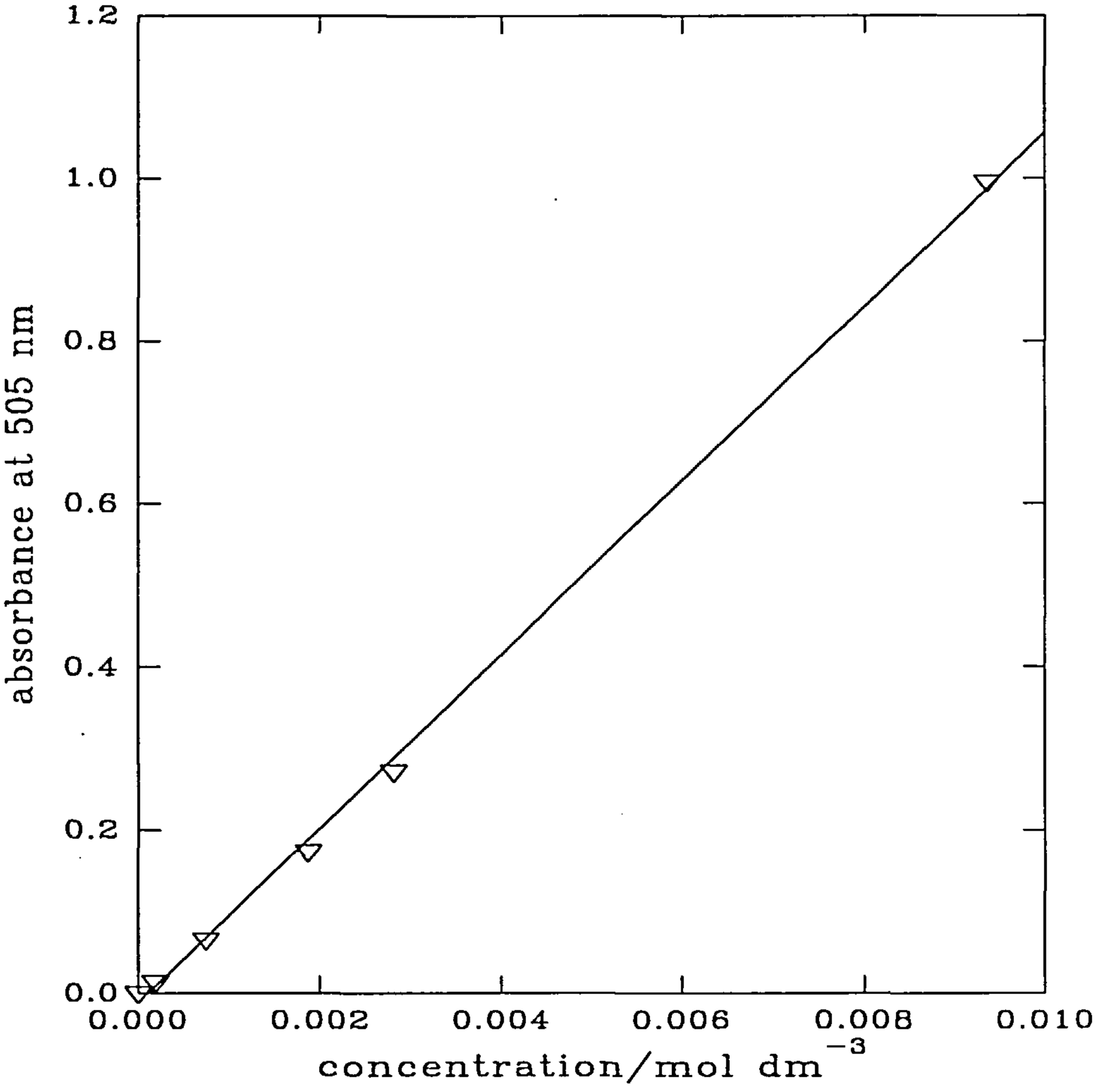

Figure 3.2

Plot of absorbance at 505 nm vs concentration of ferrate (VI) in 10 M NaOH / 14 % NaClO solution.

Known volumes of the solution were removed and diluted with 10 M NaOH. After each dilution an aliquot was removed and the spectrum was recorded between 350

and 900 nm. It was noted that the peak at 505 nm decreased in height with increasing dilution with 10 M NaOH. Figure 3.2 shows a plot of absorbance at 505 nm vs ferrate (VI) concentration. The straight line plot which passes through the origin follows the Beer Lambert law.[132] From the slope of the graph, an extinction coefficient of 1070 ± 5 $dm^3\ mol^{-1}\ cm^{-1}$ was calculated. This value is similar to that reported by Wood [81] and Ezhov [127 128] (1075 $dm^3\ mol^{-1}\ cm^{-1}$).

The intense colour of the ferrate (VI) solutions provides a convenient method to monitor ferrate (VI) concentration in the range 0.2 - 10 mM. The absorbance at 505 nm. can be converted to concentration of ferrate (VI) by using the Beer Lambert calibration plot.

3.3 Stability of ferrate (VI) ion in sodium hydroxide solutions.

The ferrate (VI) ion decomposes according to the equation below:

$$4\ FeO_4^{2-} + 6\ H_2O \rightarrow 3\ O_2 + 8\ OH^- + 4\ FeOOH \qquad (1)$$

Here, FeOOH is a "convenient name" for the Fe (III) precipitate since the exact stoichiometry of the solid is unknown. The product is however an oxide/hydroxide of Fe (III) which is insoluble in 10 M NaOH.

3.3a Effect of temperature.

(I) Decomposition at room temperature.

A solution of approximately 10 mM ferrate (VI), (determined from the calibration plot in figure 3.2), was prepared in 10 M NaOH, in a small glass H cell, (see figure 2.4) by applying 3 V between two iron wool electrodes at room temperature. When the voltage was applied the solution around the anode turned purple as ferrate (VI) was formed along with the evolution of oxygen. The cathode reaction was hydrogen evolution. With increasing time, the colour of the anolyte darkened as more ferrate (VI)

was formed. The concentration of ferrate (VI) was monitored through the absorbance at 505 nm.

The ferrate (VI) was removed from the cell and transferred to a flask. An aliquot was removed and placed in an optical cell thermostatted at 298 K, a visible spectrum was recorded. Any oxygen bubbles present in the optical cell were removed by degassing the solution in an ultrasonic bath for several seconds. The spectrometer was programmed to record the absorbance every 12 hours. The remainder of the sample was placed in a thermostatted water bath at 298 K.

During the course of the experiment, it was discovered that the ferric hydroxide species formed in the decomposition began to deposit on the side of the walls of the cuvette.

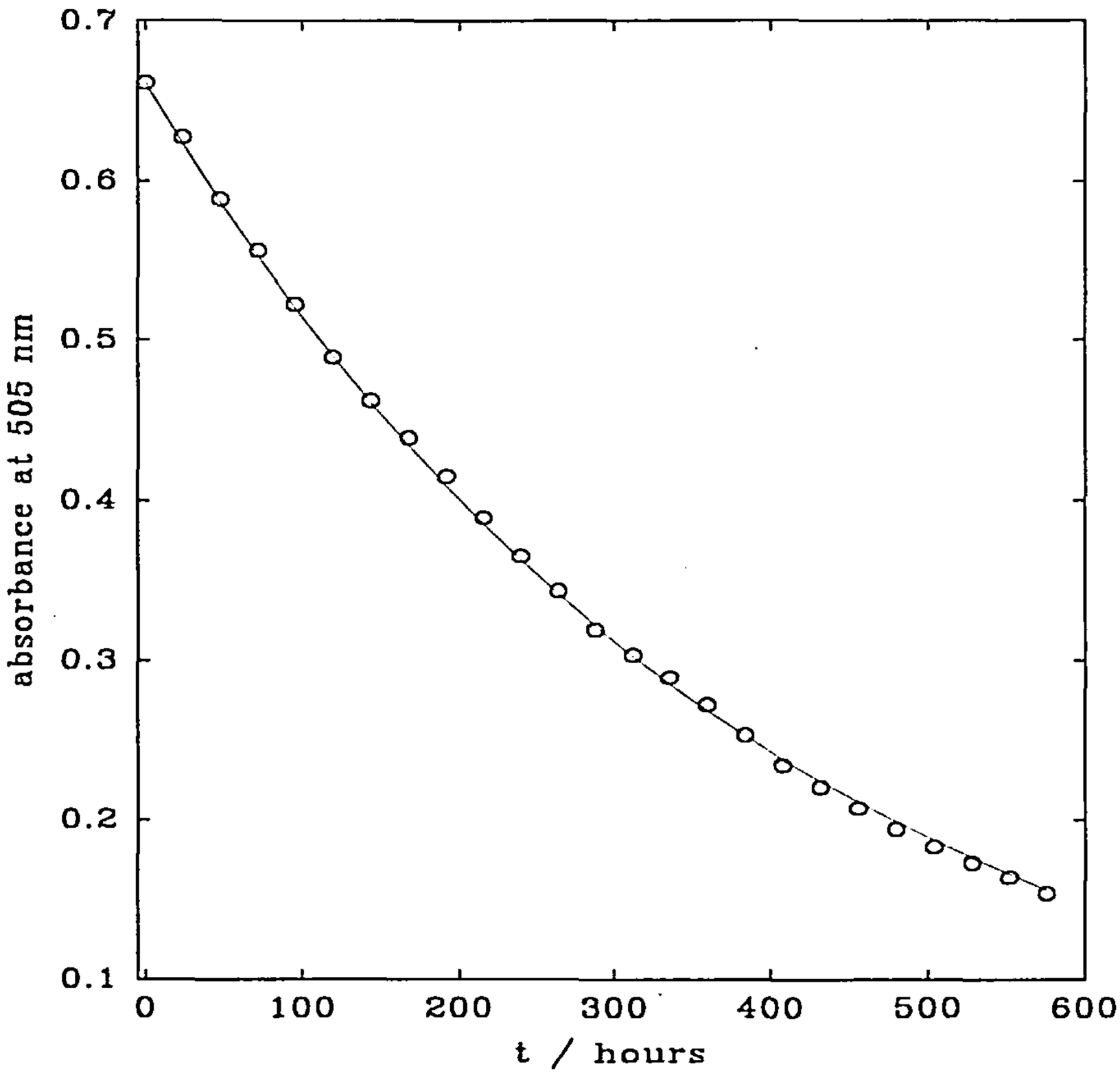

Figure 3.3

Plot of absorbance at 505 nm vs time for a solution of ferrate (VI), initially 10 mM, in 10 M NaOH solution at 298 K.

The removal of the oxide film was achieved by washing with dilute acid solution followed by repeat washing with distilled water. The cuvette was then refilled from the stock solution and replaced in the spectrometer. The absorbance dropped slowly with time (see figure 3.3) in what seemed to be an exponential decay. The data was replotted as ln $[A]_t / [A]_0$ vs time and this is shown in figure 3.4.

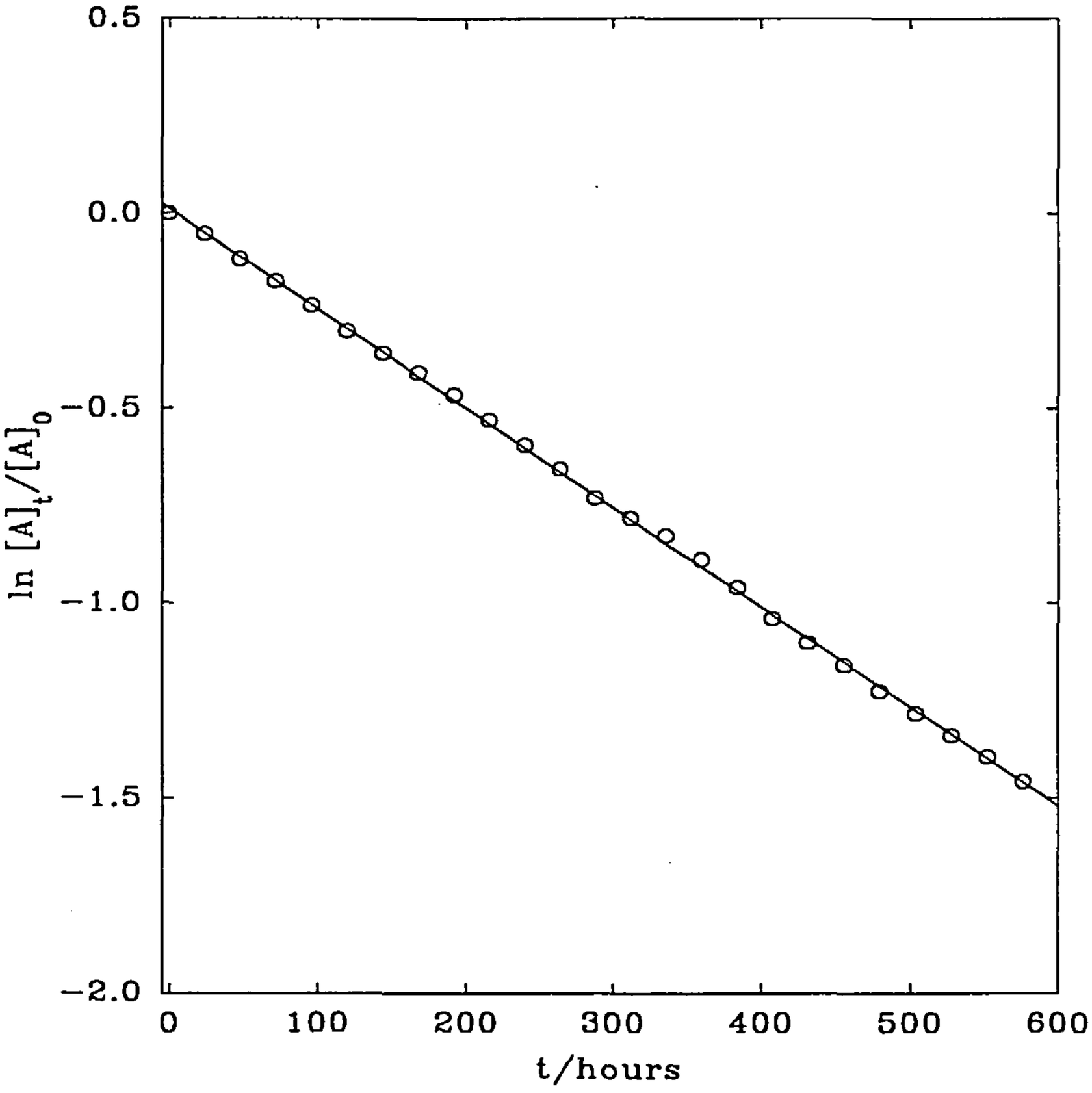

Figure 3.4

Plot of ln $[A]_t / [A]_0$ vs time for a solution of ferrate (VI) initially 10 mM, in aqueous 10 M NaOH solution at 298 K. $[A]_t$ is the absorbance of the solution at 505 nm at time t and $[A]_0$ is the absorbance at time = 0.

The linear plot shows that the decomposition follows first order kinetics and the slope is the rate constant for the reaction (1). The slope was calculated as 7.2×10^{-7} s^{-1}. From the

results it can be seen that ferrate (VI) decomposes very slowly in aqueous 10 M NaOH at 298 K with a half life of 280 hours. The decomposition is first order with respect to ferrate (VI) with a rate constant for the reaction of 7.2×10^{-7} s^{-1}.

(II) Decomposition at elevated temperatures.

A solution of ferrate (VI), approximately 10 mM, in 10 M NaOH was prepared by electrolysis at room temperature. The ferrate (VI) solution was removed from the cell and placed in a flask thermostatted at 333 K. Periodically an aliquot was removed, placed in an optical cell and the spectrum recorded.

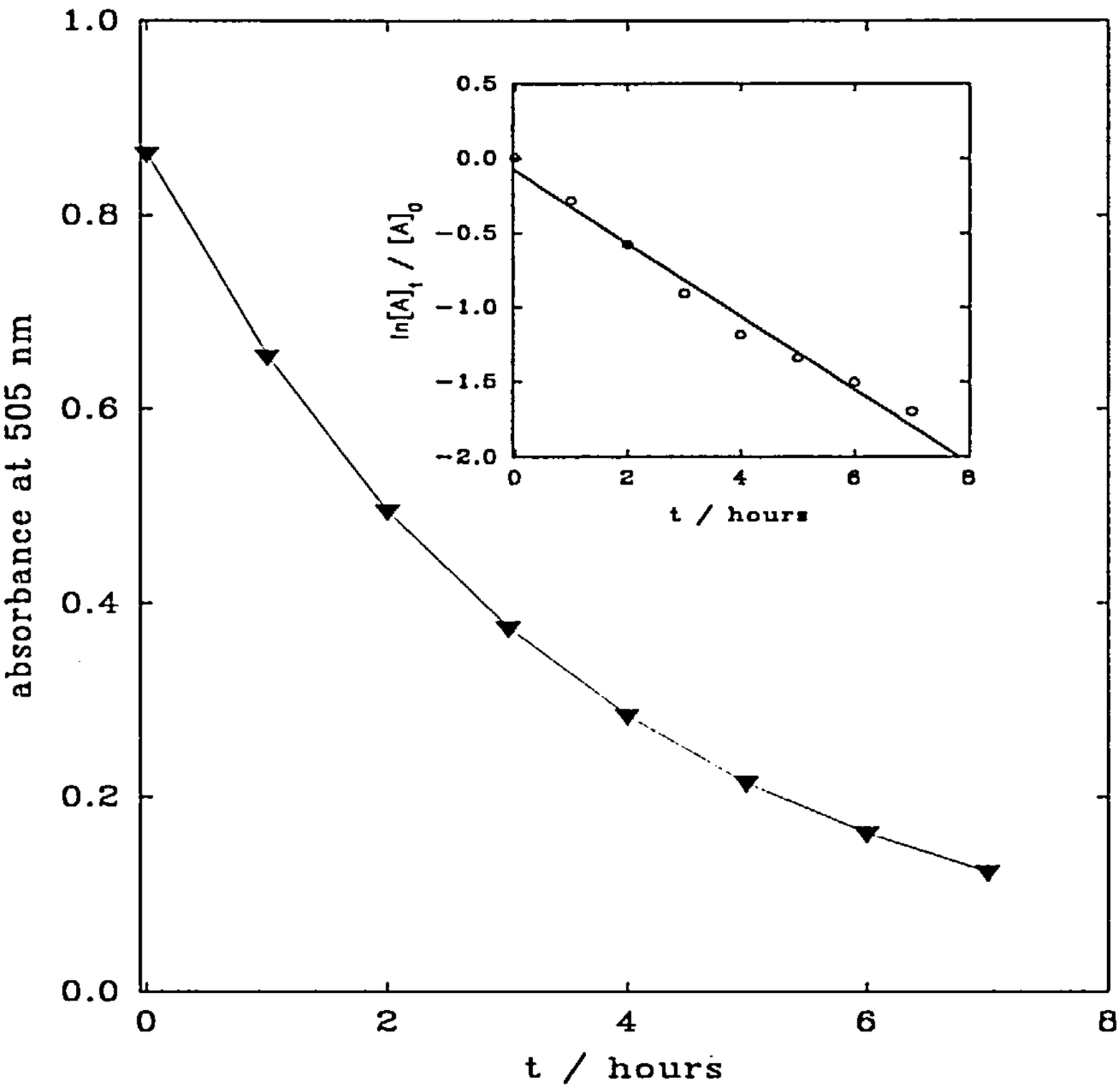

Figure 3.5

Plot of absorbance vs time for a solution of ferrate (VI) initially 10 mM, in aqueous 10 M NaOH solution at 333 K. The inset shows a plot of ln $[A]_t$ / $[A]_0$ vs time for the data shown in the main figure. $[A]_t$ is the absorbance of the solution at 505 nm at time t and $[A]_0$ is the absorbance at t = 0.

When the ferrate (VI) solution in the cuvette was returned to the thermostatted flask the optical cell was cleaned with dilute acid and water. This process was repeated every hour.

Figure 3.5 shows there is a relatively rapid drop in absorbance at 505 nm at 333 K. The shape of the curve is similar to that shown in figure 3.3. A plot of ln $[A]_t/[A]_0$ vs time gave a straight line with a slope of 6.8×10^{-5} s^{-1}. These results show that the decomposition of ferrate (VI) is almost 1000 times faster, (the half life of the ferrate (VI) being 2.5 hours), at 333 K than at 298 K. At 333 K, also, it can be seen from the plots that the decomposition reaction still follows first order kinetics but, with a rate constant of 6.8×10^{-5} s^{-1}.

The experiment was repeated at 323 and 313 K. The data collected from the experiments was treated in the same manner as the 298 and 333 K experiments and is shown in table 3.1.

Temperature, T / K	Rate constant k / s^{-1}	Log_{10} k	1/T K^{-1}
298	7.2×10^{-7}	-6.14	3.37×10^{-3}
313	6.14×10^{-6}	-5.12	3.19×10^{-3}
323	1.30×10^{-5}	-4.89	3.10×10^{-3}
333	6.80×10^{-5}	-4.16	3.00×10^{-3}

Table 3.1

Data collected from the plots of ln $[A]_t / [A]_0$ vs time for the decomposition of ferrate (VI) at 298, 313, 323, 333 K in aqueous 10 M NaOH solution.

At all temperatures the decomposition was found to follow first order kinetics with the rate constant for the decomposition reaction increasing with increasing temperature. A plot of log_{10} k vs 1/T was constructed (see figure 3.6). From this Arrhenius plot an energy of activation for the decomposition of ferrate (VI) in aqueous 10 M NaOH of 99 kJ mol^{-1} was obtained from the slope.

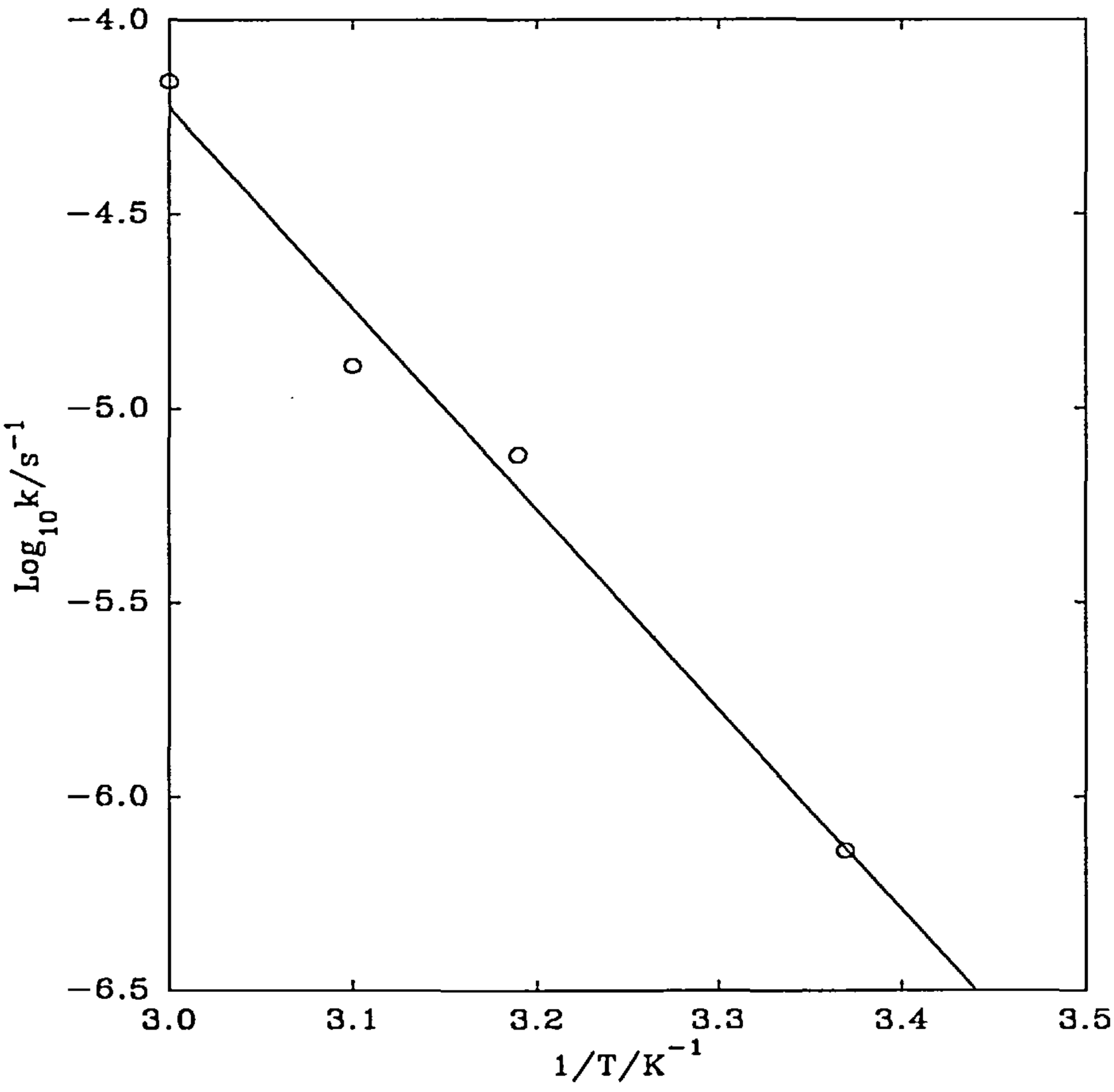

Figure 3.6

An Arrhenius plot of the rate constant for the ferrate (VI) water reaction (taken from the slopes of ln $[A]_t / [A]_0$ vs time plots) as a function of temperature.

Ferrate (VI) ion is very stable in 10 M NaOH solution at room temperature with a half life for the decomposition reaction, of approximately one month. The reaction follows first order kinetics, suggesting that ferrate (VI) could be generated electrochemically without significant decomposition. As the temperature increases the rate of decomposition also increases, although it still follows first order kinetics. In order to prepare ferrate (VI) at temperatures significantly above room temperature the product must be to removed continually from the electrolyte.

3.3b Decreasing the NaOH concentration.

A ferrate (VI) solution, approximately 10 mM, in 10 M NaOH was prepared by electrolysis at room temperature. A 1 cm^3 portion of the ferrate (VI) solution was removed and placed in a flask thermostatted at 273 K. The ferrate (VI) solution was diluted by a factor of 10 with water at 273 K. The resulting solution was mixed for 30 seconds. An aliquot was transferred to an optical cell and placed in the spectrometer. The absorbance was recorded every 30 seconds between 350 and 900 nm.

The ferrate (VI) in solution had completely disappeared after 7 minutes. There was a colour change in the solution from purple to colourless to cloudy yellow. The change in the spectrum of the ferrate (VI) solution as a function of time is shown in figure 3.7.

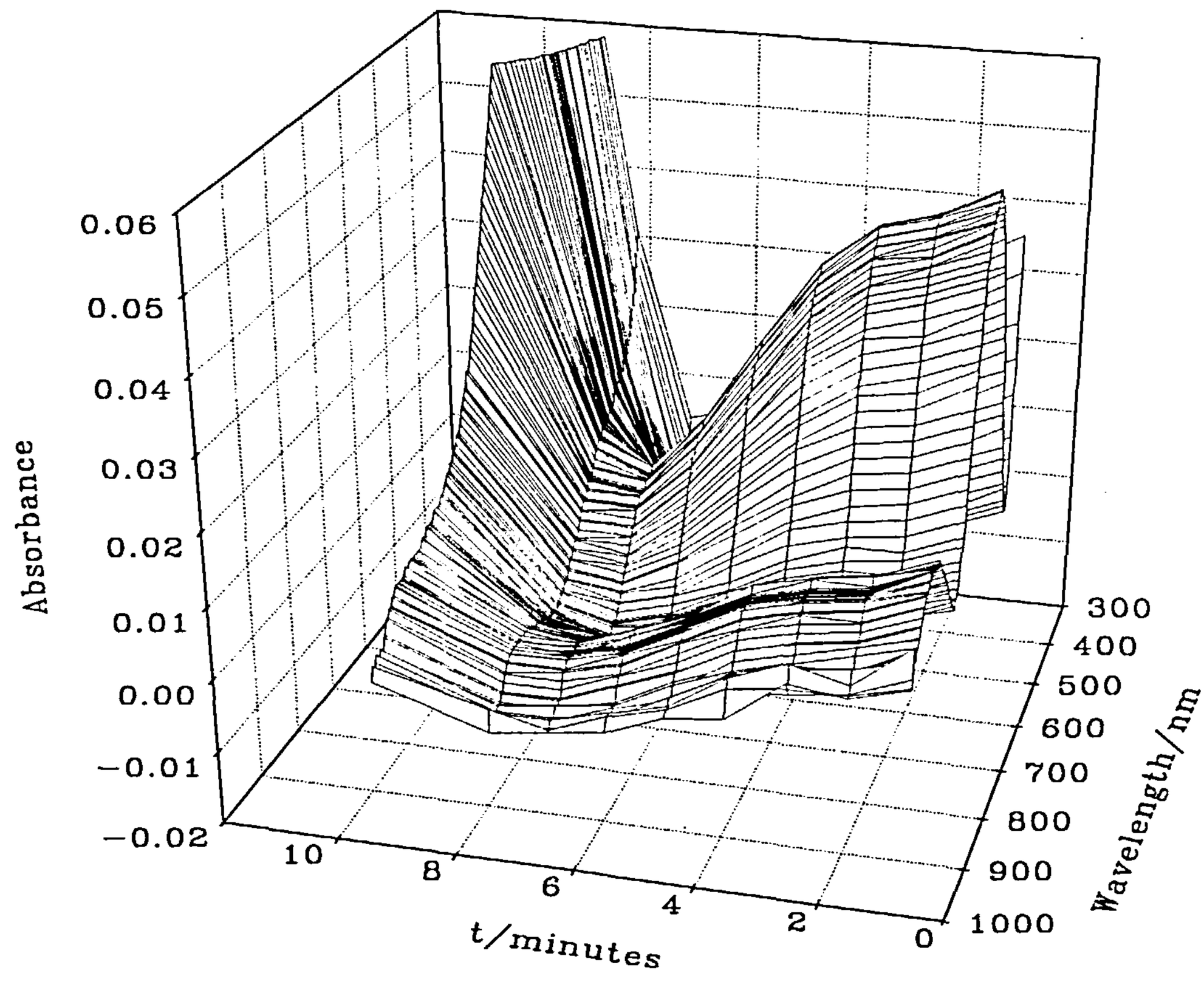

Figure 3.7

Spectra of a solution initially 1 mM ferrate (VI) in 1 M aqueous NaOH solution at 298K as a function of time.

The initial spectrum recorded after 30 seconds showed the same features as the ferrate (VI) in 10 M NaOH which is shown in figure 3.1. Figure 3.7 shows that, (a) there is a decrease in the absorbance at 505 nm with time and (b) some species is being formed with a strong absorbance in the u.v and as this species builds up, then the spectrum begins to tail into the visible region.

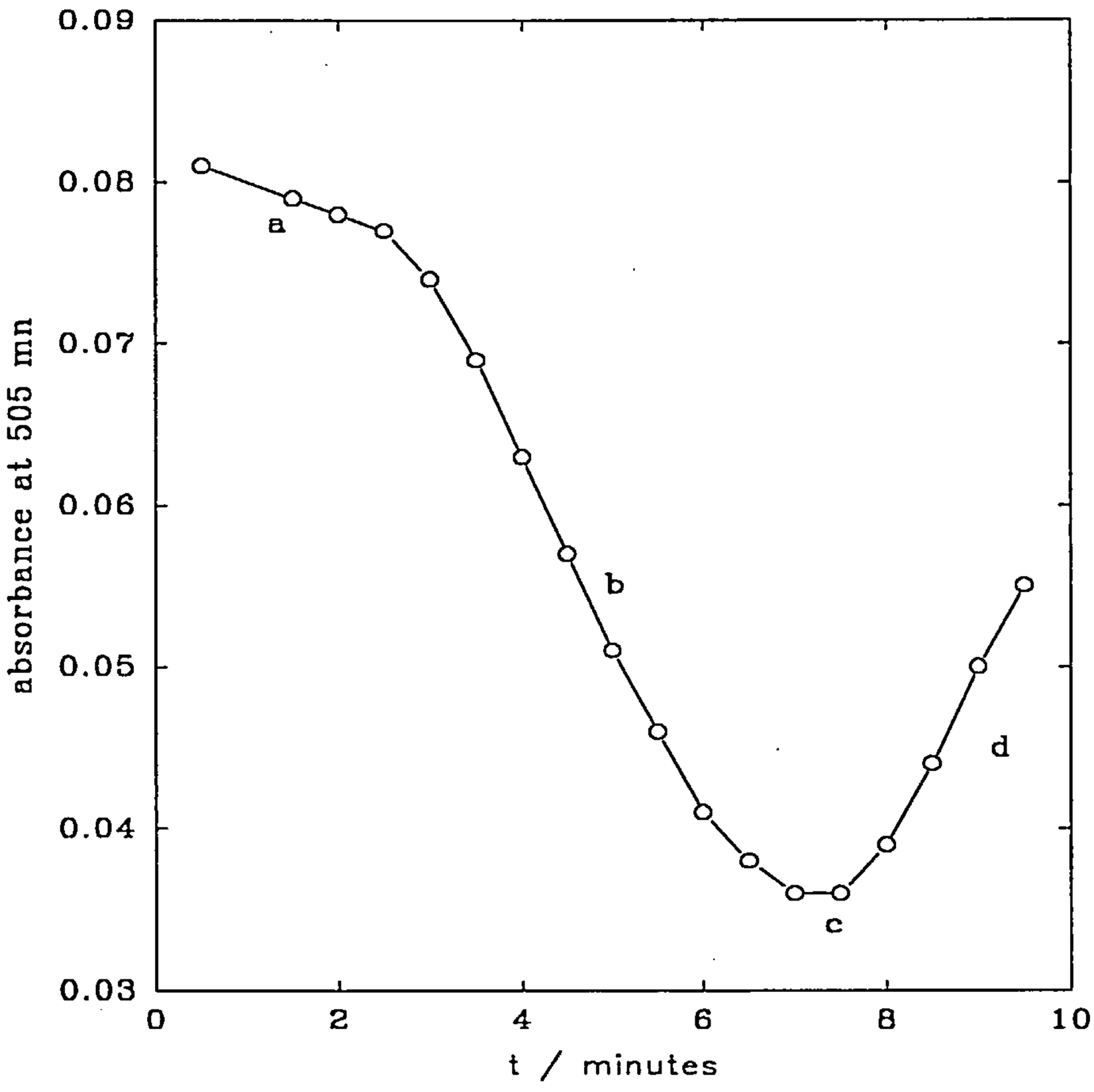

Figure 3.8

Plot of absorbance at 505 nm vs time for a ferrate (VI) solution 1 mM, in 1 M aqueous NaOH solution at 298 K.

When compared to the absorbance vs time plot recorded in 10 M NaOH it can be seen that figure 3.8 has several different features. The decrease in the absorbance is very fast, occurring over a period of a few minutes. The plot in figure 3.8 has 4 distinct regions:

(a) In the first 2 minutes there is a slow linear decrease in the absorbance at 505 nm. The solution showed no visible colour changes.

(b) There is a marked increase in the slope of the line indicating an increased rate of ferrate (VI) decomposition. There is also a rapid decrease in the intensity of the purple coloured solution in this region of time along with a considerable amount of gas bubbles dispersed throughout the solution.

(c) The solution is colourless for a few seconds.

(d) The absorbance begins to increase as the solution turns from a transparent yellow to a deeper and cloudy yellow colour.

Figure 3.7 shows more clearly that that the rise in the absorbance at 505 nm is due to the formation of a species that absorbs strongly in the u.v. region. As more of this species is formed, the absorbance increases, tailing into the visible region forcing the absorbance to increase.

The yellow colour may be due to the formation of a ferric oxide/hydroxide. Initially these particles would be very small, but then they coalesce giving the yellow colour to the solution. It should be noted that this was not the same as the solid product obtained in the 10 M NaOH reactions which was much coarser and darker brown in colour. The shape of the absorbance time curve also shows that there is clearly a change in mechanism occurring leading to an increase in the rate of decomposition of ferrate (VI) with time in 1 M NaOH. This change could be from a homogeneous reaction to a surface catalysed reaction. The shape of the curve indeed suggests that the reaction is autocatalytic. It would seem that in region (a) the ferrate (VI) reacts with the water slowly producing a small amount of ferric oxide/hydroxide. These small particles become involved in the reaction causing the rate of the reaction to be enhanced (region (b)) thus producing more ferric oxide/hydroxide. When all the ferrate (VI) has decomposed the solution appears colourless, region (c). As the ferric oxide/hydroxide in the solution coagulates the particles increase in size. This imparts a yellow colour to the solution which causes the absorbance to increase again.

A few experiments were carried out by dissolving solid sodium ferrate (VI) in water. Initially, the ferrate (VI) appeared to be stable as a neutral solution but, again, once a small amount of Ferric oxide/hydroxide was formed, decomposition suddenly

became rapid. The "initial" time during which the ferrate (VI) seemed to be stable was variable but it is clear that the oxidation of many organic compounds should be possible in these conditions.

3.4 Reactions with organic compounds.

The results from the previous set of experiments showed that ferrate (VI) is stable for many days in 10 M NaOH solution at room temperature. It also seems that the oxide/hydroxide formed in 10 M NaOH solutions does not have a significant contribution in the decomposition reaction. It was concluded that the reaction of ferrate (VI) with organic compounds in 10 M NaOH could be monitored through the absorbance at 505 nm.

3.4a Reaction of ferrate (VI) with concentrated organic solutions in 10 M NaOH.

(I) Reaction with ethanol.

A solution of ferrate (VI), 10 mM, was prepared electrochemically in 10 M NaOH at room temperature. A solution of 0.2 M ethanol was prepared in 10 M NaOH and placed in a thermostat at 273 K with the ferrate (VI) solution. A portion of the ferrate (VI) solution, 5 cm^3, was removed and transferred to another flask where it was mixed for 30 seconds with 5 cm^3 of the ethanol solution. An aliquot was removed and placed in an optical cell and the absorbance at 505 nm was measured at 10 second intervals. A blank solution containing no ethanol was run to compare the results.

For the solution containing ethanol there was a rapid decrease in the purple colour, coupled to the formation of a brown deposit. This deposit remained in solution as well as on the walls of the glass cuvette. No change in colour was observed for the ethanol free solution. Figure 3.9 shows the change in absorbance for the two solutions.

Curve (b) shows that the decrease in the absorbance occurs at a very fast rate for the first 150 seconds of the reaction. The absorbance, then begins to rise again probably, due to oxide forming as a brown deposit on the walls of the cuvette and flask, and flakes of the brown solid are observed in solution. Curve (a) shows that for the solution

containing no ethanol that there is no decrease in the absorbance during the time period of the reaction. Clearly, ethanol is being oxidised rapidly by the ferrate (VI).

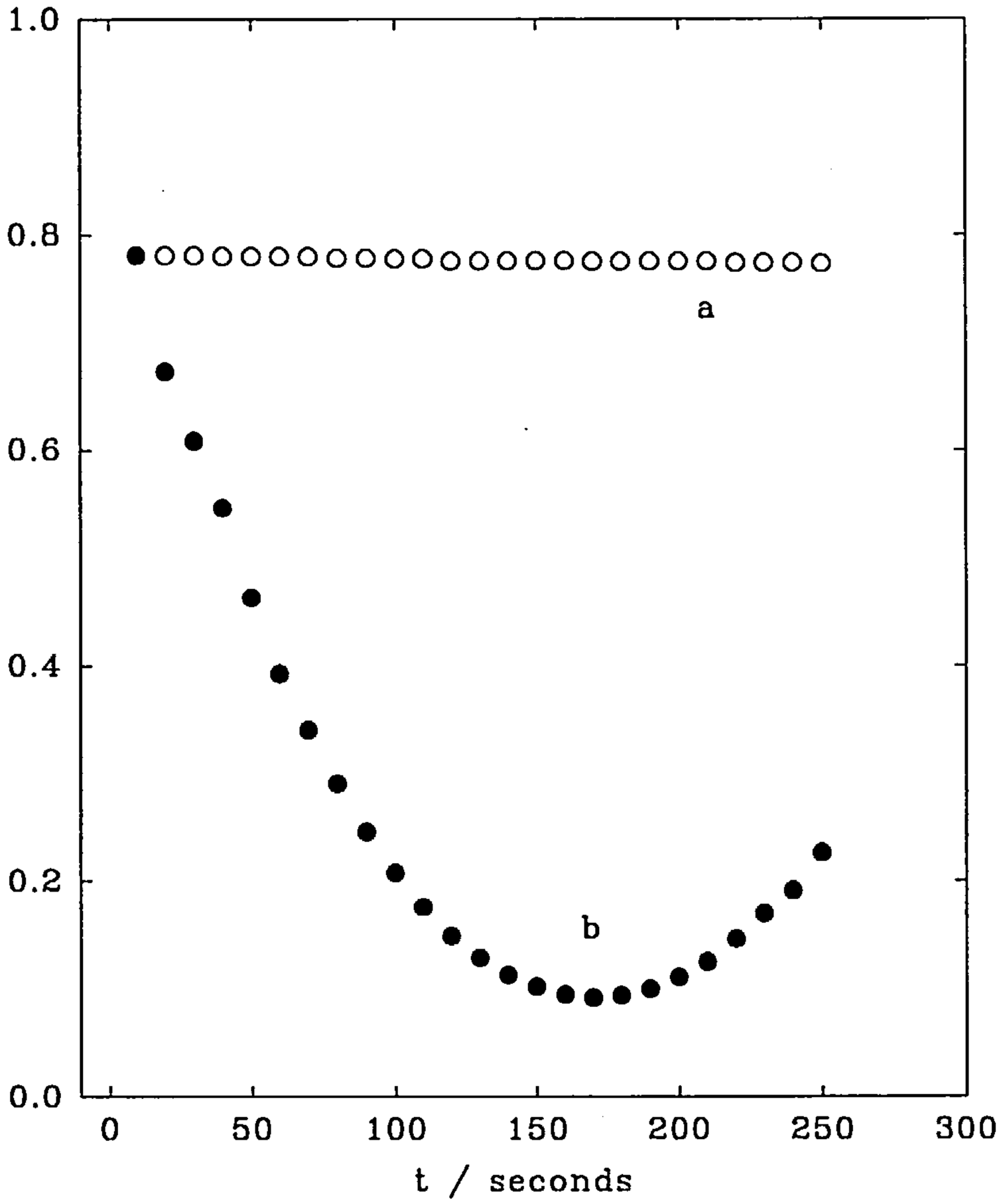

Figure 3.9

Plot of absorbance vs time for the reaction of ferrate (VI) (≈ 4 mM) in 10 M NaOH.

a) ○ Reaction with water,

b) ● reaction with 0.1 M ethanol.

(II) Reactions with other alcohols.

The experiment was repeated with the different alcohols listed in table 3.2. In all cases, the plots of absorbance at 505 nm vs time had the same form as the plot for the reaction with ethanol. The absorbance decreased rapidly, with all the purple colour disappearing from the solution within a few minutes.

Alcohol	[Alcohol] / mM	$[FeO_4^{-2}]$ / mM	Reaction time / s
CH_3OH	100	4.6	130
C_2H_5OH	100	4.3	150
C_3H_7OH	100	4.4	160
$C_2H_5CH(OH)CH_3$	100	4.7	180
$C_2H_5C(OH)(CH_3)_2$	100	4.5	180
$(CH_2OH)_2$	100	4.6	105
C_6H_5OH	100	4.3	160

Table 3.2

Data collected from the absorbance vs time plots for the reaction of ferrate (VI) with concentrated alcohol solutions in 10 M NaOH. The reaction time was the time required to remove all ferrate (VI) from solution.

As with the ethanol reaction, when the reaction was completed the solution became colourless and there was also brown solid on the side of the glass and in solution. Due to the fact that there was no ferrate (VI) left in the solution at the end of the reactions and, diluting the ferrate (VI) with 10 M NaOH did not result in decomposition, then it must be assumed that the ferrate (VI) is only reacting with the alcohols. The reaction of ferrate (VI) with alcohols has been well documented in the literature [73, 74] and it is most probable that all the ferrate (VI) is being consumed in the oxidation of the alcohols to either the corresponding ketone or acid. In order to see if there is further oxidation of the alcohols occurring, it would be necessary to have an excess of ferrate (VI) in solution.

3.4b Reactions of ferrate (VI) with dilute alcohol solutions in 10 M NaOH.

(I) Aliphatic alcohols.

A solution of ethanol, 1 mM, was prepared in 10 M NaOH. A 5 cm^3 portion was removed and placed in a flask thermostatted at 273 K. A ferrate (VI) solution, 15 mM, in 10 M NaOH was prepared electrochemically in a flow cell, (see chapter 4). The ferrate (VI) solution was transferred to a flask and 5 cm^3 removed and thermostatted at 273 K. The ethanol and ferrate (VI) solutions were mixed and the spectrum recorded between 350 and 900 nm, after which the solution returned to the flask, (which had been removed from the ice bath). Periodically, an aliquot was removed and the spectrum was recorded.

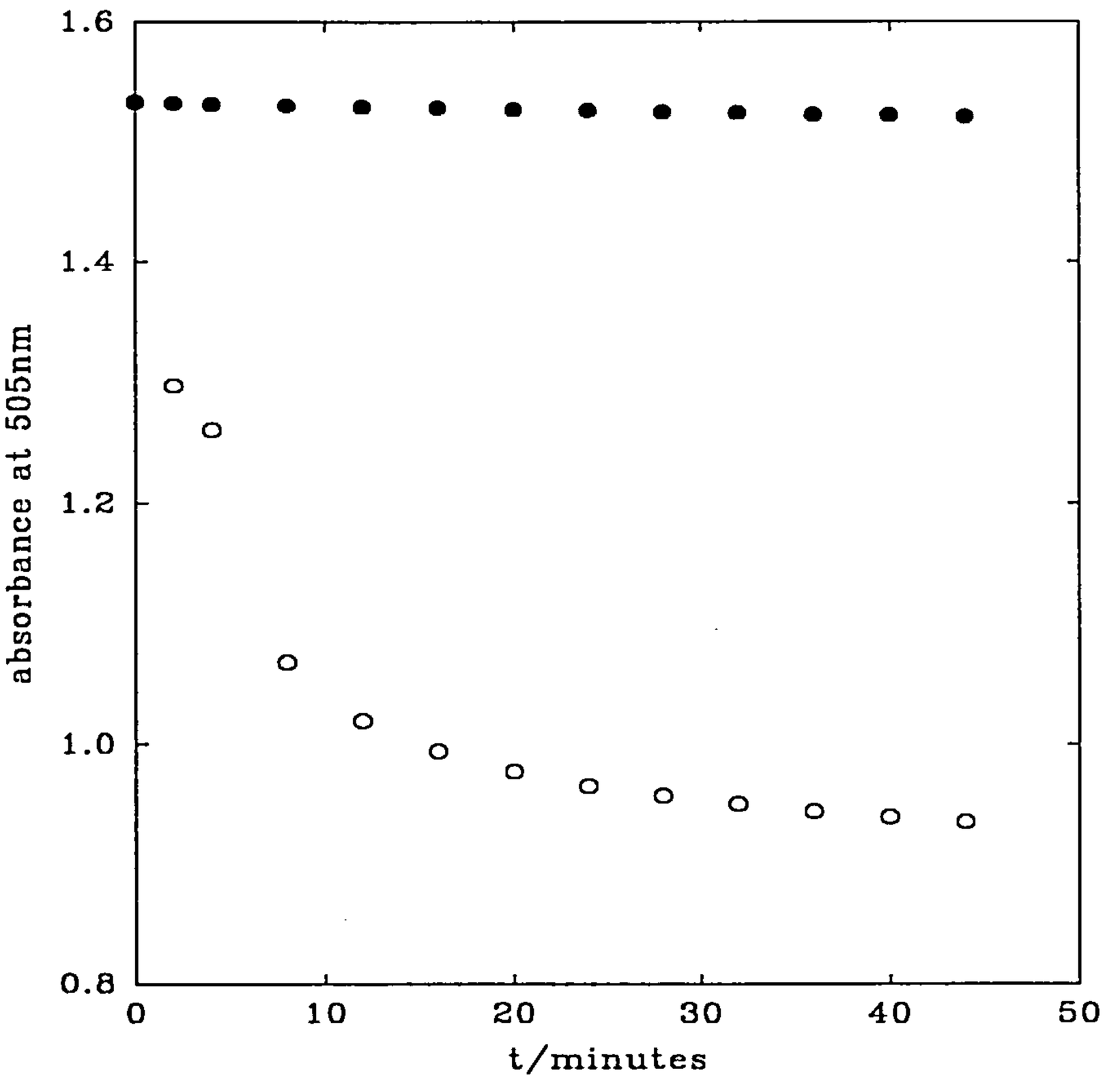

Figure 3.10

Plots of absorbance at 505 nm vs time for the reaction between

O *ferrate (VI), 7.2 mM and ethanol, 0.5 mM in 10 M NaOH*

● *and ferrate (VI), 7.2 mM, 10 M NaOH and water.*

During the first 10 to 20 minutes of the reaction the purple colour of the solution faded slightly and some gas evolution was observed in the solution. However, after 20 minutes there was no further change in the colour of the solution. There was no brown solid in the flask. Figure 3.10 shows the change in the absorbance at 505 nm vs time for the reaction. Over the first 20 minutes the absorbance dropped rapidly, but not as quickly as when the solution contained a high concentration of ethanol. After 20 minutes, the rate of change decreased and an almost constant value for the absorbance was achieved. Thereafter the rate at which the absorbance changes was similar to that observed for the reaction of ferrate (VI) and water. From the absorbance, the concentration of ferrate (VI) at the beginning of the reaction was determined as 7.2 mM. At the end of the reaction the concentration of ferrate (VI) was 5.7 mM. Therefore 1.5 mM of ferrate had reacted with the ethanol.

For complete oxidation of ethanol 12 electrons are required:

$$C_2H_5OH + 12\ OH^- - 12\ e^- \rightarrow 2CO_2 + 9\ H_2O$$

As 1.5 mM of ferrate (VI), equivalent to 4.5 mM of electrons, reacted with 0.5 mM of ethanol then 9 electrons per molecule of ethanol were used in the reaction.

The experiment was repeated with other aliphatic alcohols listed in table 3.2. In all the cases there was an initial decrease in the intensity of the solutions colour in the first 10 to 30 minutes of the reaction. For the higher alcohols the absorbance began to rise slightly as some brown solid was formed. This had to be filtered out before the next spectrum could be recorded. An example is shown in figure 3.11 which shows the absorbance time plot for the reaction between ferrate (VI) and butan-2-ol. For the smaller alcohols the absorbance decreased slowly until it occurred at the same rate as that observed for the reaction of ferrate (VI) and water.

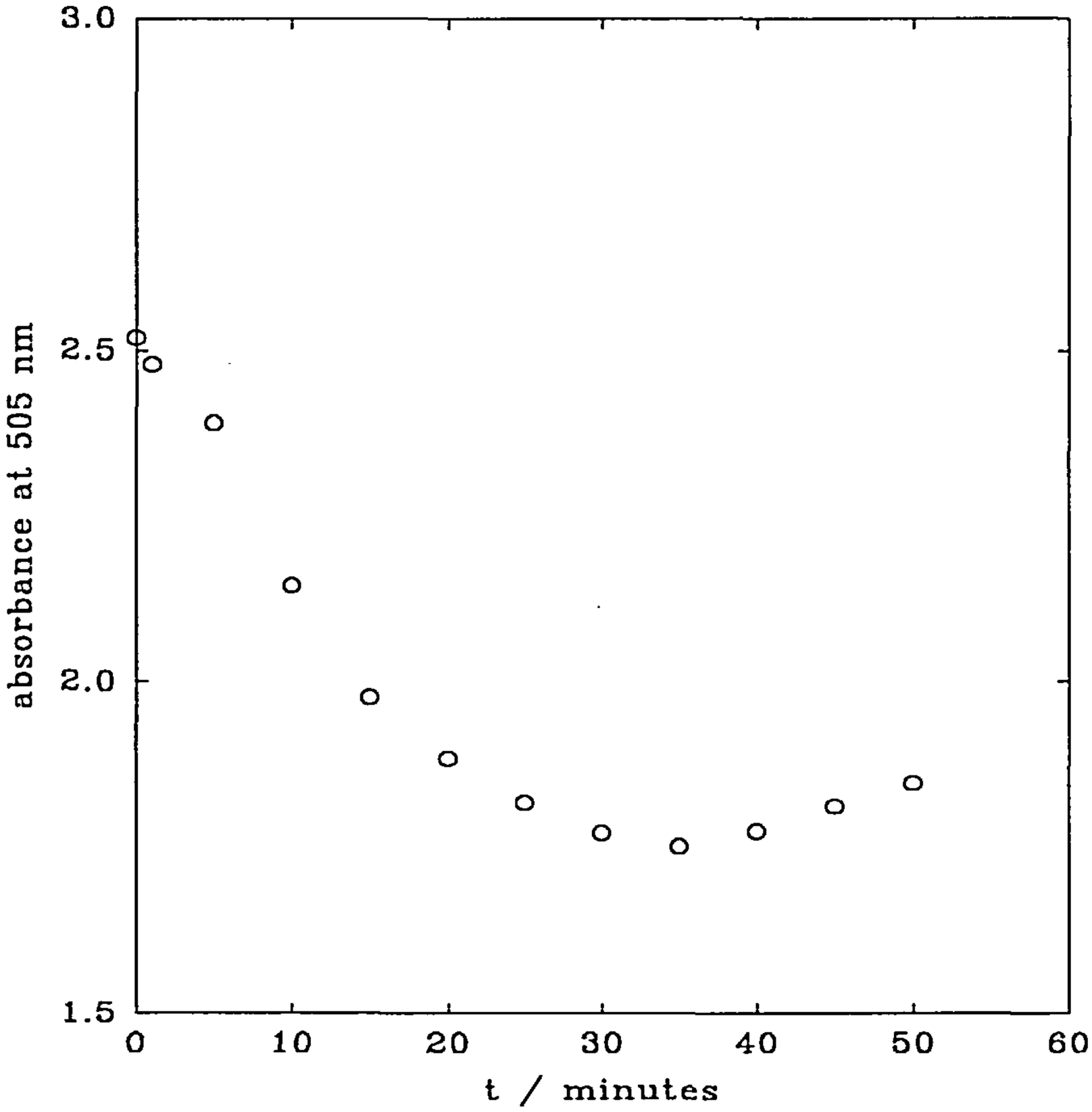

Figure 3.11

Plot of absorbance at 505 nm vs time for the reaction of ferrate (VI), 10.2 mM and butan-2-ol, 0.5 mM in 10 M NaOH solution at 298 K.

The brown precipitate that was filtered off was a ferric oxide/hydroxide. The formation of this species in solution had resulted in the increase in the absorbance. At the end of the reaction between the butan-2-ol, the amount of ferrate (VI) that had reacted was calculated as 2.9 mM, which equated to 14 electrons pre molecule of butan-2-ol. In order to fully oxidise butan-2-ol 24 electrons are required. This suggests that the butan-2-ol was only partially oxidised and the resulting molecules could not be oxidised further or, perhaps more likely some of the alcohol was absorbed on the surface of the precipitate and was removed by filtration.

Table 3.3 shows a summary of the alcohols studied in the experiments.

Alcohol	[Alcohol] / mM	[Ferrate (VI)] initial / mM	[Ferrate (VI)] final / mM	No. electrons experimental	No. electrons for complete oxidation	reaction time scale for 50 % conversion
CH_3OH	0.5	11.5	10.5	6	6	180
	1.0	11.5	9.6	6	6	420
C_2H_5OH	0.5	7.2	5.7	9	12	360
C_3H_7OH	0.5	8.3	6.3	12	18	900
$C_2H5CH(OH)CH_3$	0.5	10.2	7.3	14	24	1245
$C_2H_5C(OH)(CH_3)_2$	0.5	9.7	8.0	10	30	1560
$(CH_2OH)_2$	0.5	11.3	9.7	10	10	720

Table 3.3

Summary of results for the reaction of dilute solutions containing aliphatic alcohols in 10 M NaOH with ferrate (VI).assumingFe (VI) → Fe(III)

It can be seen that both methanol and ethandiol were completely oxidised by the ferrate (VI). There was significant reaction between the ferrate (VI) and the higher alcohols. However, these alcohols did not appear to be completely oxidised. Again the low n values may be due to the adsorption onto the precipitate. It was also found that there was a tendency for the n value to decrease with increasing alcohol concentration. For example, in the reaction between butan-2-ol, (1 mM) and 10 mM ferrate (VI) solution the number of electrons used in the oxidation was reduced to 10. This may also be a result of adsorption of the alcohol on the iron oxide/hydroxide. The rates of reaction are compared by reporting the time for 50 % oxidation of the alochols in dilute solution. Reaction of ferrate (VI) is faster for the straight chained alcohols, but it decreased as the number of carbons in the backbone of the alcohol increased. It can also be seen that secondary and tertiary alcohols react at a slower rate than the primary alcohols.

(II) Reaction of ferrate (VI) with phenol.

A solution of phenol, 1 mM, was prepared in 10 M NaOH. A 5 cm^3 portion was removed, placed in a flash which was thermostatted at 273 K. A ferrate (VI) solution, (22 mM in 10 M NaOH), was prepared electrochemically in a flow cell; 5 cm^3 was removed and thermostatted at 273 K. The phenol and ferrate (VI) solutions were mixed and the spectrum was recorded between 350 and 900 nm every 2 minutes. The optical cell was cleaned before each spectrum was recorded.

The intensity of the purple coloured reaction mixture lessened in the first 40 minutes. Then began to rise as the dark brown ferric oxide/hydroxide formed in the solution. However, removing the ferric oxide/hydroxide before each measurement showed that the absorbance was still decreasing with time. The reaction continued for several hours before it reached a steady state value.

Figure 3.12 shows the decrease in the absorbance at 505 nm vs time for the reaction of ferrate (VI), 11 mM, and phenol 0.5 mM. Again the absorbance fell for the first 40 minutes before starting to increase. This increase was due to the formation of a Fe_2O_3/FeOOH precipitate and its removal, by filtration, prior to the absorbance measurements made showed that the colour of the solution was still fading over a period of at least 24 hours. After 24 hours the absorbance is 1.1. Compared to the reaction of

ferrate (VI) with the 0.5 mM ethanol solution, the difference between the initial and final absorbance values for the phenol solution is larger and the reaction period is longer. This indicates that the extent of reaction occurring between the ferrate (VI) and phenol is greater than the reaction with the ethanol. Removal of the ferric oxide/hydroxide showed that the decrease in the absorbance was still occurring at a rapid rate and it was only after 24 hours that the decrease in the absorbance reached a rate which was comparable to the ferrate (VI) water reaction. The initial ferrate (VI) concentration was 11.0 mM and the final concentration was 5.3 mM. This meant that 5.7 mM of ferrate (VI) had reacted with the 0.5 phenol.

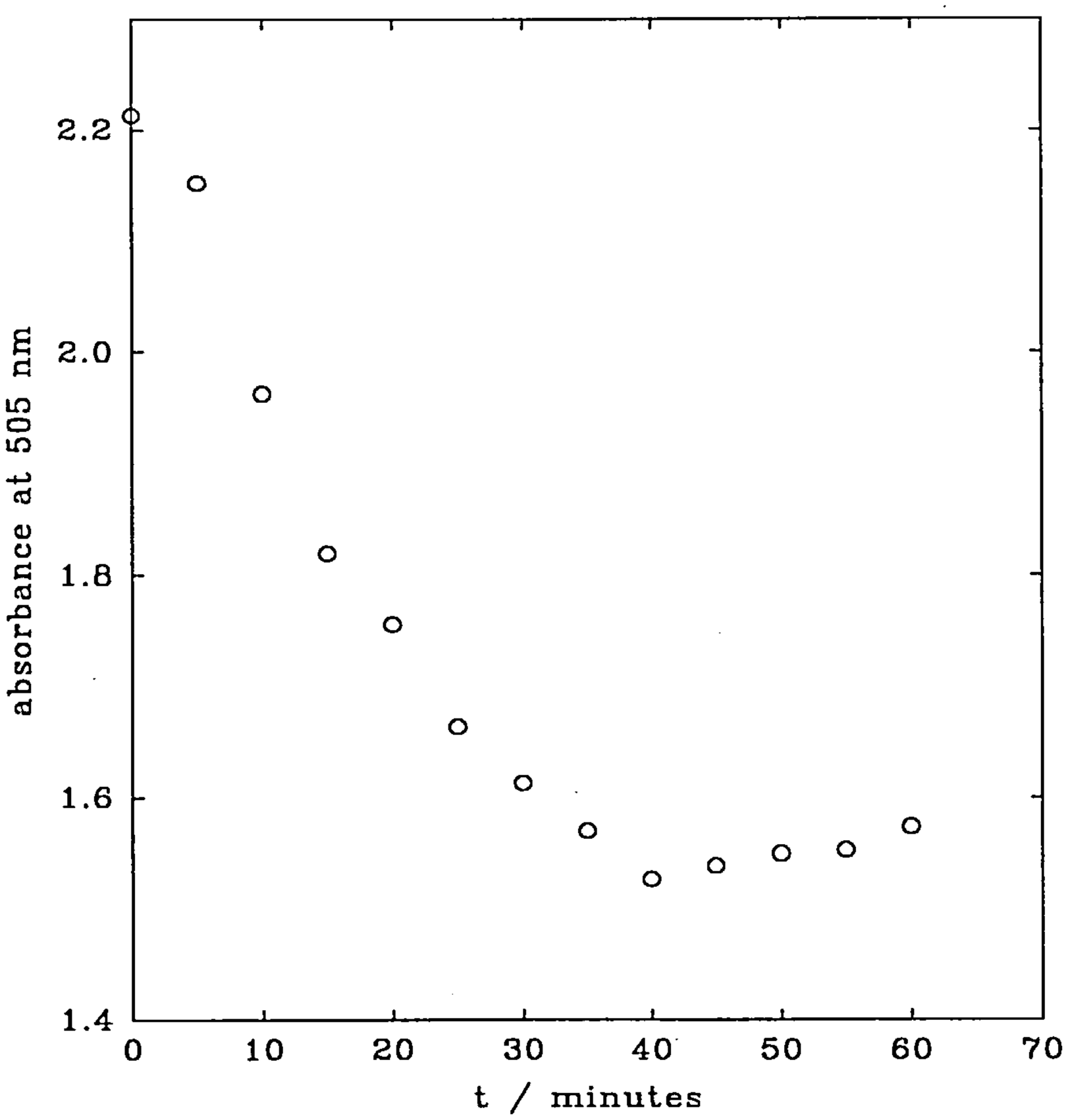

Figure 3.12

Plot of absorbance at 505 nm vs time for the reaction of ferrate (VI), 11 mM, in 10 M NaOH solution and phenol, 0.5 mM, in 10 M NaOH solution.

The ferric oxide/hydroxide formed in the reaction was the same as that described for the butan-2-ol experiment. It was dark brown in colour and had a flaky appearance. Figure 3.13 shows a three dimensional plot for the reaction of ferrate (VI), 11 mM, with phenol, 0.5 mM, in 10 M NaOH solution.

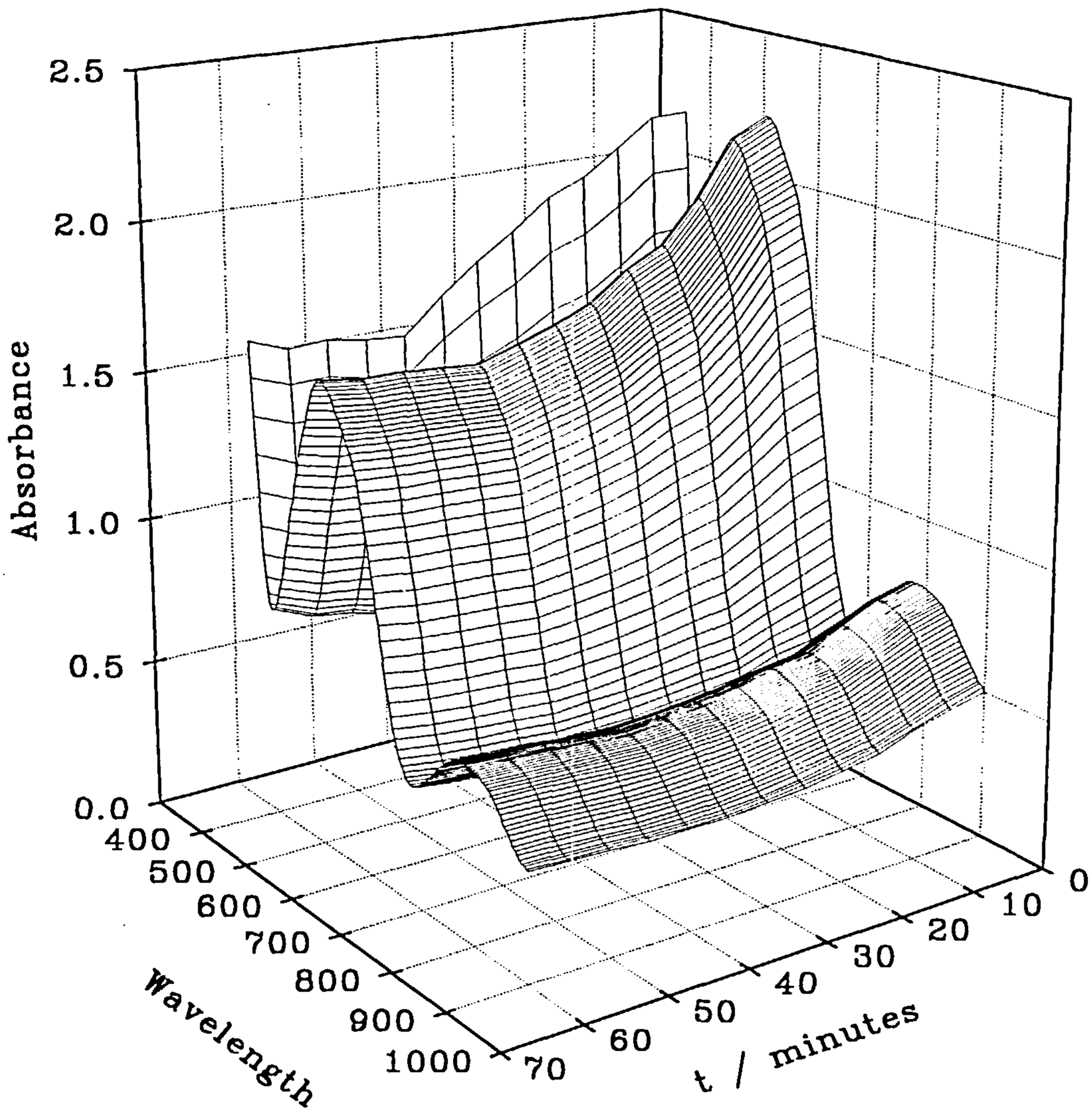

Figure 3.13

A three dimensional plot showing the change in the spectrum of ferrate (VI), 11 mM, as it reacts with phenol, 0.5 mM, in 10 M NaOH solution.

The plot shows that the main features of the ferrate (VI) spectrum, shown in figure 3.1, remain unchanged as the reaction proceeds. It is interesting to note also that the rise in the absorbance is not due to the formation of a species with that has strong

absorbance in the u.v. region which tails into the visible region, (compare with figure 3.7).

From the results it can be concluded that the ferric oxide/hydroxide formed in the reaction of ferrate (VI) in 10 M NaOH has different properties to the species formed in 1 M NaOH. Because the absorbance reaches a steady value when the reaction with the phenol (and the other alcohols tested), it must be assumed that the brown ferric oxide/hydroxide does not have a significant contribution in the decrease of ferrate (VI) concentration in 10 M NaOH solution at room temperature. Also we would postulate that the brown solid oxide contributes little to the absorbance. In contrast, the colloidal oxide causes strong absorbance in the uv/yellow region of the spectra and provides a very high surface area for a heterogeneous decomposition in water. Therefore, the decrease in the ferrate (VI) concentration must be due to the reaction of the ferrate (VI) and the phenol.

Complete oxidation of phenol requires 28 electrons:

$$C_6H_5OH + 27\,OH^- - 28\,e^- \rightarrow 6CO_2 + 16\,H_2O$$

The concentration of ferrate (VI) used in the reaction was 5.7 mM or 17.1 mM of electrons. Thus the oxidation of the phenol involved 32 electrons per molecule, indicating that the phenol was completely oxidised. The time required for 50 % reaction was 1685 seconds.

The results from all the experiments show that ferrate (VI) ion reacts with organics and has the potential to be used as a water treatment chemical. The formation of ferrate (VI) electrochemically avoids contamination of waste with chloride ions or hazardous compounds produced through chlorination. It may be that the ferric oxide/hydroxide formed in the reaction adsorbs some of the organic species onto the surface allowing them to be removed from the solution by filtration. The oxygen evolved in the reaction may also be used to oxidise certain species as well as aiding in the removal of volatile organic species from solution. Lowering the pH of the solution would probably allow the reaction to occur at an even faster rate than that observed in 10 M NaOH.

It would clearly be of interest to define the influence of a ferrate (VI) addition on the total organic carbon (TOC) of the wastewater. An experiment was attempted whereby a solution of 100 cm^3 solution of phenol in water, 1 mg/l was treated with a solution of ferrate (VI), 20 mM, in 10 M NaOH. The TOC was estimated before and after the treatment. In fact the TOC increased due to CO_2 absorption into the sample containing a high concentration of NaOH. An entirely different approach would be necessary but this was not followed up.

3.5 Electrochemistry of ferrate (VI) solutions.

(I) Electrochemistry of ferrate (VI) on a platinum disc.

A ferrate (VI) solution was produced electrochemically (4 mM) in 10 M NaOH and 30 cm^3 were transferred to a three compartment cell, as described in chapter 2. A 5 mm diameter Pt disc electrode was used to record a linear sweep voltammogram, at 298 K, between +0.4 V vs SCE and -0.1 V vs SCE. The sweep rate used in the experiment was 20 mV s^{-1}. On a Pt disc using a sweep rate of 20 mV s^{-1} there was a reduction peak which occurred at E_p = 0.1 V vs SCE.

The experiment was repeated at a range of sweep rates and the resulting curves are shown in figure 3.14. It can be seen that as the potential sweep rate, ν, increases from (a) 20 to (d) 320 mV s^{-1} the peak current increases; also E_p shifts towards negative potentials to, for example, 0.05 V vs SCE at 320 mV s^{-1}. A plot of j_p vs $\nu^{1/2}$ is linear and passes through the origin. The reduction becomes diffusion controlled beyond the peak. Reverse scans show no coupled oxidation peak. In all cases the electrode had a thin golden brown film on the surface after the voltammogram had been recorded. This film is probably an iron oxide/hydroxide and it was removed by polishing between scans. The reduction peak at 0.1 V was not evident when there was no ferrate (VI) in the solution.

These results show that ferrate (VI) shows clean electrochemistry on Pt with the ferrate (VI) reduction peak occurring at 0.1 V vs SCE in 10 M NaOH

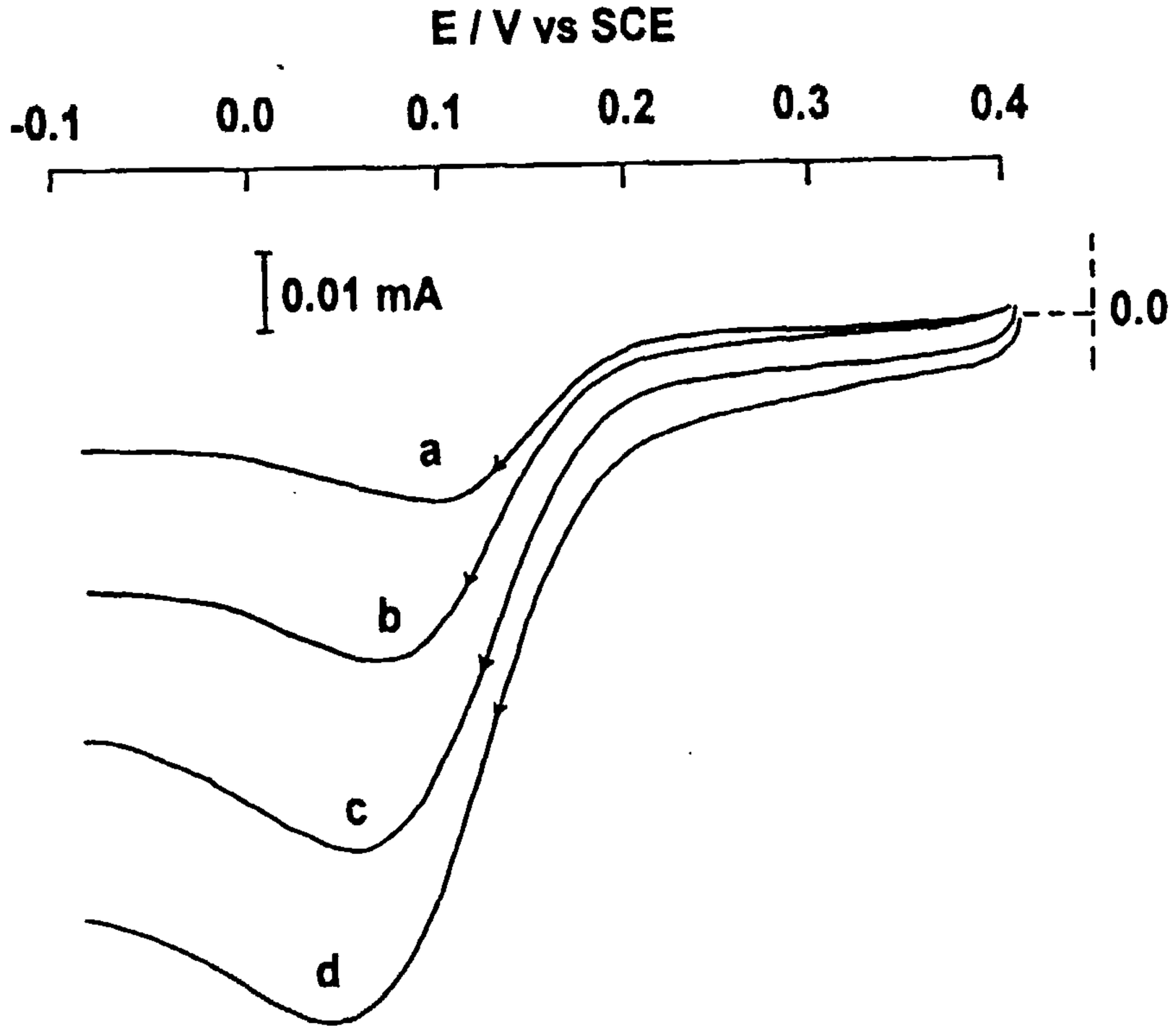

Figure 3.14

Linear sweep voltammograms for the reduction of ferrate (VI) in 10 M NaOH solution on a stationary Pt disc electrode.

Sweep rates from a to d were 20, 80, 200 and 320 mV s^{-1} respectively.

(II) Electrochemistry of ferrate on a platinum microelectrode.

A steady state voltammogram of a ferrate (VI) solution, concentration 5.6 mM was recorded on a 5μm Pt microdisc electrode in 10 M NaOH at 5 mV s^{-1}. The result of the experiment is shown in figure 3.15.

The reduction wave has a good shape, however, there is some hysteresis between the forward and reverse scan. On the forward scan the half wave potential occurs at $E_{1/2}$ = 0.12 V vs SCE. There is a good plateau from -0.1 V vs SCE to -0.5 V vs SCE. The limiting current was calculated as 0.24 nA.

The experiment was repeated with a 50 μm Pt microdisc. This resulted in a wave similar to that shown in figure 3.15 with a limiting current of 2.9 nA. It can be seen from the table 3.4 that $i_L \propto a$ and therefore, the reduction of ferrate (VI) is a diffusion

controlled reaction. The limiting current for a diffusion controlled current at a microdisc is given by the equation:

$$i_L = 4nFDca$$

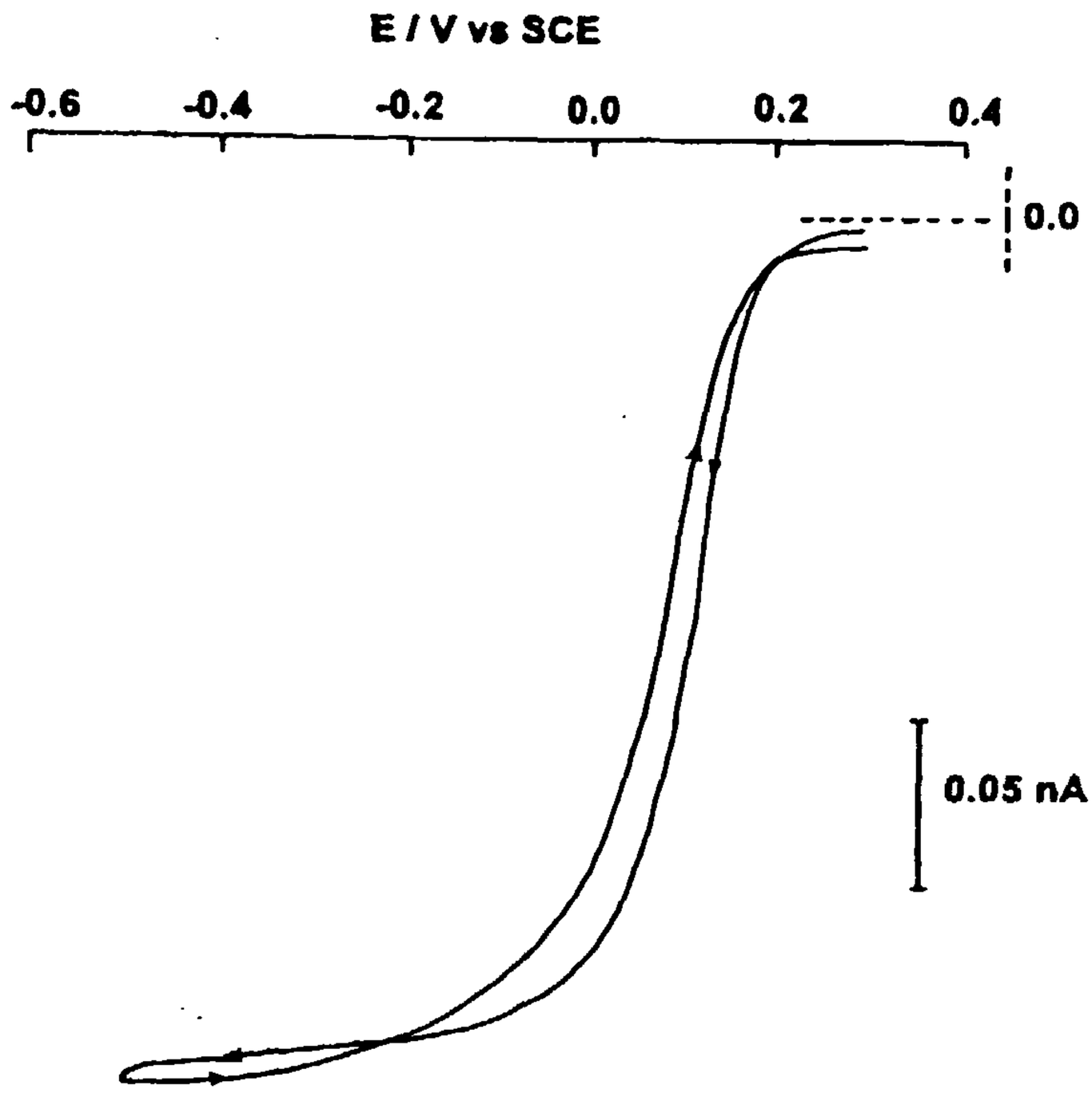

Figure 3.15

Reduction of ferrate (VI) in 10 M NaOH solution on a 5μm Pt microdisc electrode.

Knowing the value of the limiting current form the experiments, it was possible to calculate a value for nD for each. These values are shown in table 3.4.

r / μm	i_L / nA	nD / cm^2 s^{-1}
2.5	0.24	1.1×10^{-6}
25	2.9	1.3×10^{-6}

Table 3.4

Summary of results collected from the reduction of ferrate (VI) on Pt microelectrodes.

(III) Reduction of ferrate (VI) on a rotating glassy carbon disc.

The reduction of a ferrate (VI) solution, concentration 2 mM in 10 M NaOH, was recorded a glassy carbon disc, 4 mm diameter, rotated at 100 rpm between the potential limits 0.0 V vs SCE and -1.0 V vs SCE at a sweep rate of 20 mV s^{-1}. The rotation rate was increased and the voltammogram recorded again. The results are shown in figure 3.16

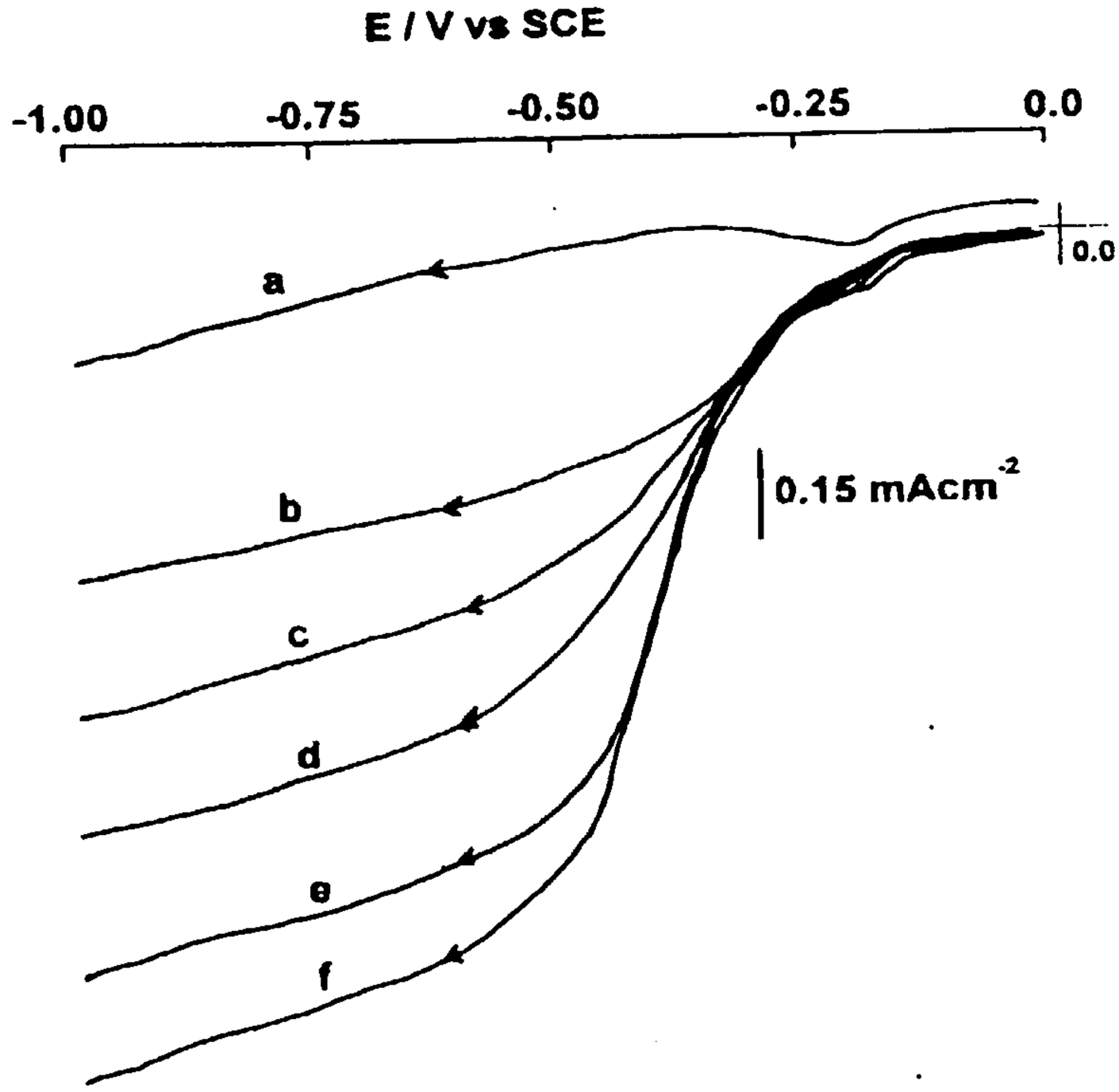

Figure 3.16

Linear sweep voltammograms of ferrate (VI) 2 mM in 10 M NaOH recorded on a rotating glassy carbon disc electrode (4 mm) at a sweep rate of 10 mV s^{-1}.

a = no ferrate (VI) in solution. Curves b to f recorded in 2 mM ferrate (VI) solution.

Curve b = 100 rpm, c = 400 rpm, d = 900 rpm, e = 1600 rpm and f = 2500 rpm.

The background current, (curve a) was recorded on the carbon disc in 10 M NaOH solution. The current response did not change with the rotation rate. Increasing the rotation rate also has no effect on the small peak at -0.2 V. When ferrate (VI) ions

were present in solution a reduction wave was observed at $E_{1/2}$ at -0.3 V vs SCE. This is a shift to more negative potentials when compared to the curves recorded on a Pt electrode. There was a good plateau observed between -0.37 V vs SCE to -1.0 V vs SCE. The small peak that was visible in curve a is also present in the curves for ferrate (VI) reduction. The limiting current was measured at -0.6 V vs SCE and was corrected for the background. Figure 3.17 shows the plot of i_L at -0.6 V vs SCE vs square root of rotation rate. The plot was linear passing through the origin.

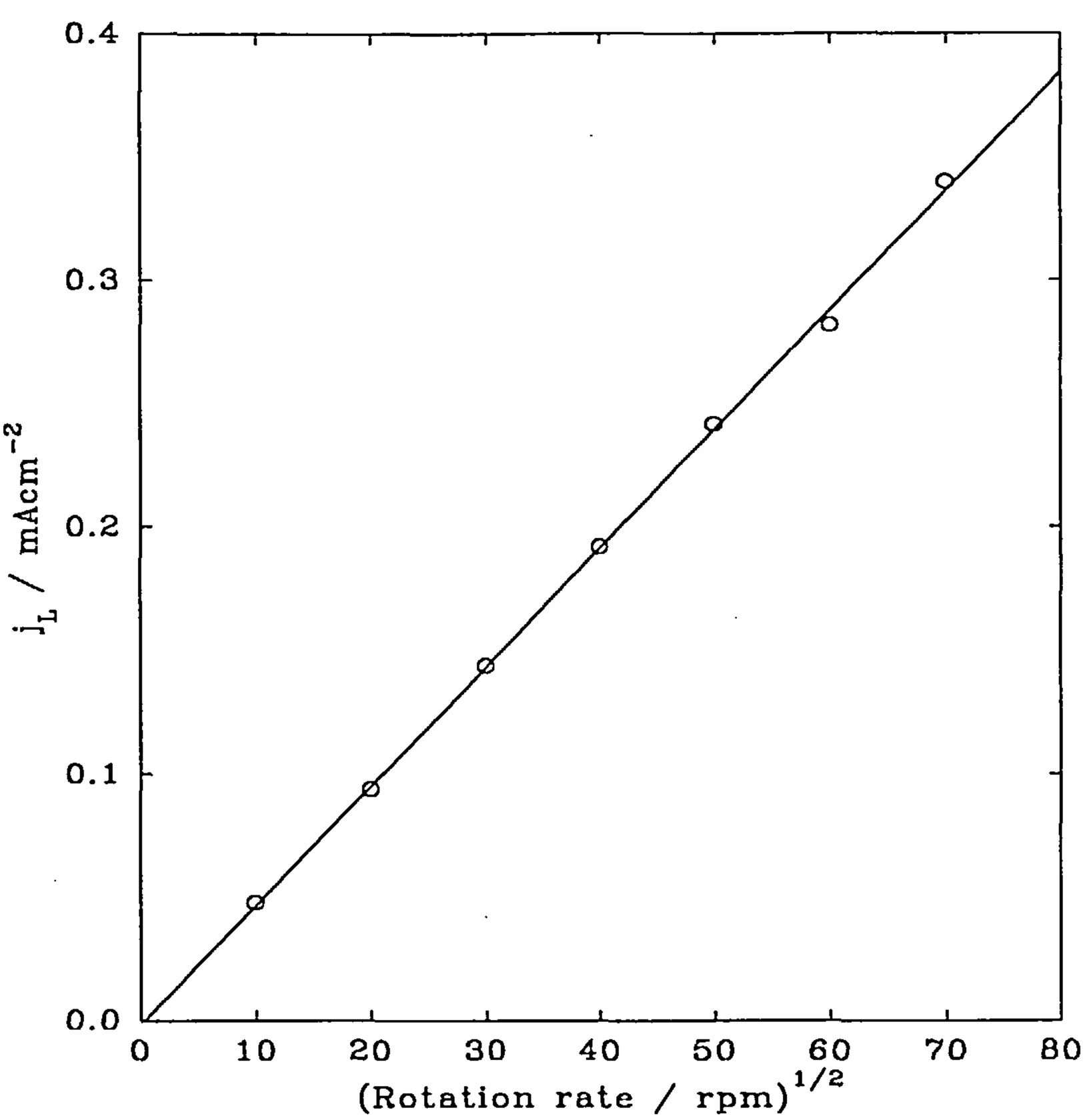

Figure 3.17

Plot of limiting current density at -0.6 V vs SCE vs square root of rotation rate for the reduction of ferrate (VI) on a rotating glassy carbon disc in 10 M NaOH at the same rotation rates for figure 3.16.

The limiting current for a rotating disc is give by the equation:

$$i_L = 0.62nFD^{2/3}\nu^{-1/6}\omega^{1/2}c$$

Thus a value of $nD^{2/3} = 1.5 \times 10^{-4}$ cm^2 s^{-1} was calculated from the slope of the graph shown in figure 3.17

The kinematic viscosity for 40 % NaOH solution, (10 M NaOH), is 24.1×10^{-2} cm^2 s^{-1} [133]. From the rotating disc experiments and the microelectrode experiments it was possible to solve the equations for n and D.

$D = 3.7 \times 10^{-7}$ cm^2 s^{-1} and n = 3.4.

Therefore, the reduction of ferrate (VI) is a three electron transfer. The diffusion coefficient of 3.7×10^{-7} cm^2 s^{-1} is very low (a typical value for aqueous electrolytes is 6×10^{-6} cm^2 s^{-1}). The value in 10 M NaOH is, however, very close to the one reported by Beck *et al.* [131] Walden's Rule [134] shown below states that for most substances the diffusion coefficient in two media 1 and 2 are related to the viscosity η_1 and η_2 of the different media.

$$D_1\eta_1 \approx D_2\eta_2$$

As the relative viscosity (η/η_0) of the 10 M NaOH solution is higher, (16.81), than normal electrolyte, (1.025), then the diffusion coefficient must be lower by a factor of around 17, which is the case.

(IV) Electrochemistry of ferrate (VI) on iron.

A cyclic voltammogram of an iron disc electrode, 5 mm in diameter, in 10 M NaOH was recorded between +0.6 V vs Hg/HgO and -1.35 V vs Hg/HgO at a sweep rate of 250 mV s^{-1}. The voltammogram showed all the characteristic oxidation and reduction reported for iron in concentrated alkaline solution.[101- 114] The electrode was polished and replaced in the cell. The potential was held at +0.7 V vs Hg/HgO for 100 seconds after which a cyclic voltammogram was recorded from +0.7 V vs Hg/HgO to -1.35 V vs Hg/HgO at a sweep rate of 250 mV s^{-1}. The results are shown in figure 3.18.

The solid line is the voltammogram recorded between + 0.6 V vs Hg/HgO and -1.35 V vs Hg/HgO. Because the experiment was commenced at +0.6 V vs Hg/HgO, the surface was already covered by oxide. On the forward scan there are several oxidation peaks occurring in the potential range -1.0 V to 0.0 V vs Hg/HgO. The current falls and then maintains a constant value until the potential reaches +0.6 V vs Hg/HgO. On the reverse scan there are no reduction peaks until -0.8 V vs Hg/HgO. When the potential was held at +0.7 V vs Hg/HgO there was a rapid rise in the anodic current. Gas bubbles observed both in solution and at the electrode surface.

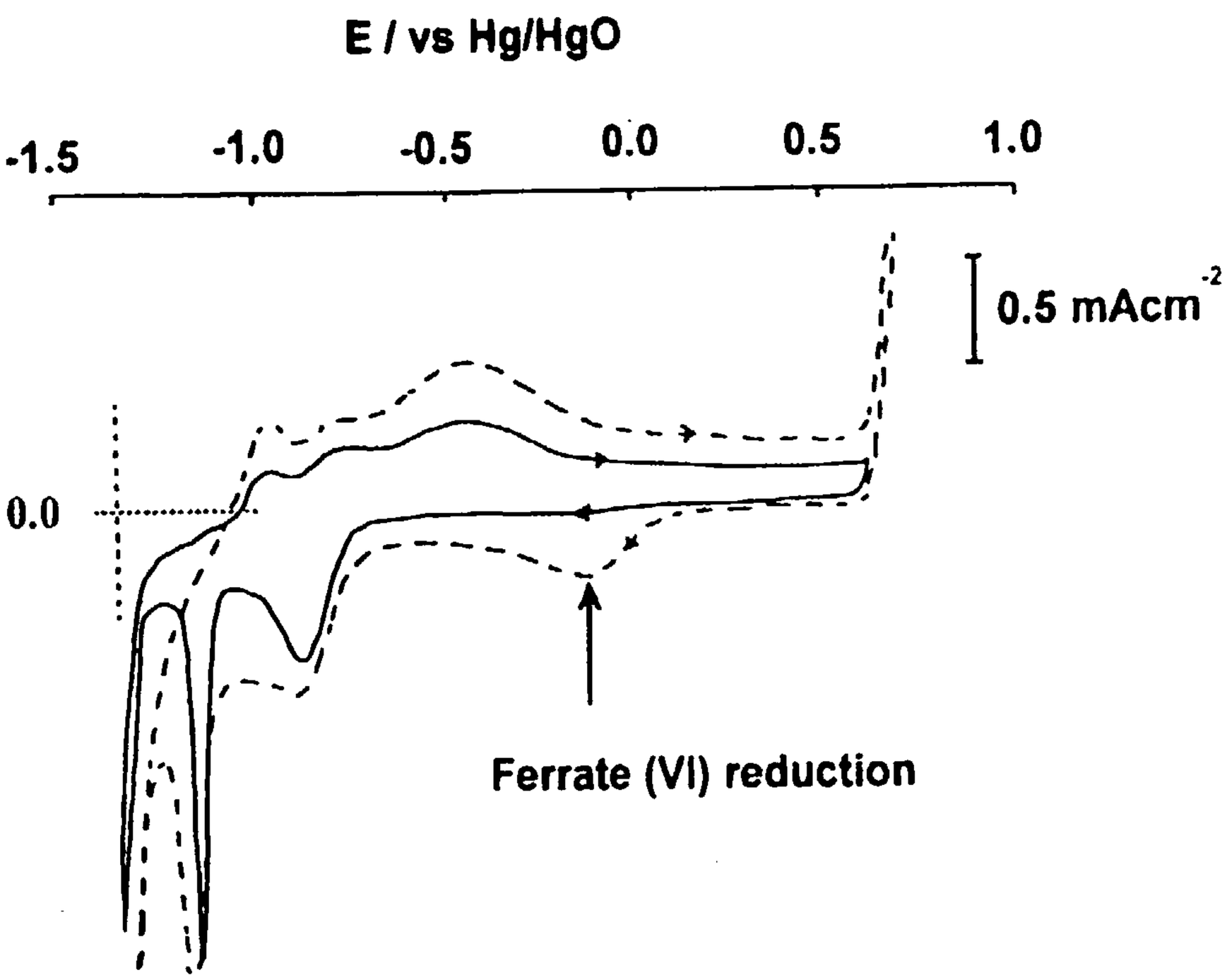

Figure 3.18

Cyclic Voltammograms of an iron disc electrode, 5mm diameter, in 10 M NaOH solution. The solid line represents the response when the potential was scanned from +0.6 V vs Hg/HgO to -1.35 V vs Hg/HgO and the dashed line shows the voltammogram when the potential was held at +0.7 V vs Hg/HgO for 100 seconds. The potential scan rate was 250 mV s^{-1}.

Electrolyte close to the electrode surface turned purple. This purple solution then diffused into the bulk electrolyte. The current potential curve (shown as the dashed line) produced a new reduction wave at -0.2 V vs Hg/HgO. This reduction wave increased in

height when ferrate (VI) was added to the solution. No corresponding oxidation wave was observed on the back scan.

The increase in the current at +0.7 V vs Hg/HgO was due to the oxidation of the water to form oxygen in conjunction with the transpassive dissolution of the iron to form ferrate (VI). On iron in 10 M NaOH, ferrate (VI) reduces at E_p = -0.2 V vs Hg/HgO. The Fe(VI) / Fe(III) couple is irreversible, no oxidation wave was observed on the reverse scan. The formation of ferrate (VI) and oxygen are competitive reactions occurring at the same potentials, problems could arise with the current efficiency when the reaction is scaled up.

(V) Electrosynthesis of ferrate (VI).

The kinetic data reported in section 3.2 showed that ferrate (VI) was very stable in 10 M NaOH solution. Thus a preliminary experiment was designed to produce ferrate (VI) in 10 M NaOH in a glass H cell on an iron flat plate electrode with an applied current density of 10 mA cm^{-2}. Upon applying the current the solution around the electrode turned purple and gas bubbles were observed. The solution was stirred and the anolyte was examined using visible spectroscopy. The concentration of ferrate (VI), determined from the absorbance at 505 nm, was used to calculate the current efficiency for the reaction.

The overall it appears that only oxygen and ferrate are the only products formed in solution. In fact, however, the current efficiency for ferrate (VI) formation is very low (between 3 and 5 %). During the electrolysis, the iron anode changed from a shiny, metallic appearance and became covered in a black film. This is presumably an oxide of iron.

Further controlled potential electrolysis were carried out at 5 mA cm^{-2} and 20 mA cm^{-2}. with the respective current efficiencies being 6 % and 3 % at the end of the reaction. The anode nature of the anode material was changed to an iron wool and the experiment repeated with an applied current of 31 mA (an effective separator current density of 10 mA cm^{-2}) Analysis of the solution showed that the current efficiency for the formation of ferrate had increased to 28 %.

The results of this preliminary experiment show that ferrate (VI) is formed with greater efficiency on a high surface area electrode than on a flat plate electrode.

3.6 Summary of conclusions.

These initial studies have shown that ferrate (VI) has considerable stability in a 10 M NaOH solution at room temperature. The stability decreases with increasing temperature. The decomposition of ferrate (VI) follows first order kinetics in 10 M NaOH. The ferric oxide/hydroxide formed in the decomposition in these conditions does not seem to interfere with the decomposition process. Decreasing the concentration of the NaOH to 1 M results in a loss of ferrate (VI) stability. The decomposition no longer follows first order kinetics and the ferric species formed in the decomposition becomes involved in the reaction, causing a change in mechanism.

Ferrate (VI) reacts rapidly when alcohols are present in high concentration. Excess ferrate (VI) in the system allows the complete combustion of phenol, ethanediol and methanol. There is also significant oxidation of higher alcohols but the extent of oxidation decreases as the number of carbons in the backbone of the molecule increases. The n value found may be underestimated because of the adsorption of the alcohol onto the iron oxide/hydroxide formed. Ferrate (VI) has, however, been shown to be an effective agent for oxidising alcohols when it is present in excess. The ferric oxide/hydroxide species formed in the reaction does not undergo further reaction with the ferrate (VI) in solution. This precipitate may, however, adsorb organics onto the surface thus allowing them to be removed by filtration.

Ferrate (VI) shows clean electrochemistry on platinum. It is reduced in a three electron transfer at E_p = +0.1 V vs SCE. On glassy carbon the reduction potential shifts more negative with E_p = -0.25 V vs SCE. The diffusion coefficient was determined as 3.8×10^{-7} cm^2 s^{-1} in 10 M NaOH at 298 K. Ferrate (VI) is formed in competition with water oxidation on iron anodes. The reduction potential of ferrate (VI) on iron is E_p = -0.2 V vs Hg/HgO. The Fe(III)/Fe(VI) couple is irreversible as no oxidation wave can be observed when the potential is scanned positive. The amount of ferrate (VI) formed by applying a specific potential or current density can thus be estimated by measuring the peak current density for the reduction, allowing, for example, different iron containing

electrodes to be compared (see Chapter 5). Also increasing the anode surface area improves the efficiency of ferrate (VI) formation

Chapter 4

The electrochemical generation of ferrate (VI) on iron wool anodes.

4.1 Introduction.

There have been many reports on the electrosynthesis of ferrate (VI) by the transpassive dissolution of iron wool anodes.[128 - 131] This work has, however, concentrated on the use of cells with flat plate anodes. In all cases, the current efficiency for these reactors has been low, less than 20 %. In this chapter, the discussion concentrates on the use of high surface area, three dimensional iron wool anodes and the factors which effect the synthesis of ferrate (VI) with such structures. Three dimensional electrodes are particularly suited to electrosyntheses which only occur at low current densities and this appears to be the case for the formation of ferrate (VI). It also enables the use of a cheap form of iron wool or scrap as the source of iron.

4.2 Electrosynthesis of ferrate (VI) in a flow cell at room temperature.

(I) Effect of applied current.

The flow cell was constructed as shown in figure 2.7, chapter 2 with a clean iron wool anode. Both the anolyte and catholyte used in the experiment were 10 M NaOH solutions, 450 cm^3, and they flowed around the system at 0.8 l/min. A constant current of 1 A, (an effective membrane current density of 17 mA cm^{-2}) was applied and the absorbance of the anolyte was monitored between 350 and 900 nm.

On applying the current density the cell voltage to increased slowly and the final value was 2.2 V. The anolyte remained clear for 2 minutes, but with increasing time it began to take a slight purple hue. The purple colour of the anolyte intensified with time. Gas bubbles were also seen well dispersed throughout both the anolyte and catholyte compartments though none of the purple colour seen on the anolyte side was observed in the catholyte compartment.

The spectrum of the anolyte exhibited all the features shown in figure 3.1. A plot of absorbance (at the absorbance maximum) vs time is shown in figure 4.1.

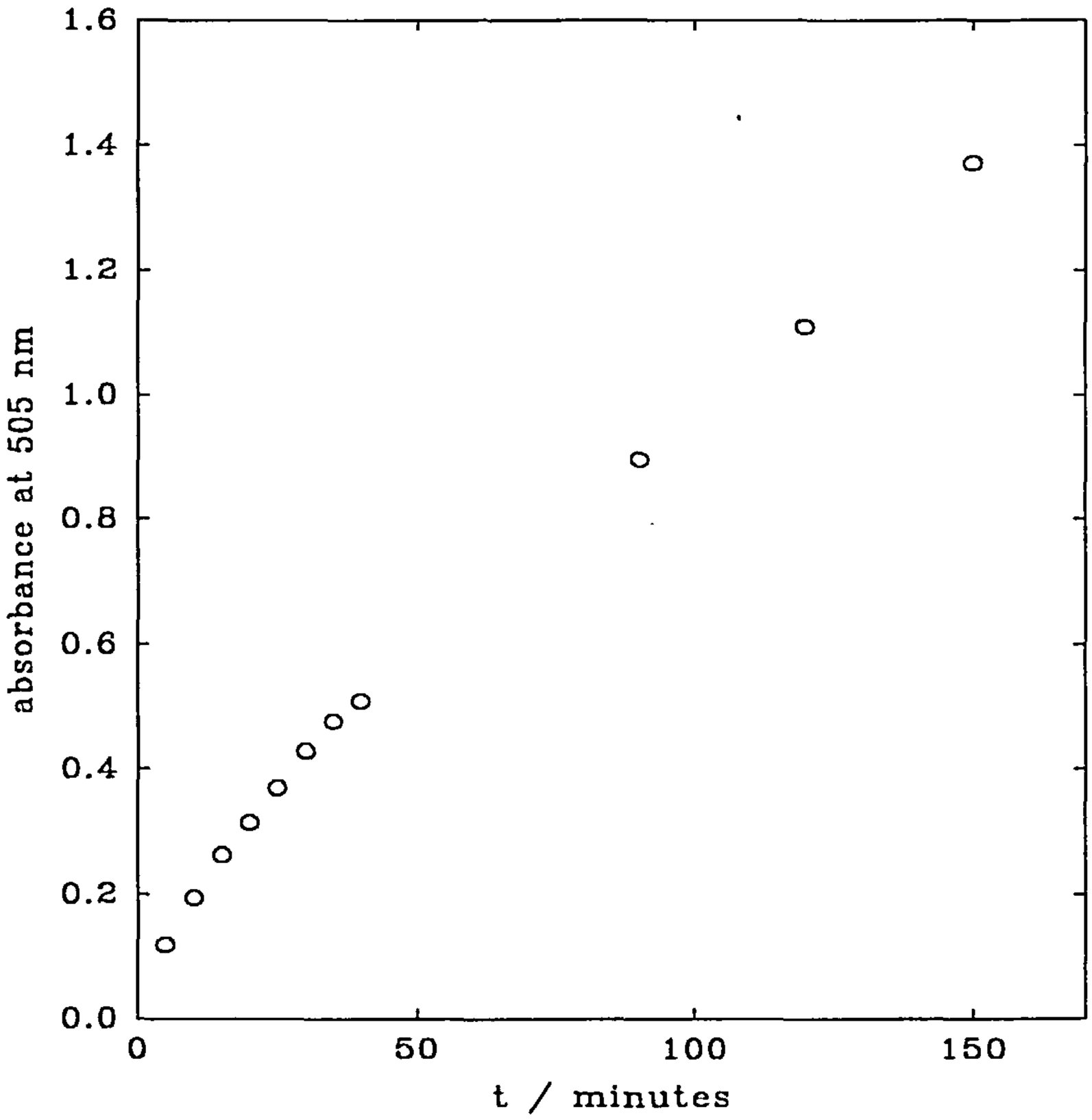

Figure 4.1

The plot of absorbance at 505 nm vs time for the anolyte during the formation of ferrate (VI) in a flow cell at room temperature on an iron wool anode. The anolyte, 10 M NaOH was flowed through the system at 0.8 l/min. The ferrate (VI) was formed by applying a constant current of 1 A (17 mA cm^{-2} membrane current density).

The change in the absorbance is smooth, curving slightly in the first 40 minutes of the reaction before becoming linear as the electrolysis proceeds. No ferric oxide/hydroxide species were seen in the anolyte compartment at the end of the reaction, but the surface of the anode had turned black.

Applying the current of 1 A resulted in ferrate (VI) being formed by the transpassive dissolution of the iron wool anode. The evolution of oxygen was occurring

as a competitive electrode reaction and was not due to the reaction of the ferrate (VI) with the water. The concentration of the ferrate (VI) was determined from the calibration plot and it was found that after 150 minutes 7 mM of ferrate (VI) had been produced. Therefore, using the flow cell in this manner enables ferrate (VI) to be prepared in a useful concentration.

(II) Effect of changing the applied current.

The experiment was repeated, on an oxide free anode, with an applied currents of 5 A, (a membrane current density of 85 mA cm^{-2}), and 0.4 A, (6.8 mA cm^{-2}). In both cases the solutions turned purple in colour but, with a current of 5 A, the colour of the solution was much darker. Measuring the absorbance of the anolytes showed that the change in the absorbance occurred in a similar manner to that shown in figure 4.1. At the end of the reactions, it was found that the final absorbance for the 5 A electrolysis was 3 times higher that that recorded in the 1 A experiment, whereas the final absorbance in the 0.4 A electrolysis was half of that recorded for the reaction using 1 A. In all experiments the anode surface was found to have a black oxide coating, when examined at the end of the reaction. From the spectroscopic data the concentration of ferrate (VI) in the anolyte was determined. The cell voltage at the end of the 5 A electrolysis was measured at 4.4 V. The final cell voltage for the 0.4 A electrolysis was much less, only 1.9 V.

Figure 4.2 shows a plot of ferrate (VI) concentration vs time for the reaction at 1 A and 5 A. It can be seen that in both cases there is a slight curve in the increase in ferrate (VI) concentration with time. There was a 3 fold increase in ferrate (VI) concentration when the applied current for the electrolysis was increased from 1 A to 5 A

From these experiments it has been shown that the concentration of ferrate (VI) in the anolyte can be improved by operating the cell at higher current densities.

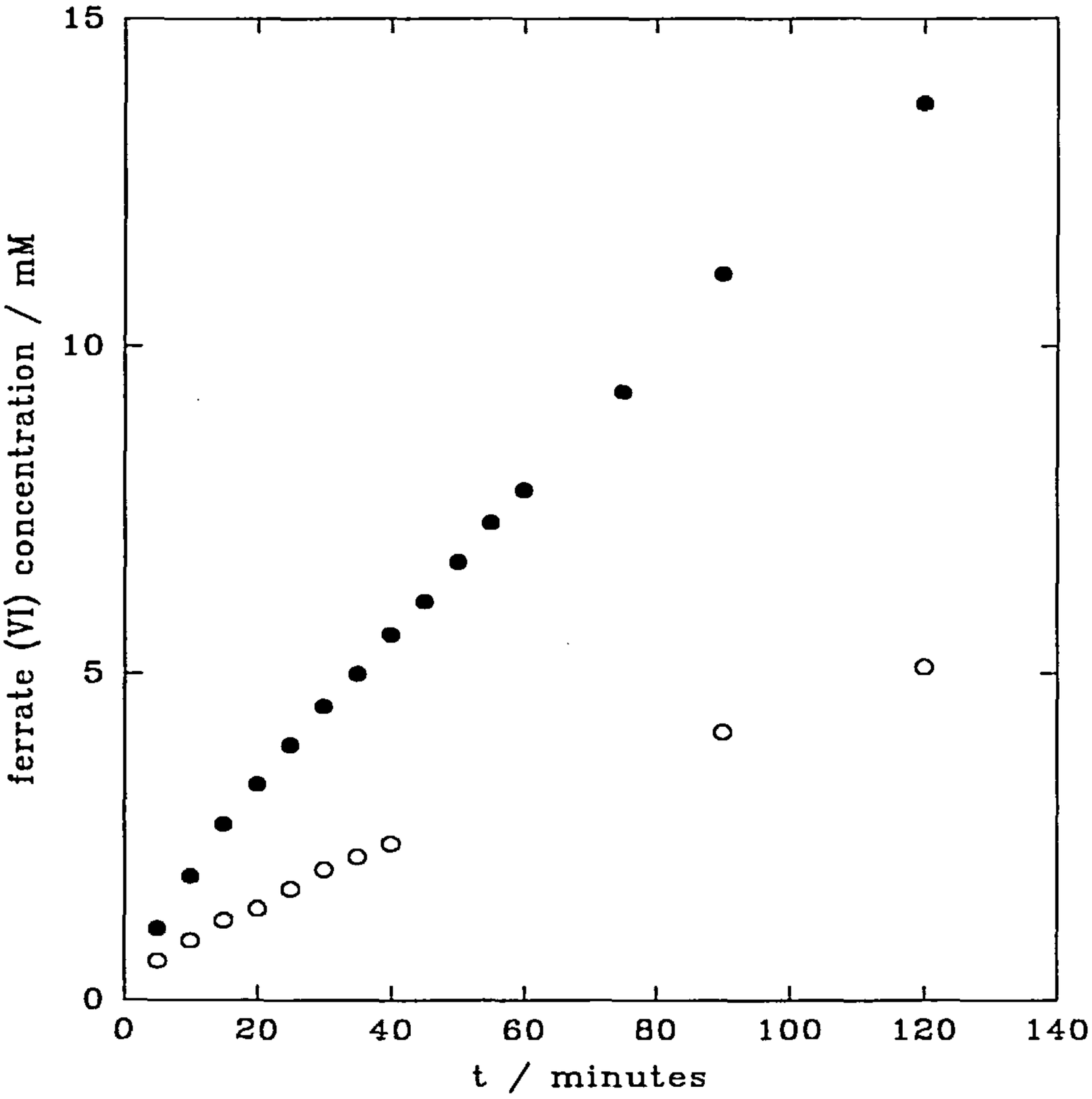

Figure 4.2

Plots of ferrate (VI) concentration in 10 M NaOH vs time. The ferrate (VI) was synthesised at room temperature in a flow cell at ● 5 A and ○ 1 A .

Having obtained values for the concentration of ferrate (VI) in the anolyte it was possible to determine the current efficiency for each of the reactions by using the equation:

$$\phi = \frac{mnF}{it}$$

Plots of current efficiency vs time for the reactions are shown in figure 4.3.

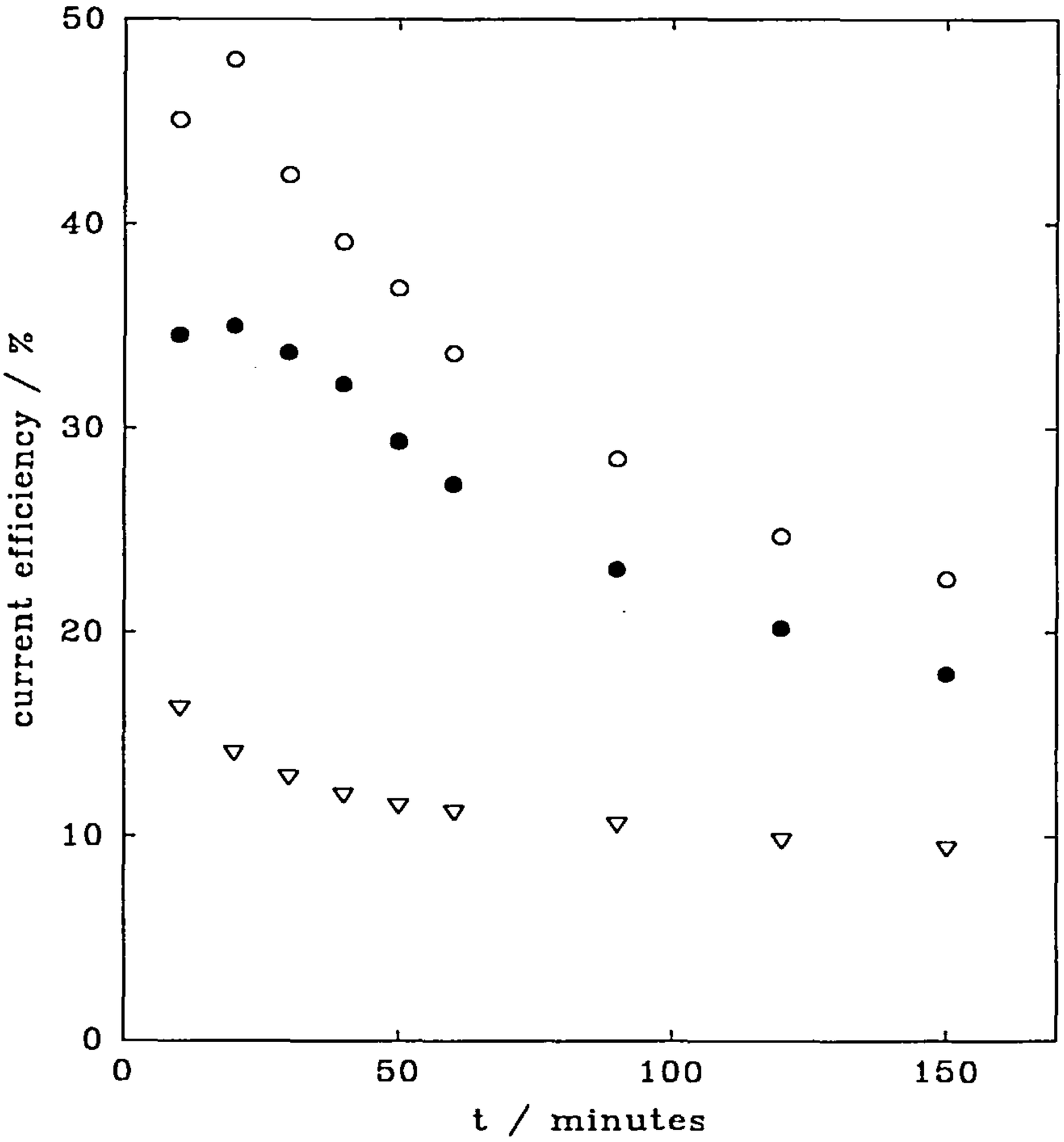

Figure 4.3

Plots of current efficiency vs time for the formation of ferrate (VI) in a flow cell at 298K in 10 M NaOH solution. The current efficiencies were calculated from the absorbance at 505 nm for the electrosyntheses at ∇ *5 A*, ○ 1 A *and* ● *0.4 A*

The plots show that the current efficiency is higher for the electrolysis at 1 A and lowest at 5 A. In all the experiments the current efficiency dropped with time before reaching a steady state value. During the electrolysis at 1 A, the difference in the current efficiency between the initial value and the steady state value is around 20 %. A similar difference in initial and steady state current efficiencies is seen in the 0.4 A electrolysis, over the same amount of time. On the other hand, with an applied current of 5 A used to generate the ferrate (VI), the loss in the current efficiency, from the beginning to the end of the experiment is relatively small, around 6 %.

From the experimental results described in chapter 3 it has been shown that ferrate (VI) is very stable in 10 M NaOH solution. Therefore the loss in current efficiency as the reaction proceeds is not due to the reaction of the ferrate (VI) with water. This evidence is supported by the fact that none of the characteristic decomposition product were observed in the anolyte compartment at the end of the reaction. It must be concluded that the loss in current efficiency is due to a portion of the current being used in competitive reactions. Visual observations of the anolyte in all the electrolyses showed the presence of oxygen bubbles. Therefore during the electrolyses a portion of the current was being used in oxygen evolution.

However, the current efficiency also dropped with increasing reaction time. This suggests that there is another process occurring during the electrolyses which alters the ratio of ferrate (VI) to oxygen produced in the electrolysis. It may be possible that as the reaction proceeds the surface of the oxide layer on the anode surface changes in composition, structure or thickness over the course of the reactions to produce a surface which inhibits the production of ferrate (VI) or catalyses oxygen evolution.

(III) Ferrate (VI) formation at 0.2 A.

Repeating the experiment with an applied current of 0.2 A (a membrane current density of 3.4 mA cm^{-2}) resulted in the formation of an orange species in the anolyte in the first 15 minutes of the electrolysis. This was removed by filtration to give a colourless liquid. No ferrate (VI) had been formed. The anolyte was changed for a fresh 10 M NaOH solution and the electrolysis started over again. Upon applying the current the anolyte turned purple. This purple colour intensified as the reaction time increased. At the end of the reaction the electrode had a black oxide coating, and there was no brown deposits on the walls of the anolyte compartment. The cell voltage at the end of the reaction was measured at 1.6 V.

Figure 4.4 shows the absorbance vs time plot for the electrolysis at 0.2 A. There are three distinct regions on the plot. For the first 15 minutes, after the orange species has been removed from the solution, there is no increase in absorbance. But with increasing time, (and after a change in electrolyte), it can be seen that it rises steeply in a

linear fashion for 45 minutes. After 60 minutes the slope becomes less steep and has the form of a slight curve. It must also be noted that the absorbance of the solution is very low when compared to the previous experiments.

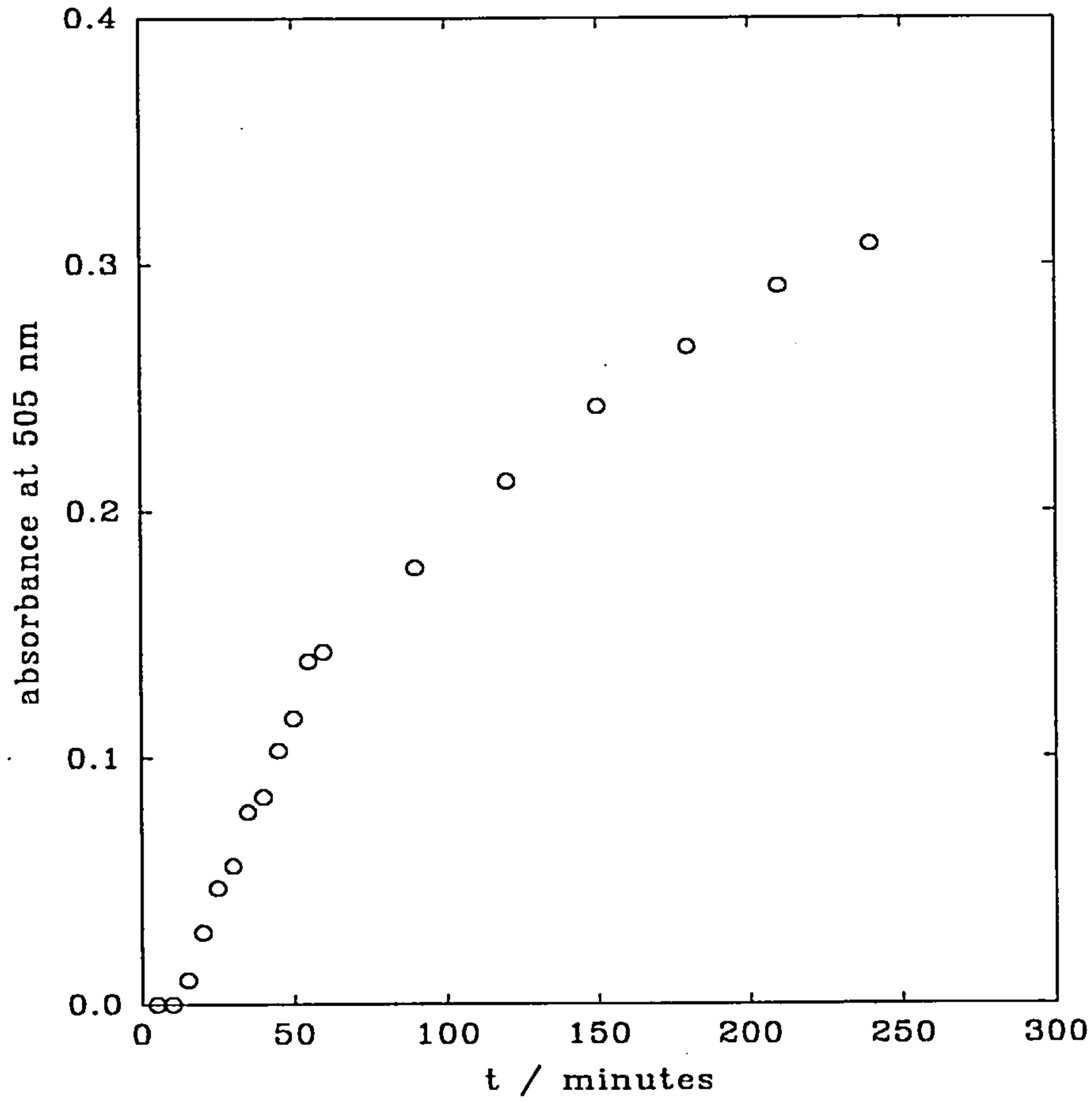

Figure 4.4

Plot of absorbance at 505 nm vs time for the electrolysis at 0.2 A (3.4 mA cm^{-2}) in 10 M NaOH solution at 298 K.

From the data collected in the experiment the current efficiency for the electrolysis was calculated. Figure 4.5 shows the change in the current efficiency with time.

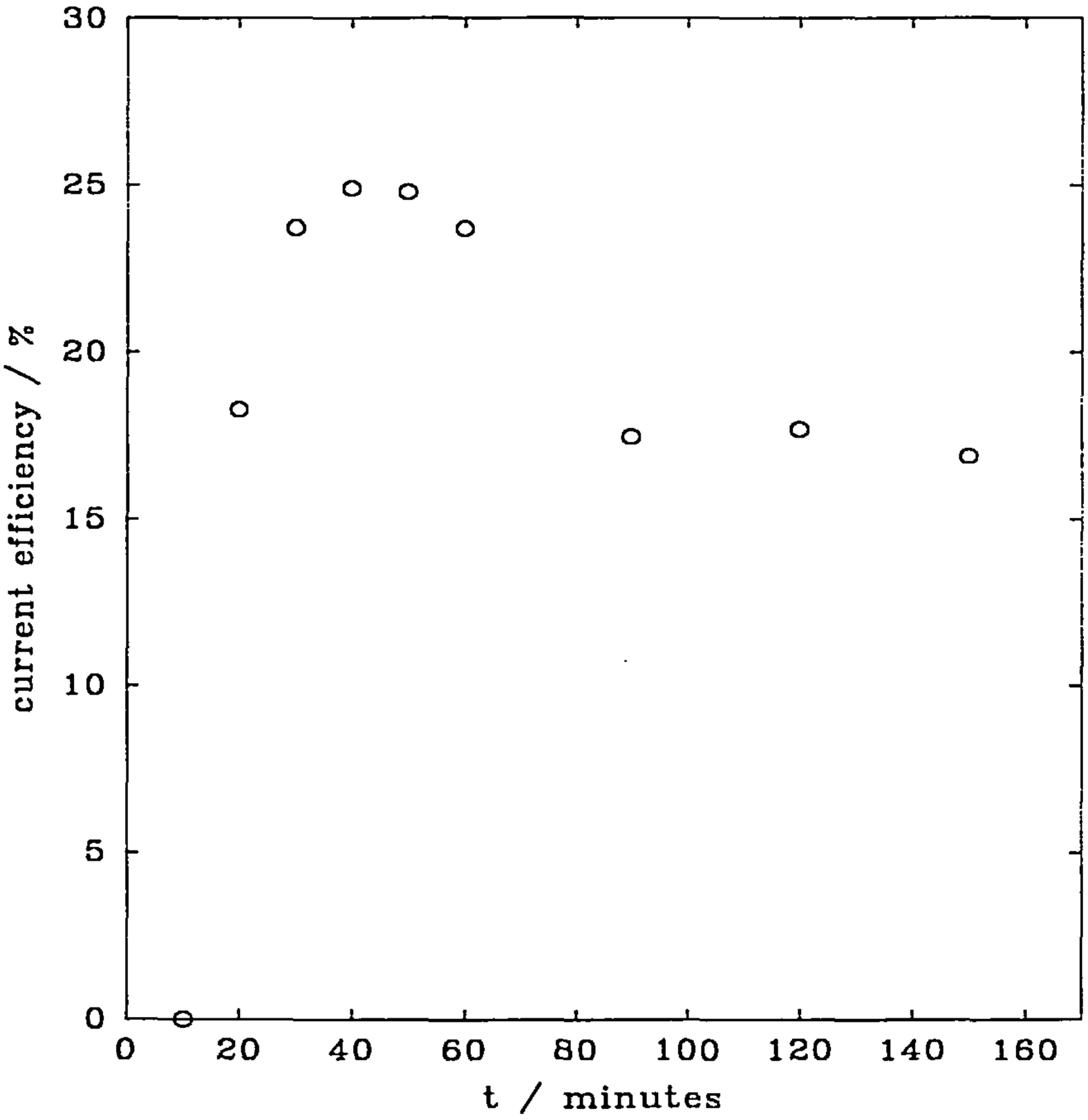

Figure 4.5

Plot of current efficiency vs time for the formation of ferrate (VI) with an applied current of 0.2 A at 298 K in 10 M NaOH.

Here again it can be seen that the shape of the curve is different to those observed in figure 4.3. In the initial 15 minutes of the reaction, the current efficiency for the reaction is 0 %. It then increases to 25 % over a period of 45 minutes where it is maintained. This corresponds to the straight line part of figure 4.4. As the reaction proceeds further, the current efficiency falls sharply to 18 % where it remains until the end of the reaction.

The initial period could be interpreted in two ways. (I) It is necessary to condition the surface of the iron before ferrate (VI) is produced at this low current density, or, (II) it is necessary to remove any impurities from the cell (which react with ferrate (VI)) and this effect is only observed because of the low rate of production in the

experiment. The first reason is the most probable. When compared to the 0.4 A and 1 A experiments it can be seen that they also show a small increase in the current efficiency at the start of the reaction before it starts to decrease, but these last for a much shorter time. This is expected because the electrode processes are occurring at a faster rate. From these results it may be assumed that during the electrolyses, the oxide surface is continually changing. Also during this change the oxide has a structure or composition which improves the ferrate (VI)/oxygen ratio for the reaction, thus resulting in an increase in the current efficiency. As this oxide changes further, (for example in thickness), this ratio is decreased again and the current efficiency drops.

Applied current Amps	Current efficiency after 5 minutes / %	Rate of ferrate formation after 5 minutes/ mol/cm^2/s	Current efficiency after 150 minutes /%	Rate of ferrate formation after 150 minutes mol/cm^2/s
0.2	0.0	0.0×10^{-7}	18.0	0.6×10^{-7}
0.4	31.5	2.2×10^{-7}	20.2	1.4×10^{-7}
1.0	45.0	7.8×10^{-7}	22.0	3.8×10^{-7}
5.0	17.5	15.0×10^{-7}	11.3	9.7×10^{-7}

Table 4.1

Summary of experimental results obtained from the flow cell experiments in 10 M NaOH solution at 298 K at different applied currents.

Table 4.1 has a summary of data collected from these experiments. With the exception of the 0.2 A the current efficiency and the rate of ferrate (VI) formation is higher in the first 5 minutes of the electrolyses. The rate at which the ferrate (VI) is formed increases with increasing applied current but decreases with reaction time. The current efficiency for the reaction is highest at 1 A.

From the information obtained it has been shown that ferrate (VI) is formed along with oxygen evolution in 10 M NaOH solution. The ratio of ferrate (VI) and oxygen is strongly dependant on the applied current for the electrolysis. Increasing the

current increases the rate at which the ferrate (VI) is produced, but it alters the ferrate (VI):oxygen ratio and the steady state current efficiency for the reaction is lower. Lowering the applied current to 1 Amp increases the steady state current efficiency for the formation of ferrate (VI), but this is coupled with a decrease in the rate in which the ferrate (VI) is produced. Lowering the applied current even further also results in a decrease in the current efficiency. In all these experiments the current efficiency was observed to fall with time, (until a constant value was attained) as a change in the composition, thickness or structure of the oxide on the electrode surface occurred. At some stage during the electrolyses an oxide is formed which favours the formation of ferrate (VI) or does not catalyse oxygen evolution as strongly. However, the life time of this species depends on the applied current, it is short lived at high currents, but exists for a longer time at the lower currents.

4.3 Effect of temperature on the current efficiency.

(I) Electrolysis at 333 K

Having established that 1 A provided the best current efficiency for the formation of ferrate (VI) it was decided to repeat the flow cell electrolysis at elevated temperature. The electrolyte, 10 M NaOH, was circulated through the thermostat at 333 K until it had attained a constant temperature. Before starting the experiment the anode was acid washed to remove any oxide on the surface. All glassware such as flow meters were wrapped in aluminium foil to prevent heat loss as the electrolyte flowed through the system. The absorbance was recorded between 350 and 900 nm periodically.

As before, upon applying the current, the anolyte attained a purple colour which increased in intensity as the experiment proceeded. Examination of the anode at the end of the reaction showed that the surface had a coating of black oxide, also there were thick brown deposits on the surface of all the glass components used in the cell set-up. The brown species was also seen in the anolyte compartment and this had to be filtered out before the absorbance could be measured.

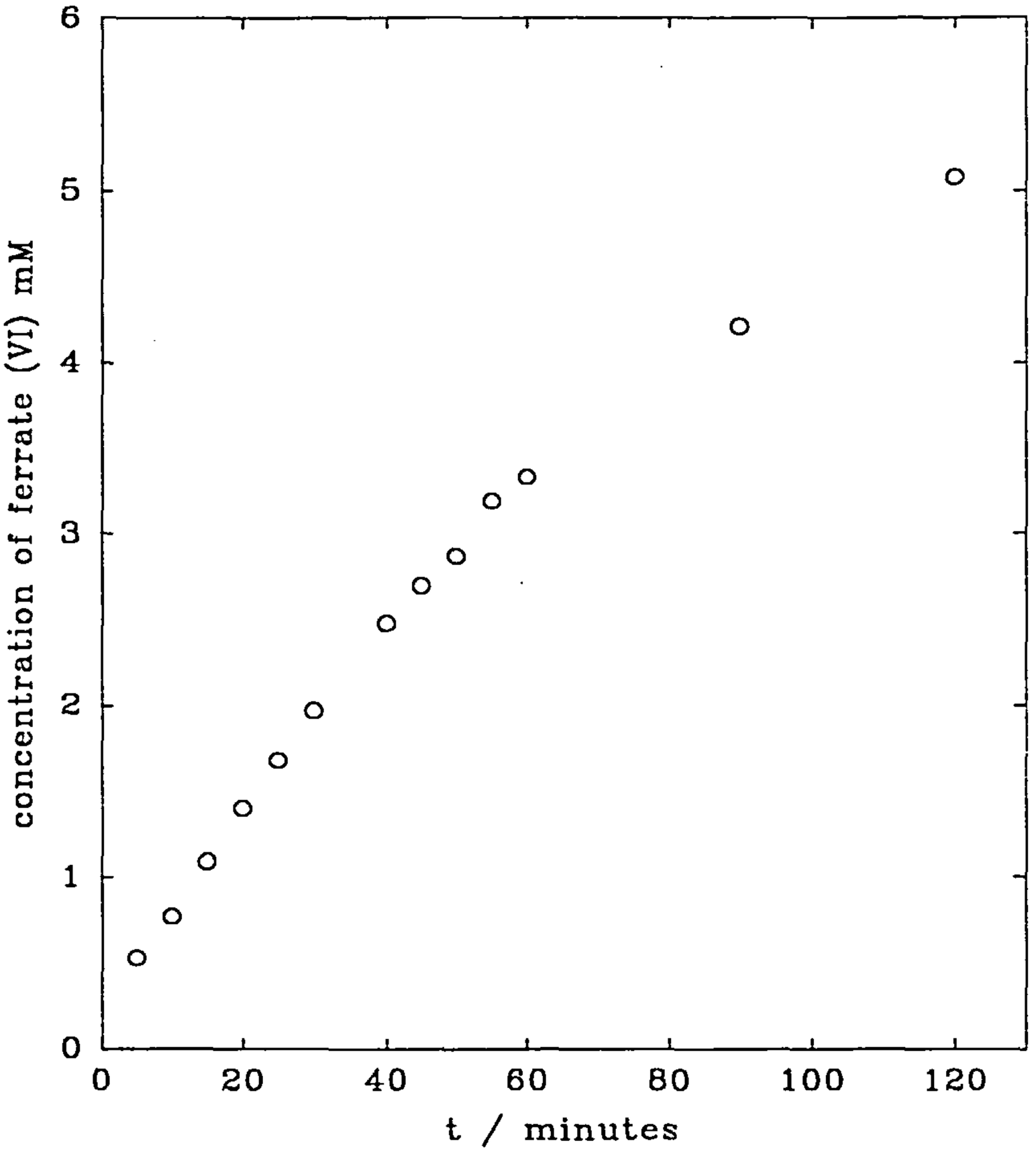

Figure 4.6

Plot of concentration of ferrate (VI) vs time for the electrolysis at 333 K in 10 M NaOH solution with an applied current of 1 A, (membrane current density of 17 mA cm^{-2}).

As was previously reported in this chapter, using an applied current of 1 A at 298 K the absorbance increased with a slight curve. From this the concentration of ferrate (VI) was calculated. Figure 4.6 shows the change in the concentration of ferrate (VI) in the anolyte with increasing reaction time. The plot shows that the concentration of ferrate (VI) in the anolyte after the passage of 7200 C at 333 K is slightly lower than 298 K electrolysis (see figure 4.2). However, at 333 K there were thick oxide deposits on all the glassware which were not seen in the 298 K experiment. This oxide had the same appearance as that seen in the kinetic reactions described in section 3.3, chapter 3.

The experimental results show that at 333 K the final concentration of ferrate (VI) in the anolyte was comparable to the 298 K electrolysis. However, the large excess of ferric oxide/hydroxide seen on the glassware suggests that there was considerable decomposition of the ferrate (VI) during the reaction. As this was not observed in the electrolysis at lower temperature it must be assumed that running the cell at high temperatures results in extensive decomposition of the ferrate (VI). This is supported by the experimental evidence which was reported in section 3.3; the half life of ferrate (VI) was only 2.5 hours. Thus at 333 K both the rate of ferrate (VI) formation, and its decomposition is higher at elevated temperatures. Therefore the synthesis of ferrate (VI) at elevated temperatures offers no advantages when compared to the same experiment at 298 K.

(II) Changing the temperature.

The experiment was repeated at 273 K and 313 K. the results of the experiment are summarised in table 4.2. In all cases the current efficiency for the electrolyses was initially high.

Temperature K	Ferrate concentration at 5 minutes / mM	Ferrate concentration at 150 minutes/ mM	Current efficiency after 5 minutes/ %	Current efficiency after 150 minutes/ %
273	0.7	6.1	59	18
298	0.5	6.0	38	20
313	0.3	5.5	35	
333	0.5	5.0	46	15

Table 4.2

Summary of results obtained for electrolyses at different temperatures using an applied current of 1 A (a membrane current density of 17 mA cm^{-2}) in 10 M NaOH solution.

In the first 5 minutes of the reaction the current efficiency at 273 K is the highest but decreases to almost the same value as the 298 K experiment. The current efficiency at 333 K is also higher than at 298 K, but, at the end of the electrolysis it has a lower value. Comparing the concentration of ferrate (VI) after passing 9000 C shows no significant differences.

The lower current efficiency at elevated temperatures results from factors other than ferrate(VI) and oxygen production. Even though ferrate (VI) is produced at a faster rate, it is the fast decomposition kinetics that produce a lower ferrate (VI) concentration and not the electrode reaction. Working at 273 K results in a slightly higher ferrate (VI) concentration. This may be due to the fact that the change in the oxide/hydroxide on the electrode is occurring at a slower rate. It was hoped that a lower temperatures the formation of the inhibiting oxide would be greatly reduced, but the rapid drop in current efficiency for the reaction suggests that this is not the case. Therefore, altering the temperature at which the electrolysis is run does not have a positive contribution to make towards increasing the ferrate (VI) concentration in the anolyte or the slowing down the formation of an inhibiting oxide on the anode surface.

4.4 Methods of oxide removal.

(I) Acid washing.

An electrolysis was carried out in 10 M NaOH solution with an applied current of 1 A at 298 K and a flow rate of 0.8 l/min. The concentration of the ferrate (VI) was calculated from the absorbance at 505 nm. It was found that as expected the current efficiency started high at 48 % but dropped to 20 % by the end of the reaction (see figure 4.7). The anolyte was changed for a fresh 10 M NaOH solution and the experiment continued. The anode was not acid washed and still had the black oxide/hydroxide on the surface. From the absorbance at 505 nm the concentration of ferrate (VI) was calculated. The concentration was found to increase in a linear fashion and the rate of formation of ferrate (VI) did not change as with the acid washed anode. The concentration of ferrate (VI) at the end of the reaction was lower than that obtained for the acid washed anode

over the same time period. The current efficiency was calculated and plotted against time. This is shown in figure 4.7.

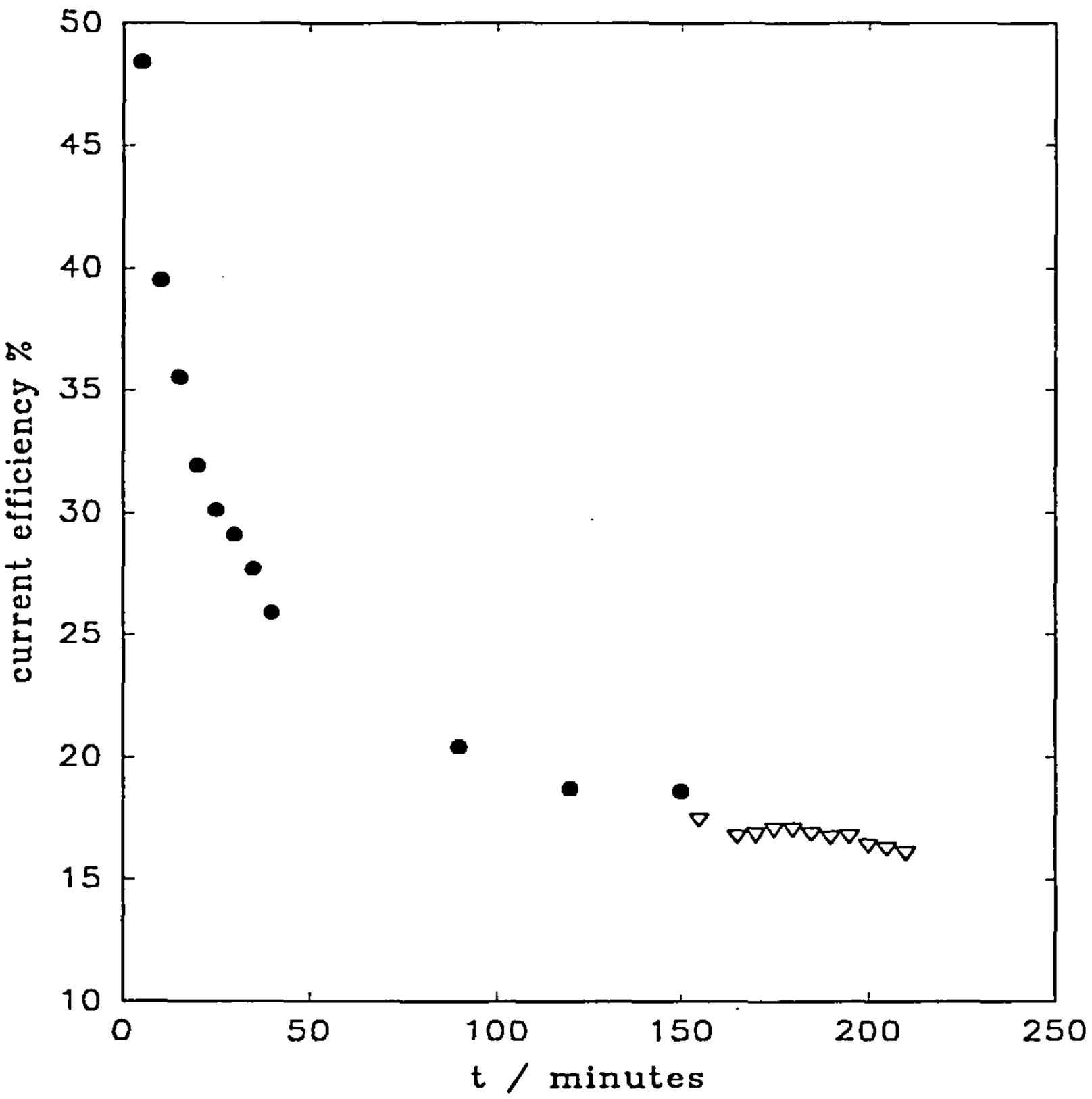

Figure 4.7

Plot of current efficiency vs time for the formation of ferrate (VI) in 10 M NaOH with an applied current of 1 A at 298 K.

Acid washed anode shown by ●, and anode with a black oxide on the surface ∇.

These results prove that it is the presence of an oxide on the anode which causes the drop in current efficiency for the formation of ferrate (VI) in 10 M NaOH solution.

(II) Addition of chloride ions.

In order to acid wash the electrode, the cell must be dismantled. If the process was scaled up the amount of down time necessary to maintain the electrode would be unacceptable as would the labour. It is therefore necessary to be able to treat the electrode with out having to dismantle the cell. Deininger *et al*[126, 126] reported that the addition of chloride ions to the electrolyte increased the amount of ferrate (VI) formed on a flat plate electrode. The presence of chloride ions in the electrolyte causes pitting which results in the breakdown in the oxide film. It has also been shown in chapter 3 that hypochlorite oxidises Fe(III) to Fe(VI) in 10 M NaOH solution.

A 10 M NaOH solution containing 0.1 mM of NaCl was used as the electrolyte for an electrolysis with an applied current of 1 A on an anode that had been acid washed. As before, the anolyte turned purple and gas bubbles were also observed. There was no smell of chlorine emanating from the anolyte compartment and the anode had a black oxide coating the surface when examined at the end of the reaction. The final absorbance of the solution was determined as 0.65, half the value obtained when no chloride was present in the electrolyte. The experiment was repeated at with an applied current of 5 A on an acid cleaned anode. From the absorbance at 505 nm the concentration of ferrate (VI) in the anolyte was calculated Figure 4.9 shows the difference between electrolyses carried out in the presence of trace NaCl and electrolyses in 10 M NaOH only. As expected the higher applied currents produce more ferrate (VI). The most obvious feature is that in the presence of 0.1 mM NaCl the amount of ferrate (VI) formed is mush lower. When ferrate (VI) is formed at 1 A there is almost twice as much ferrate (VI) produced than when there is no NaCl in the electrolyte. At 5 A, however, the concentration of ferrate (VI) in the anolyte is only a third less for the electrolyte containing NaCl.

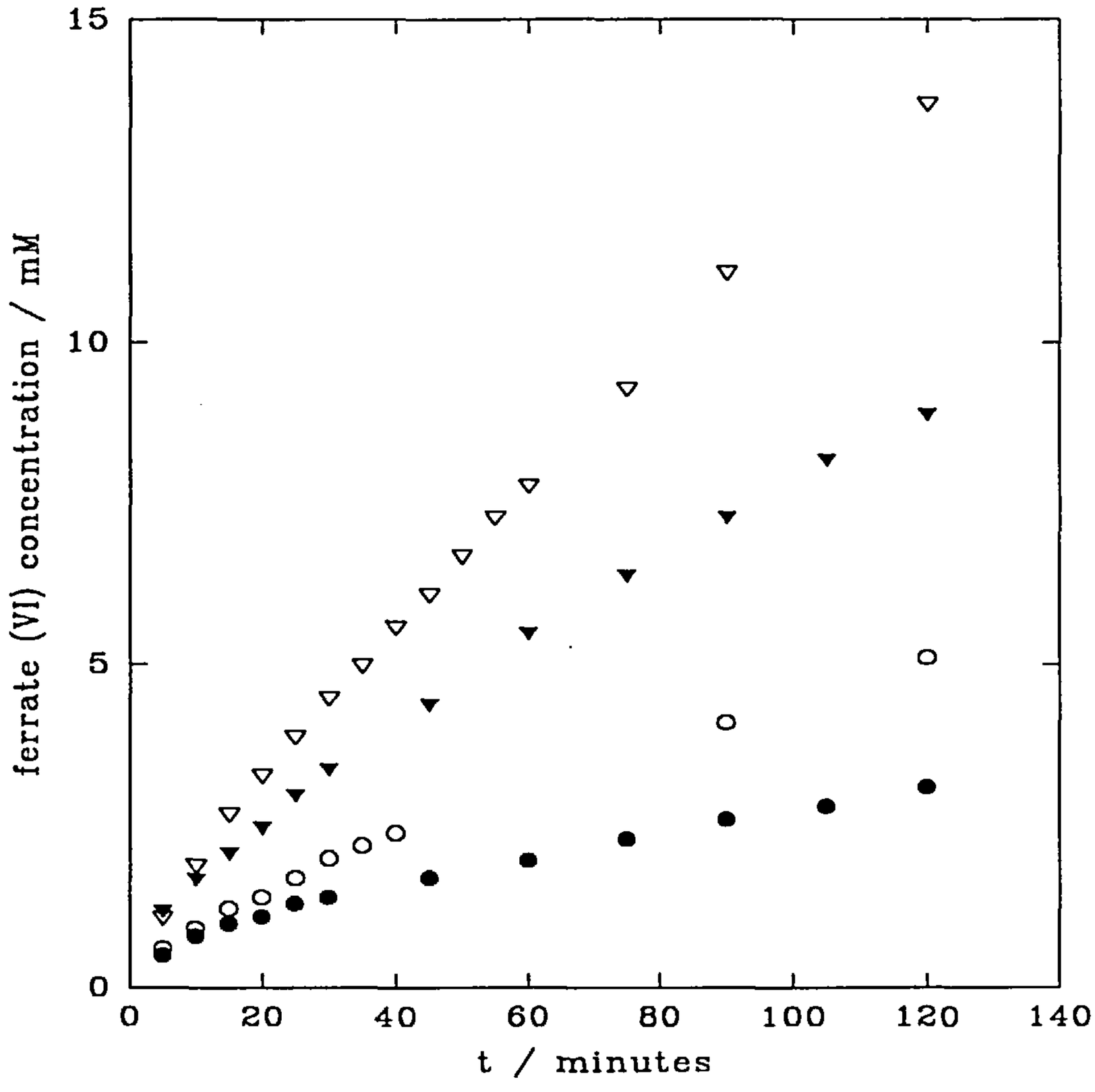

Figure 4.9

Plots of ferrate (VI) concentration vs time for electrolyses at different applied currents in different electrolytes.

○ *1 A in 10 M NaOH* ● *1 A in 10 M NaOH with 0.1 mM NaCl*

▽ *5 A in 10 M NaOH* ▼ *5 A in 10 M NaOH with 0.1 mM NaCl*

These results show that the addition of 0.1 mM chloride ions to the electrolyte does not prevent the formation of the oxide/hydroxide responsible for the drop in current efficiency.

A further electrolysis was carried out in 10 M NaOH with 10 mM NaCl as the electrolyte at a constant current of 1 A. The solution turned purple in the first 5 minutes. however as time progressed the anolyte turned a brown colour and pieces of the anode

were seen floating around in it. When the cell was dismantled the strands of wire that made up the anode had all been broken and they had a rusted all the way through.

In conclusion the addition of chloride ions to the electrolyte did not improve the current efficiency for the formation of ferrate (VI) on the iron wool anode in the flow cell.

(III) Current reversal.

There have been several reports in the literature that current reversal techniques [121] or ac current [128] improve the current efficiency on flat plate anodes

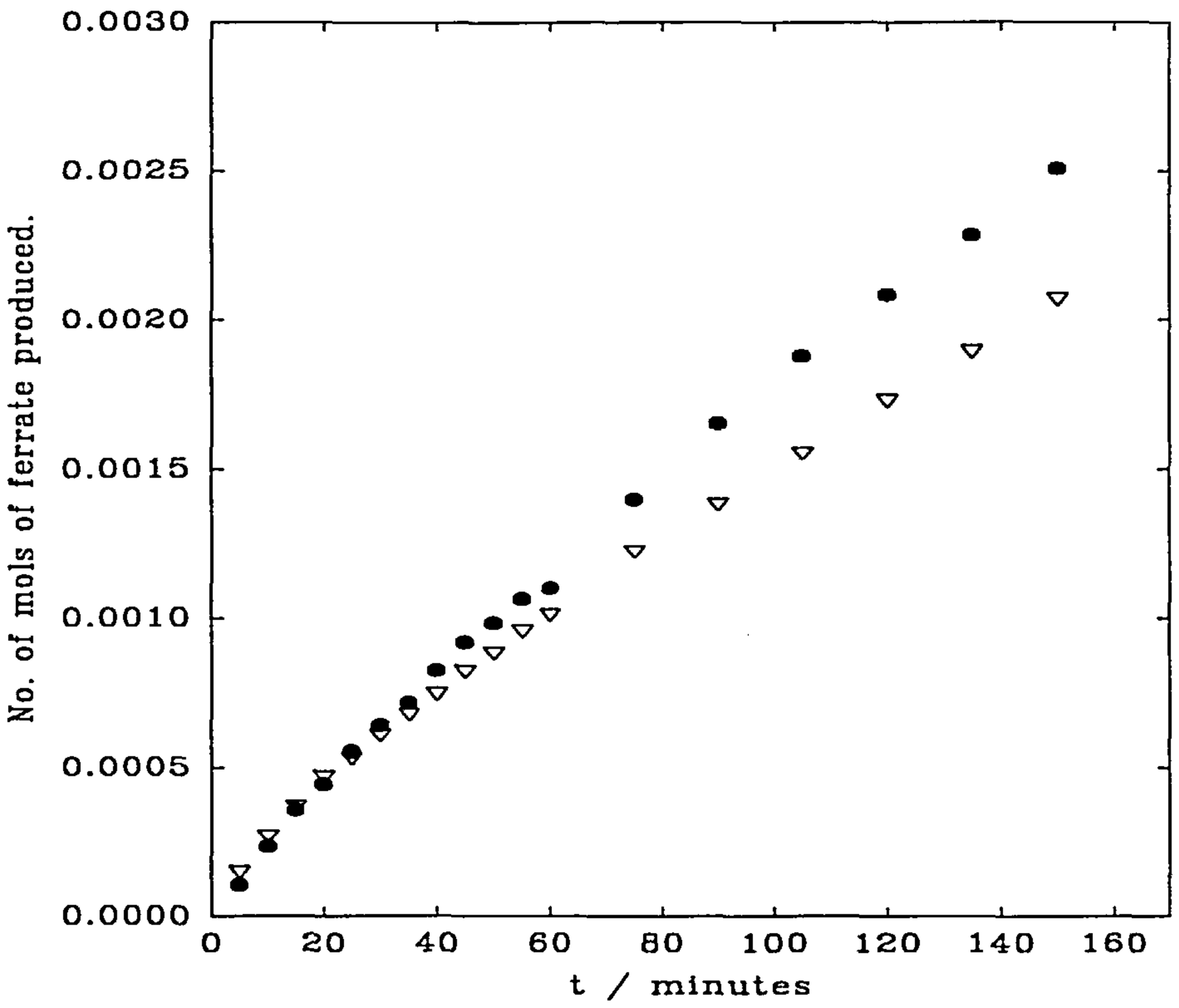

Figure 4.10

Plots of the number of mols of ferrate (VI) formed vs time for an electrolysis on an acid washed anode in 10 M NaOH at ∇ 1 A and an electrolysis where the period of anodic dissolution was 15 minutes followed by a current reversal for 5 minutes in 10 M NaOH at ● 1 A.

An electrolysis was run in 10 M NaOH with an acid cleaned anode at 1 A. When the current efficiency had reached a steady value the electrolysis was stopped and the electrolyte changed for a fresh 10 M NaOH solution. A cathodic current was applied for 5 minutes and then an anodic current was passed through the iron wool anode. This current reversal regime was then continued for the remainder of the electrolysis.

As expected the solution turned purple and oxygen was evolved. there was no sign of ant ferrate (VI) decomposition products. When the cell was dismantled at the end of the experiment it was found that the electrode surface was black. The change in the amount of ferrate (VI) formed vs time is shown in figure 4.10.

The plot shows that for the acid washed anode the increase in the amount of ferrate (VI) formed increases in the same manner as the previous electrolyses. The amount of ferrate (VI) formed in the reverse current electrolysis follows a similar trend. In fact it is clear from the plot that there is more ferrate (VI) being formed in the reverse current experiment than the normal electrolysis. The data was used to calculate the current efficiency for the electrolyses.

In the normal electrolysis the ratio of ferrate (VI) to oxygen formed is relatively high, (a current efficiency of 30 %), but as the reaction proceeds this ratio changes to favour the oxygen evolution reaction and the current efficiency at the end of the reaction has fallen to 14 %. For the reverse current electrolysis the ratio of ferrate (VI) to oxygen increases for the first 15 minutes and at the end of the electrolysis the current efficiency was 18 %.

The experimental results show that higher concentrations of ferrate (VI) are achieved by periodically reversing the current to the working electrode. There was no evidence that any of the ferrate (VI) was being reduced during the reverse current phase however it would be unlikely to think that none had occurred. This may account for a small loss in current efficiency especially at longer times when the concentration of ferrate in solution was high. However, the fact that the current efficiency is decreasing at a slower rate indicates that reversing the current reduces some of the oxide on the anode surface back to a condition where ferrate (VI) formation is more favourable. Given that the oxide on the anode was still black at the end of the reaction shows that it was not completely removed under the conditions used.

Applied current for anodic dissolution / A	Time for anodic dissolution / mins	Applied current used in reversal phase / A	Time of reversal phase / mins	current efficiency after 5 mins / %	Current efficiency after 150 mins/ %
1	150	0	0	29	12
1	5	1	5	22	10
1	15	1	5	19	15
1	15	5	5	32	8
1	5	5	15	28	6

Table 4.4

Summary of results from the electrolyses with current reversal.

Some further electrolyses with current reversal were carried out where the duty cycle or current was varied and the results are reported in table 4.4. In no condition investigated could a further improvement in current efficiency be obtained.

4.5 ferrate (VI) synthesis in low alkali concentration electrolyte.

From the experiments discussed so far it has been shown that, in 10 M NaOH, ferrate (VI) can be synthesised in with reasonable current efficiencies and good yields. This means that using a flow cell and an iron wool anode a solution of ferrate (VI) could be prepared in high enough concentrations where it could be precipitated out as a solid, or be bled directly into an effluent stream. The other option that was suggested at the beginning of chapter 3 was to produce the ferrate (VI) directly in the effluent stream where the alkali concentration would be low. The problem with this procedure is that even in 1 M NaOH solution, ferrate (VI) is very unstable and they decompose in a matter of minutes.

An electrolysis in 1 M NaOH with an applied current of 1 A was performed on a clean anode. The absorbance was measured between 350 and 900 nm. In the first 5 minutes of the electrolysis the anolyte turned a very pale purple. The absorbance of the anolyte increased for 60 minutes after which it seemed to become constant for 4 hours, see figure 4.11. Thereafter, the solution began to take on a faint yellow colour. Within 1 hour of this happening the solution had turned orange. During no stage of the reaction did the temperature of the anolyte change. At the end of the reaction the electrode had a coating of black oxide on the surface.

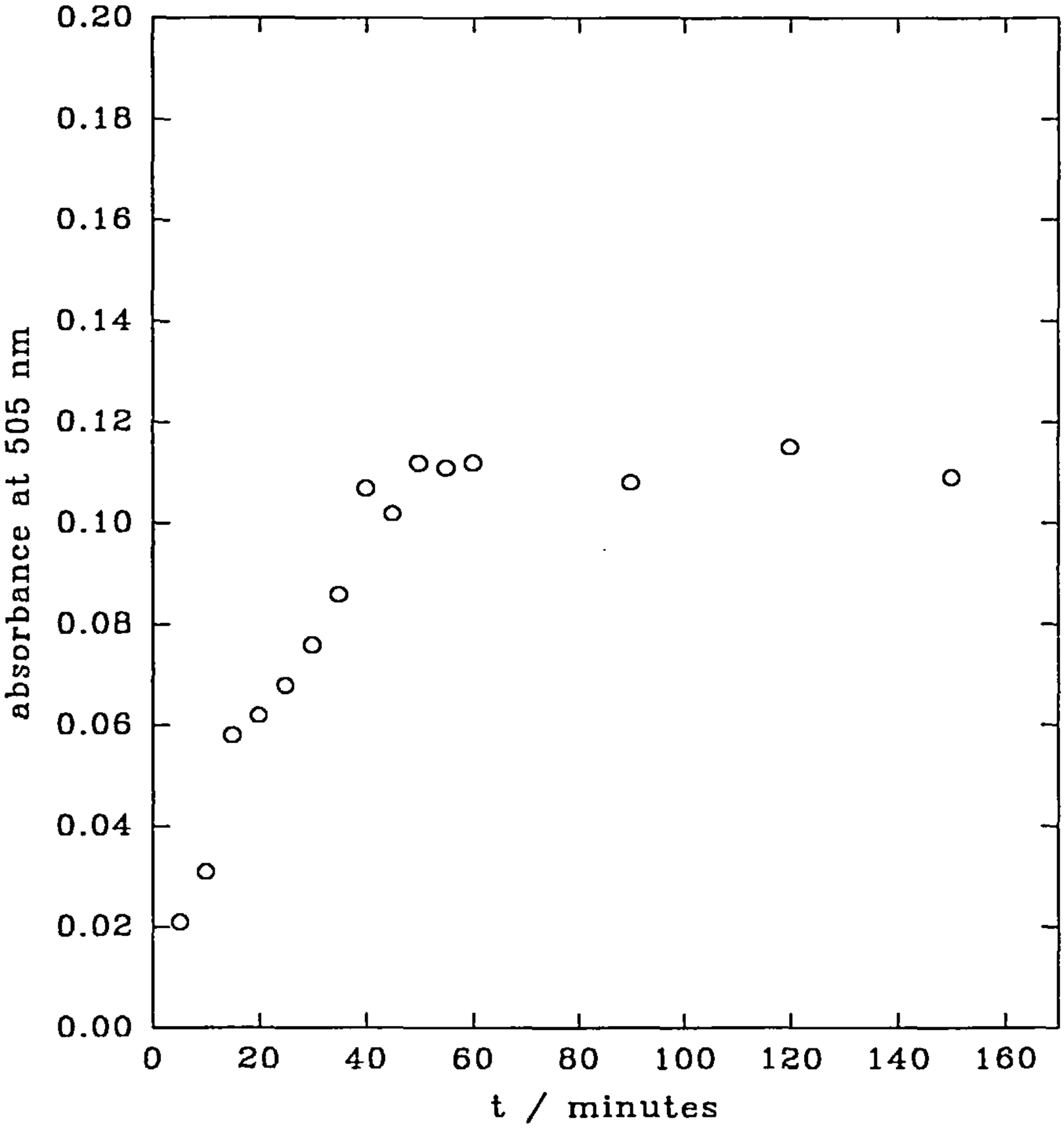

Figure 4.11

Plot of absorbance at 505 nm vs time for the formation of ferrate in 1 M NaOH solution at 298 K with an applied current of 1 A.

From the data it must be assumed that in the first 60 minutes of the electrolysis ferrate (VI) is being formed faster than it can decompose. It has already been reported in chapter 3 that in 1 M NaOH the ferric oxide/hydroxide formed by the reaction of ferrate (VI) with water in 1 M NaOH enhances the rate of decomposition. Thus, it must be assumed that this species is not present in high enough concentration in the anolyte to catalyse. ferrate (VI) decomposition. However, as the experiments proceeds the concentration of decomposition products build up and thus the rate of ferrate (VI) decomposition increases. The surface oxide species on the anode also changes, and the

ratio of ferrate (VI) to oxygen is decreased. The combination of these two factors means that the ferrate (VI) is decomposing as fast as it is made thus the concentration of ferrate in the anolyte remains constant. In the extreme case, at longer times, it can be seen that ferrate (VI) is decomposing faster than it can be formed resulting in its complete elimination from the anolyte.

[NaOH] / M	Current efficiency after 5 mins / %	current efficiency after 150 mins / %
0.1	0	0
1	1	0
2	2	0
5	37	11
10	45	22

Table 4.5

Summary of the results for electrolyses in anolytes with different NaOH concentrations at an applied current of 1 A.

Table 4.5 reports the current efficiency for ferrate (VI) formation in several sodium hydroxide concentrations. With 5 M NaOH, the efficiency is only slightly worse than in 10 M NaOH but, when the NaOH concentration is 1 M or 2 M, the efficiency is negligible. In 0.1 M NaOH there is no evidence that ferrate (VI) ever forms.

4.6 Summary of conclusions.

From the experiments reported in this chapter it has been shown that using a membrane flow cell with an anode fabricated from iron wool allows the formation of ferrate (VI) in acceptable concentration at a reasonable rates and good yields. The rate at which the ferrate (VI) is formed increases with increasing applied current but the current efficiency for the electrolysis was found to be the highest when an applied current of 1 A was used in the synthesis.

The ferrate (VI)/oxygen ratio always falls during the electrolysis but appears to reach a steady state value. This is due to a change in the structure, thickness or composition of the oxide/hydroxide on the anode surface. This change occurs faster at high applied currents.

Increasing the temperature of the anolyte increases the rate at which the ferrate (VI) is formed. However, the rate at which ferrate (VI) decomposes occurring at a much faster and there is no overall increase in current efficiency.

The best method for removing the oxide/hydroxide film is by washing the anode material in acid. However, this would need to be done on a regular bases as the results show that the current efficiency reaches a steady value after only 60 minutes. This does not prove to be a practical approach. Current reversal techniques allow the formation of ferrate (VI) to occur at higher current efficiencies as they reduce the rate at which the inhibiting oxide is formed. It is possible to produce more concentrated ferrate (VI) solutions using this method when compered to the normal electrolyses. It was shown that in the cell used in these experiments the best duty cycle was to apply an anodic current of 1 A for 15 minutes followed by a reverse current of 1 A for 5 minutes.

As the concentration of NaOH in the electrolyte is lowered, so is the amount of ferrate (VI) produced. For anolytes with NaOH concentrations less than 5 M ferrate (VI) is never the major product of the electrolyses. It is possible to produce low concentration ferrate (VI) solutions in 1 M NaOH, but these are only stable for a few hours. As the ferrate (VI) decomposes in the cell the colloidal ferric oxide/hydroxide species forms and thereafter catalyses ferrate (VI) decomposition.

Chapter 5

Effect of anode composition on ferrate (VI) synthesis.

5.1 Introduction.

It has been established in the previous two chapters that ferrate (VI) can be formed by the transpassive dissolution of an iron anode in 10 M NaOH solution. In the reports by Grubb *et al.*[121] and Pick [120] the composition of steels used in the anode were shown to influence the amount of ferrate (VI) produced in the electrosynthesis. Unfortunately the exact composition of the anodes were not reported and only three were examined. In this chapter, the effect of anode composition on ferrate (VI) synthesis will be discussed; in particular, the role of carbon content will be examined.

5.2 Voltammetry of different steels.

A cyclic voltammogram of alloy (E) (C 0.90 %) was recorded between -1.35 V vs Hg/HgO and +0.6 V vs Hg/HgO in 10 M NaOH at a sweep rate of 250 mV s^{-1}. The electrode was removed and polished before being placed back in the cell. The potential was held at +0.7 V for 100 seconds before the current potential curve was recorded again between +0.7 V vs Hg/HgO and -1.35 V vs Hg/HgO.

On the first sweep there were a series of oxidation peaks occurring between -1.0 V vs Hg/HgO and 0.0 V vs Hg/HgO. The current levelled out and no other oxidation peaks were seen until oxygen evolution. On the reverse scan no reduction peaks were recorded until the potential had reached -0.8 V vs Hg/HgO. When the potential was held at +0.7 V vs Hg/HgO and scanned, a new reduction wave was seen at -0.3 V vs Hg/HgO, (see figure 5.1). The solution around the surface of the electrode had turned purple during the period when the potential was held at +0.7 V.

From figure 5.1 it can be seen that alloy E exhibits all the same oxidation and reduction peaks that were recorded on an iron disc electrode, alloy C (C 0.20) (figure 3.18). However, the peak current density for the reduction occurring at

E_p = - 0.3 V vs Hg/HgO is much larger than that recorded for alloy C under the same conditions.

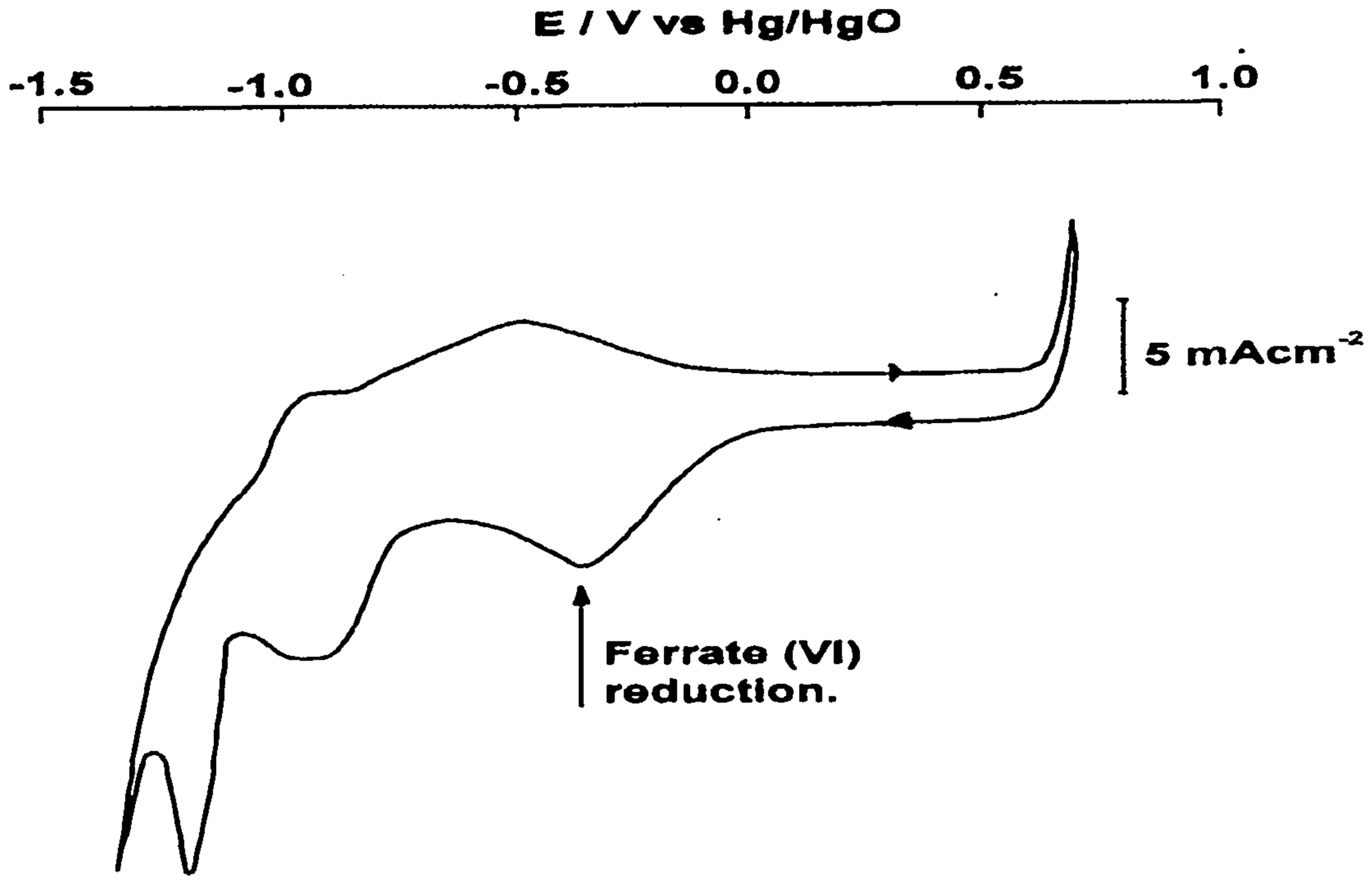

Figure 5.1

Cyclic voltammetry of a high carbon steel electrode (alloy E) between +0.7 V vs Hg/HgO and -1.35 V vs Hg/HgO in 10 M NaOH at a sweep rate of 250 mV s^{-1}. Prior to recording the voltammogram the potential was held at +0.7 V vs Hg/HgO for 100 seconds.

The experiment was repeated on alloys A to G. The resulting voltammograms exhibited the same features as that shown in figure 5.1. It was however, noted that changing, the alloy used as the anode material, altered the peak current density for the reduction of ferrate (VI). The largest reduction peak was recorded on alloy E, while the smallest was recorded on alloy A. Thus from these experiments it can be concluded that, the composition of the alloy does seem to effect the amount of ferrate (VI) produced by the transpassive dissolution of the anode material.

5.3 Effect of alloy composition on ferrate (VI) formation.

It has been shown that the reduction of ferrate (VI) on iron containing electrodes produces well defined responses. An experimental procedure was developed where:

a) A constant current , usually the same value used in (c), was passed for 100 seconds to ensure that the alloy was covered in a pseudo steady state film of oxide hydroxide.

b) A fast stream of N_2 was passed for a few seconds to remove from the vicinity of the electrode surface, all the ferrate (VI) formed.

c) Ferrate (VI) was formed using a constant anodic current for 20 seconds.

d) The electrode potential was immediately scanned from +0.6 V to -0.7 V vs Hg/HgO at 250 mV s^{-1}

The technique described above can only be used as a semi analytical method for the determination of ferrate (VI). There are several points that must be addressed to explain why:

(i) As pointed out before in chapter 4, a porous oxide species must be present on the anode material before ferrate (VI) can be formed. Beck [131] reported that there is a fixation of Fe (VI) species in the oxide pores and although well defined responses can be produced on iron containing electrodes, the presence of the oxide may introduce some undefined errors into the results.

(ii) When the ferrate (VI) is generated, the time used must be long enough as to produce a steady state concentration profile for the ferrate (VI) ions. Once the steady state is reached, increasing the generation time will not result in an increase in the reduction peak current density.

(iii.) As ferrate (VI) is generated in competition with oxygen, there is some risk that ferrate (VI) ions may be displaced into the bulk solution by the stirring effect of oxygen bubbles.

Using the pulse ramp technique, a series of linear sweep voltammograms was recorded for electrode materials E, D, C and A. Figure 5.2 shows the current/potential responses for the experiments described above. While in all experiments, a cathodic peak for the reduction of ferrate (VI) was observed, the peak

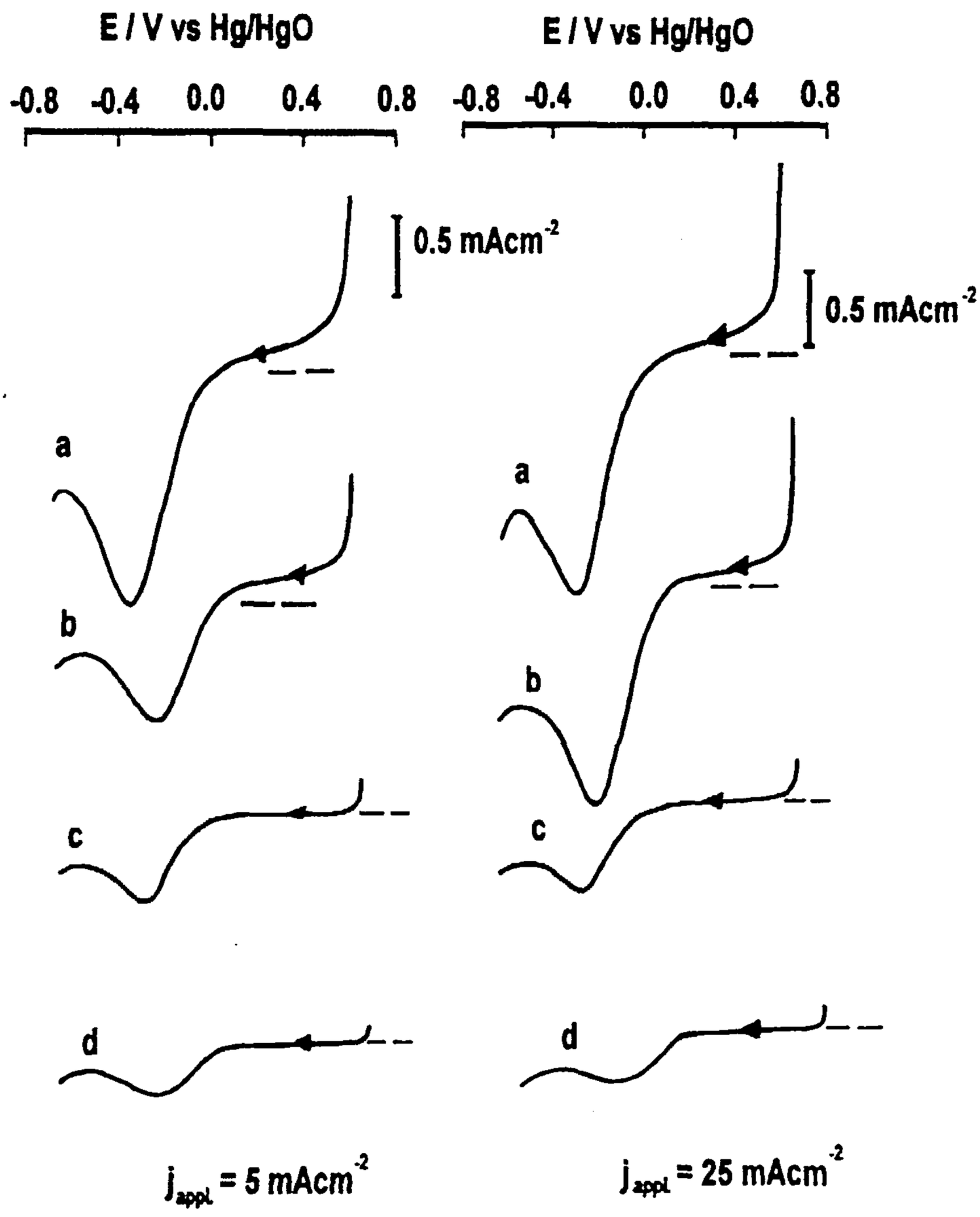

Figure 5.2

Current/potential curves to monitor the formation of ferrate (VI) during a constant current pulse for 20 seconds. The iron alloys were pre-treated by passing the same current density for 100 seconds and then dispersing the ferrate (VI) formed during this pre-treatment with a fast stream of nitrogen. The current densities are shown on the figure and the alloys used were **a** *alloy E (C 0.90 %),* **b** *alloy D (C 0.65 %),* **c** *alloy C (C 0.20 %) and* **d** *alloy A (C 0.04 %). Temperature 298 K. Potential scan rate 250 mV* s^{-1}

current densities vary greatly with the different alloy materials. With a current density of 5 mA cm^{-2} and at alloy E the ferrate (VI) reduction peak was some five times larger than alloy A. Moreover, it can be seen that the trends were the same with both current densities used in the ferrate (VI) generation phase. The reduction peak current densities were slightly larger at 25 mA cm^{-2}, reflecting a higher rate of ferrate (VI) production, (although not higher current efficiency). Two other features of the curve should be noted. Firstly, at the positive limit for these scans, +0.6 V vs Hg/HgO, there was significant anodic currents for alloys D and E but not for alloys A and C. Secondly, the peak potentials for the ferrate (VI) reduction also varied slightly between -0.25 V (alloy D) and -0.4 V vs Hg/HgO (alloy E).

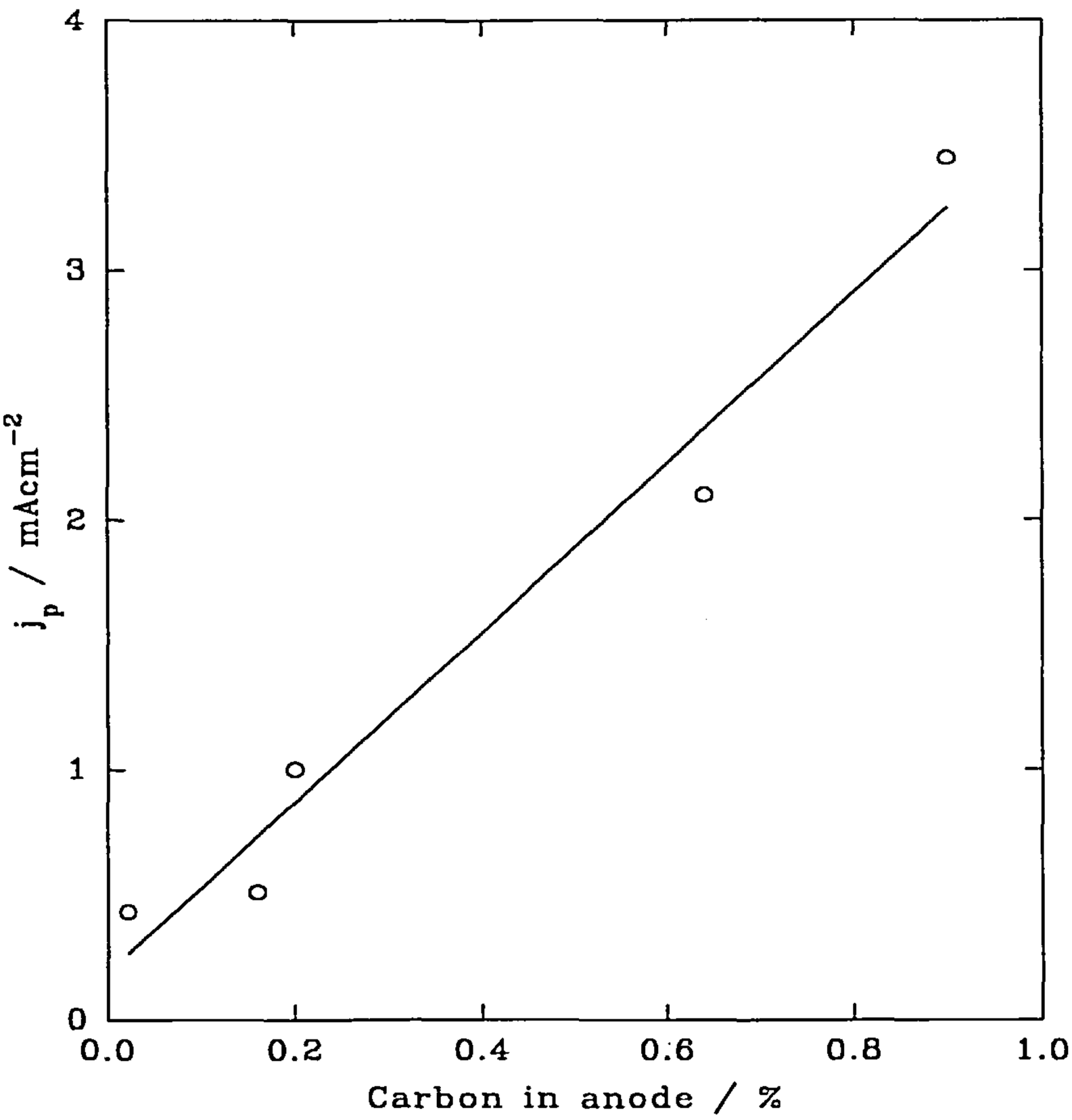

Figure 5.3

Plot of peak current density for the reduction of ferrate (VI) formed during a constant pulse (5 mA cm^{-2} for 20 seconds) vs the carbon content in the iron alloy.

Figure 5.3 shows the plot of reduction peak current density vs the percentage of carbon in the iron alloy anode and it can be seen that there is a good linear correlation. Visual observation also supports this trend shown in the voltammetry. At alloys D and E, the purple ferrate (VI) ion could be seen to accumulate at the anode surface during the constant current pulse. The ferrate (VI) was poorly visible on the other alloys.

The major elements found in the alloys tested were silicon and manganese, but there was no correlation between the percentage of these elements and the rate of ferrate (VI) formation. As was reported in the other sections of this chapter as well as in chapter 3, the reduction peak potential of ferrate (VI) is strongly related to the nature of the oxide/hydroxide formed on the electrode surface as well as electrode material and thus the observed shift in the peak potential was expected.

5.4 Electrosynthesis of ferrate (VI) on flat plate anodes.

(I) Alloy E.

The alloys used in the pulse ramp experiments were supplied in a form that made the suitable only as two dimensional electrodes. A flat plate electrode (diameter 4 cm) was polished and placed in a pipe cell. The electrolyte, 10 M NaOH was added to the cell and a constant current of 1 mA cm^{-2} was passed. The concentration of ferrate (VI) produced was calculated form the absorbance at 505 nm. Upon applying the current the surface of the anode was immediately covered in a layer of fine bubbles. After 2 minutes the surface of the disc turned purple and ferrate (VI) ions began to diffuse into the bulk solution. As more charge passed the intensity of the purple anolyte increased. No ferrate (VI) was observed crossing through the glass frit into the catholyte compartment.

Figure 5.4 shows a plot of current efficiency vs time for the ferrate (VI) reaction. Initially the current efficiency is very high, around 70 % but, it dropped quite rapidly and after 1 hour to a value of 28 %.

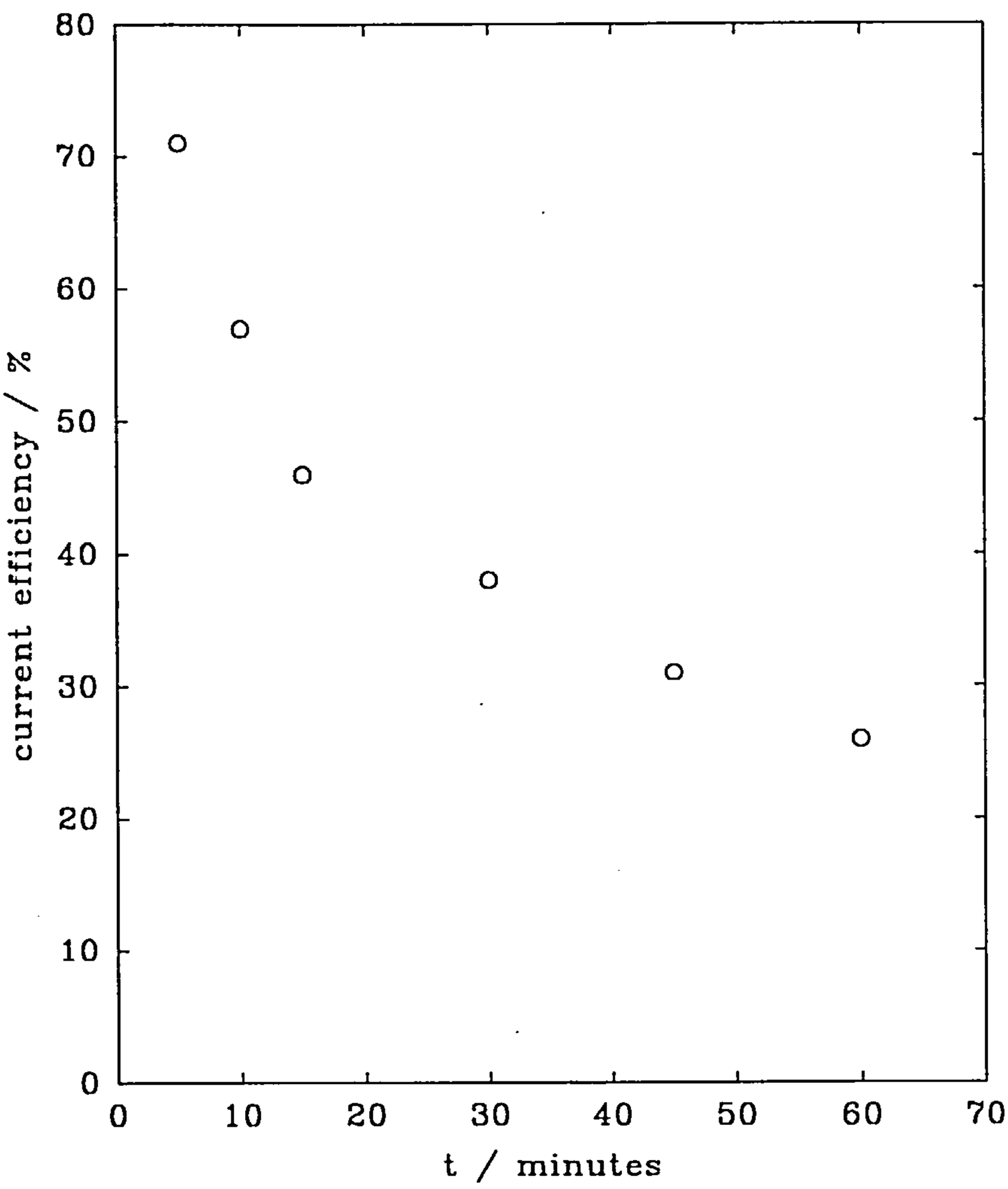

Figure 5.4

Plot of current efficiency vs time for the formation of ferrate (VI) on electrode E in 10 M NaOH with an applied current density of 1 mA cm^{-2}

The decrease must be due to changes in the corrosion film on the surface of the electrode. This is similar to what was seen in the flow cell experiments. The experiment was repeated over a range of current densities from 0.5 mA cm^{-2} to 25 mA cm^{-2}. The plots of current efficiency vs time are shown in figure 5.5.

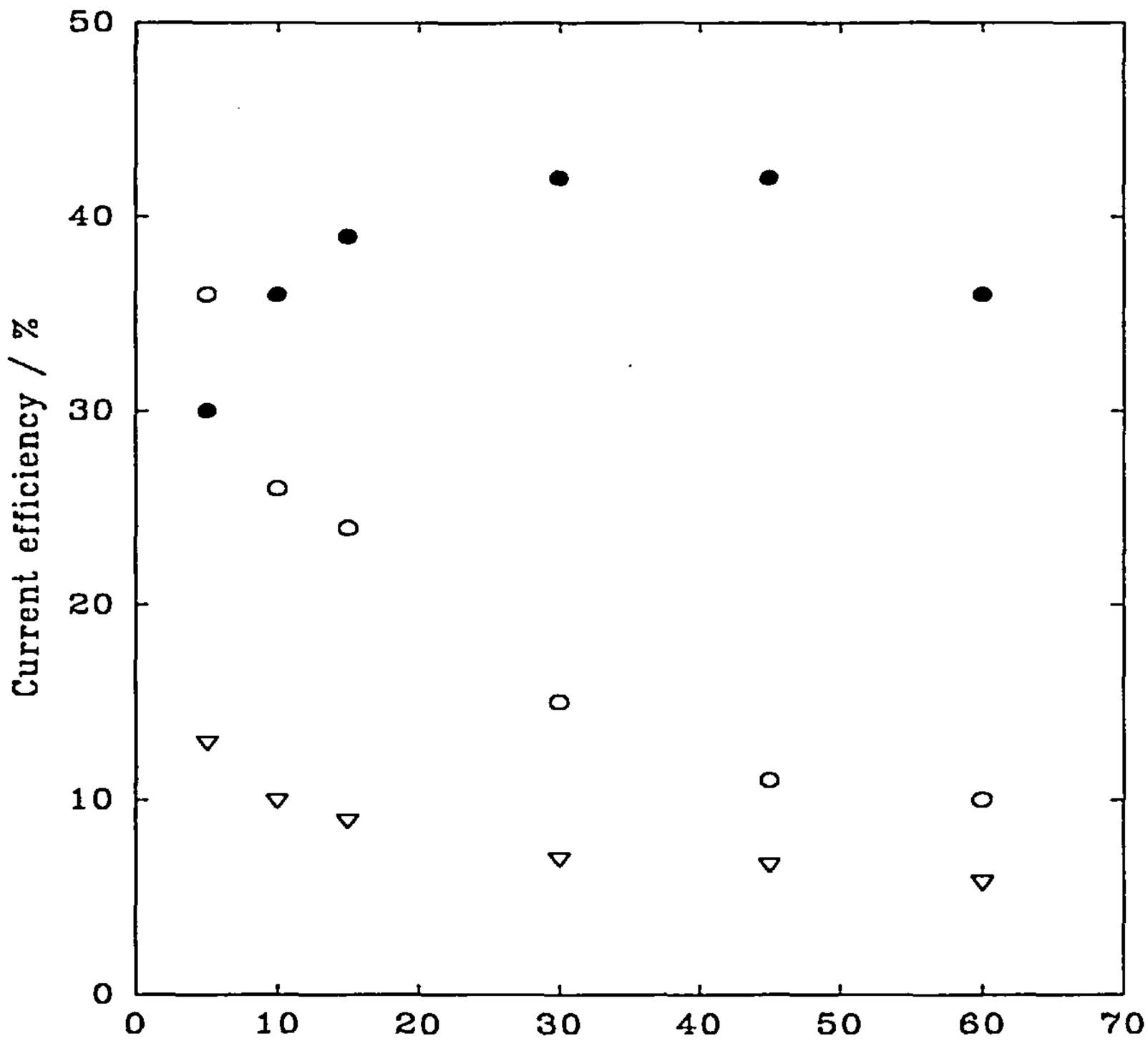

Figure 5.5

Plots of current efficiency vs time for the generation of ferrate (VI) on alloy (E) in 10 M NaOH at 298 K. The applied currents used were

∇ *25 mA* cm^{-2} O *10 mA* cm^{-2} ● *0.5 mA* cm^{-2}.

With the lowest current density the current efficiency for the formation of ferrate (VI) increases initially with time until reaching a value of 40 % afterwhich it decays slowly. For the higher current densities the current efficiency falls with time and the higher the applied current density the lower the corresponding current efficiency. For the 0.5 mA cm^{-2} electrolysis the initial increase in current efficiency must reflect a change in the anode surface layer which improves the selectivity of the desired reaction. However,

as with the electrolyses performed at the other current densities the surface film changes, causing the current efficiency to fall. The highest current efficiency occurred at a current density of 1 mA cm^{-2}. As with the flow cell electrolyses, the most ferrate (VI) was generated when high current densities were used.

(II) Other alloys.

Figure 5.6 compares the performance of three alloys, E, F, G and iron in electrolyses carried out at 1 mA cm^{-2}. Although the current efficiencies fall with reaction time it is clear from the plots that the current efficiency is higher for the alloy with the highest carbon content. Alloys F C 0.22 % and G C 0.25 % have similar carbon content and this is reflected by nearly identical current efficiency values throughout the electrolyses.

The current efficiency for the formation of ferrate (VI) could increase either by improved transpassive dissolution or a reduction on the rate at which oxygen is evolved. In order to investigate these possibilities current potential curves were recorded on alloy A C 0.04 % and alloy E C 0.90 % after the surface of the electrode had been pre-treated to form the passive layer by passing a constant current density of 5 mA cm^{-2} for 1000 seconds. Figure 5.7 shows the curves for the electrodes in 10 M NaOH recorded at a potential scan rate of 2.5 mV s^{-1} between 0.65 V vs Hg/HgO and 0.85 V vs Hg/HgO.

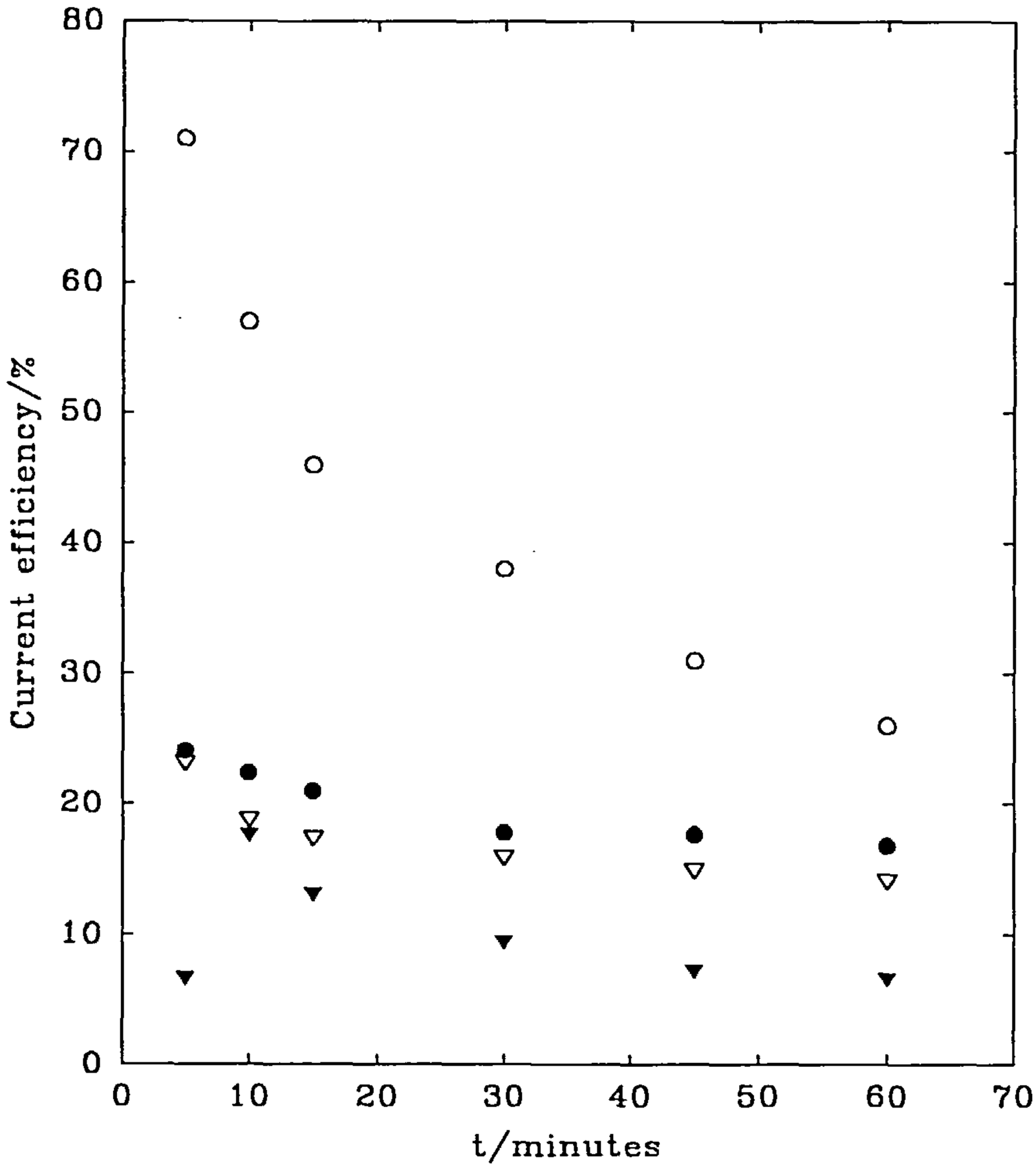

Figure 5.6

Plots of current efficiency vs time for the generation of ferrate (VI) in 10 M NaOH with an applied current of 1 mA cm^{-2}. Alloys used were

○ *E (C 0.90 %)* ∇ *F (C 0.22 %)* ● *G (C 0.25 %)* ▼*Fe (C 0.08 %)*

It can be seen that over this potential range the current density was significantly higher for alloy E, clearly confirming that the improved current efficiency in ferrate (VI) generation results from an increased rate of iron dissolution.

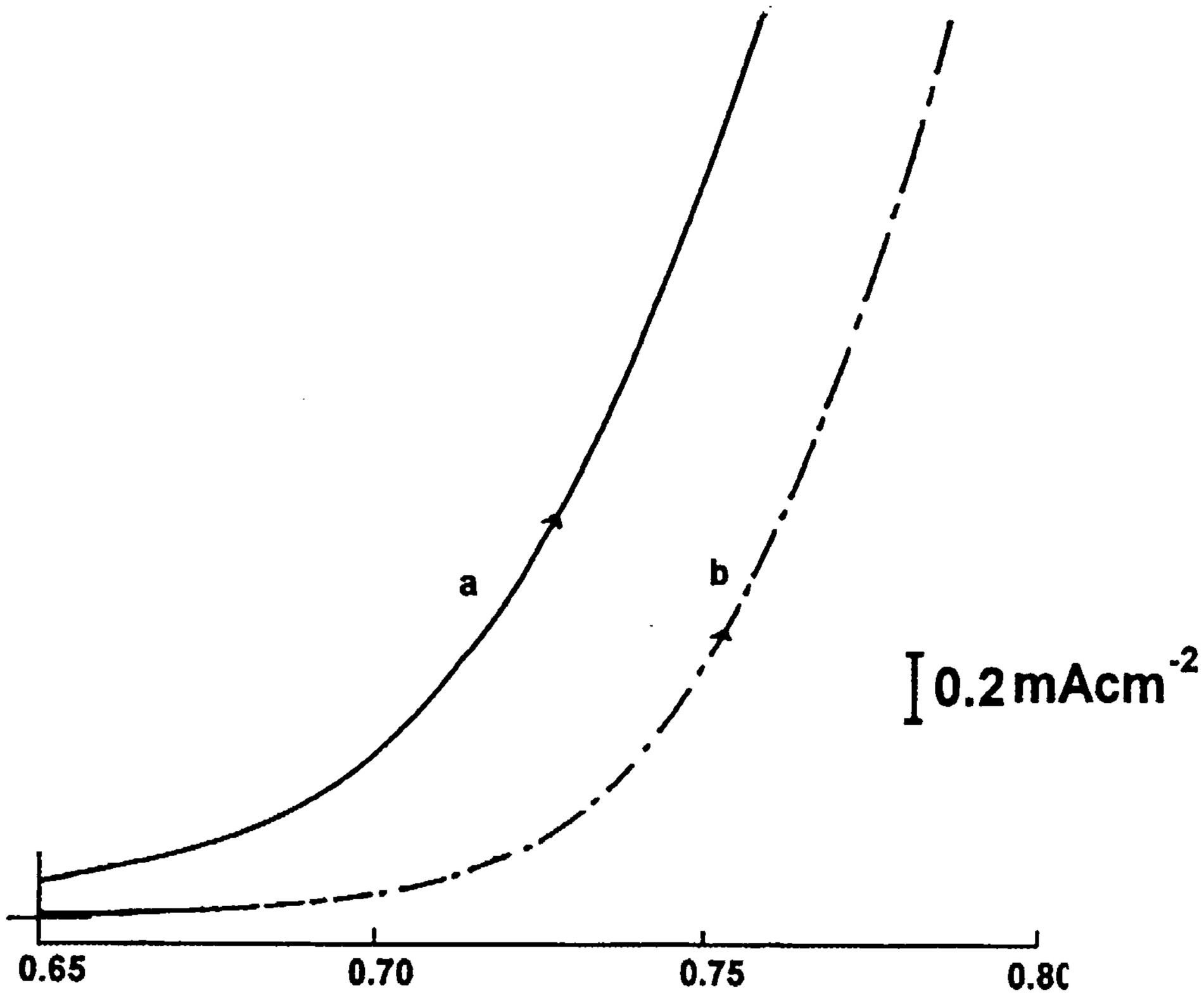

Figure 5.7

Current potential curves for (a) alloy E C 0.90 % and (b) alloy A C 0.04 %. The alloys were pre-treated by passing a constant current density of 5 mA cm^{-2} for 1000 seconds then dispersing the ferrate (VI) formed with a fast stream of nitrogen. Temperature 298 K. Potential scan rate 2.5 mV s^{-1}.

The results from the experiments pose the question. Why do iron alloys with high carbon contents dissolve more readily in 10 M NaOH, to form ferrate (VI)? The alloys used in these studies all have low non-ferrous metal content and such carbon steels are produced for their mechanical properties, including hardness, corrosion resistance and strength.[135] This information, however, relates to conditions of active corrosion, or more commonly, those where the surface is passivated. Ferrate (VI), on the other hand, is produced in the transpassive region. Carbon steels have a structure two phases

coexist. In alloys with low carbon contents, iron and iron carbide coexist. The structure is made up of many small grains with crystals of iron carbide at the inter grain boundaries. Increasing the carbon content further to 0.5 % results in the formation of a solid solution of iron carbide and iron along with iron carbide. These have more complex structures and laminar arrangements of the phases are found. We have found that the current efficiency for the formation of ferrate (VI) appears to increase smoothly through the structural changes. It may be possible that the carbon modifies the properties of the oxide layer. Irish *et al.* [106] reported that carbon activates the grain boundaries in carbon alloyed steels by preventing the formation of a passivating layer even though the rest of the grain is protected.

5.5 Effect of conditioning times on the formation of ferrate (VI).

(I) Alloy E

Alloy E was cleaned and polished and replaced in the cyclic voltammetry cell with 10 M NaOH. A series of electrolyses were carried out by applying a constant current density of 25 mA cm^{-2} for 20 seconds. The surface conditioning pulse was applied for 10 seconds. The current potential curve, shown in figure 5.8, curve (a), showed a reduction peak at -0.4 V vs Hg/HgO.

The experiment was repeated at conditioning times of 100 seconds, 400 seconds and 1000 seconds. The resulting voltammograms are shown in figure 5.5, curves (b) to (d). From the voltammograms it is clear that the reduction peak current density falls with increasing conditioning time. There is also a shift in the reduction peak to more positive potentials as the amount of conditioning is increased. Visual observations of the electrolyte showed that, at conditioning times greater than 400 seconds the electrolyte turned a faint purple colour, as the ferrate (VI) was formed, and it needed to be changed before the next experiment could be run. It is most probable that it is the change in the surface film formed on the electrode surface during the conditioning that results in the decrease in the ferrate (VI) reduction peak current density.

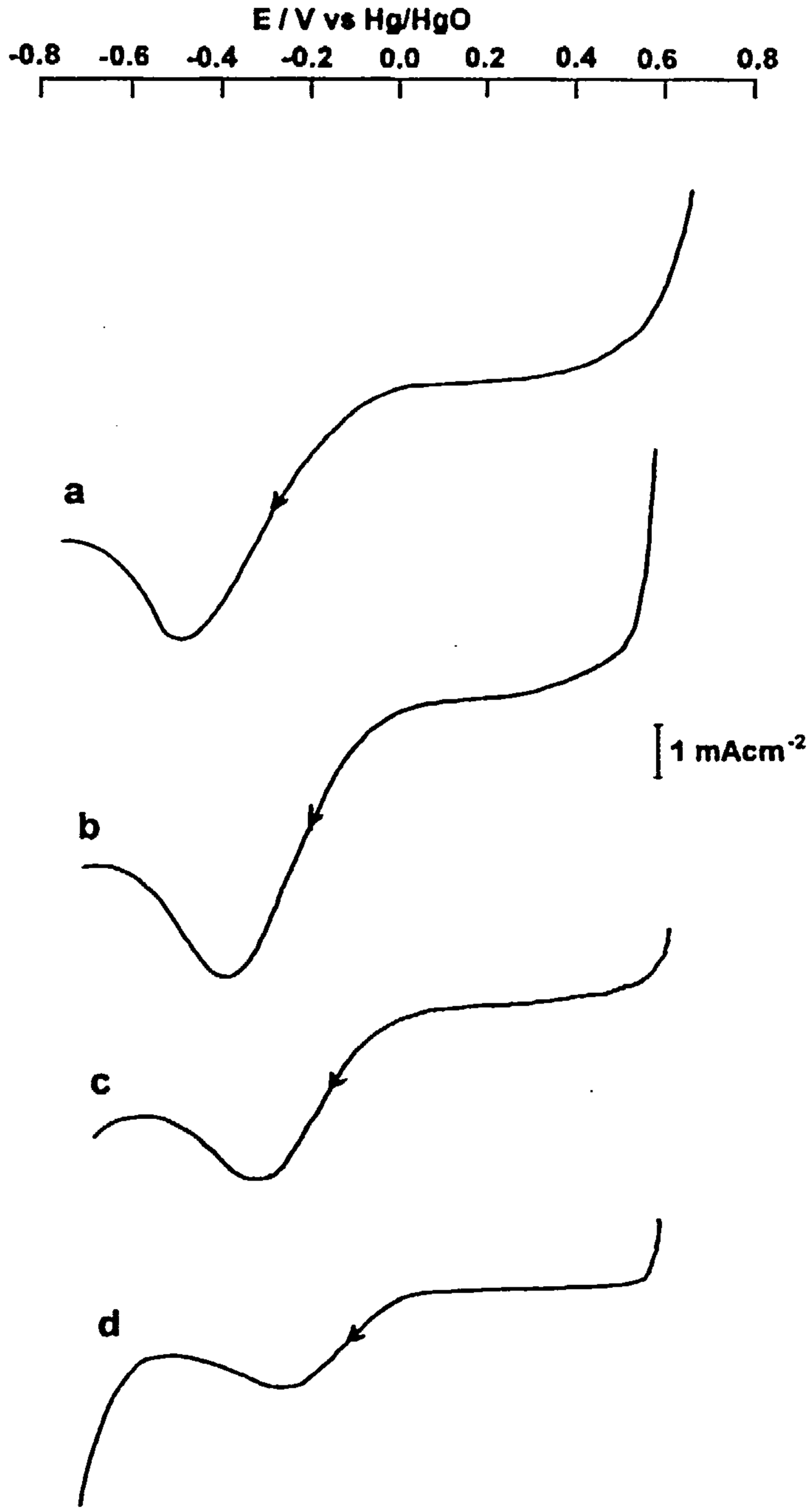

Figure 5.8

Linear sweep voltammograms recorded on alloy E at a sweep rate of 250 mV s^{-1} in 10 M NaOH. The ferrate (VI) was generated by applying a constant current density of 25 mA cm^{-2} for 20 seconds. Immediately prior to the generation, the surface of the electrode was conditioned by applying a constant current density of 25 mA cm^{-2} for (a) 10 seconds, (b) 100 seconds, (c) 400 seconds and (d) 1000 seconds.

Conditioning current density / mA cm^{-2}	Current density applied to generate ferrate (VI) / mA cm^{-2}	Conditioning time / s	Reduction peak current density / mA cm^{-2}
1	1	10	0.28
1	1	100	0.43
1	1	1000	0.87
5	5	10	2.17
5	5	100	2.30
5	5	1000	1.70

Table 5.1

Summary of results obtained from linear sweep voltammograms recorded on alloy E in 10 M NaOH. The ferrate (VI) was generated by passing a constant current density for 20 seconds. Immediately prior to the experiment the electrode was conditioned for various lengths of time by applying the same current density.

The experiment was run again at different applied current densities of 1 mA cm^{-2} and 5 mA cm^{-2} and the results from the voltammetry is shown in table 5.1.

These results clearly demonstrate that alloy E undergoes transpassive dissolution in 10 M NaOH solution to form ferrate (VI). With 1 mA cm^{-2} being used to condition and generate ferrate (VI), it can be seen that the peak current densities for the reduction have low values, associated with a low rate of ferrate (VI) formation. They do however, increase in size as the charge passed in the conditioning phase is increased.

With 5 mA cm^{-2} ferrate (VI) is formed at a faster rate, hence the larger values for the reduction peaks. The corrosion film formed after 100 seconds seems to provide the best conditions to achieve good current efficiency for the ferrate (VI) reaction. At longer times the current efficiency drops as the charge passed in the conditioning phase is increased. A slight shift towards positive potentials was observed.

(II) Other alloys.

The experiment was repeated on all the other alloys (A to G). with an applied current density of 25 mA cm^{-2} a typical set of responses is shown in figure 5.9.

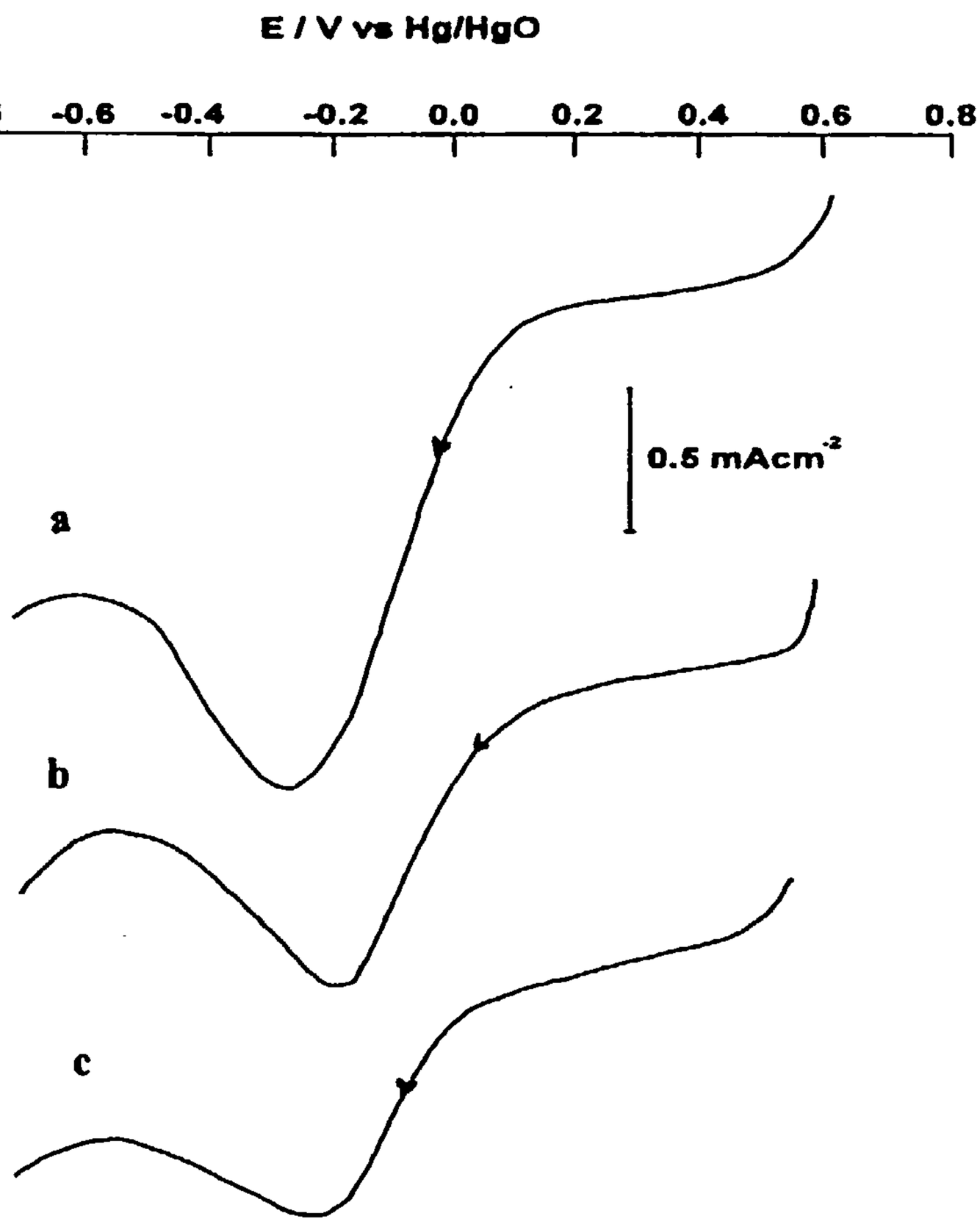

Figure 5.9

Linear sweep voltammograms recorded on alloy B at a sweep rate of 250 mV s^{-1}. The ferrate (VI) was generated by applying a constant current density of 25 mA cm^{-2} for 20 seconds. Immediately prior to the experiment the electrode surface was conditioned by applying a constant current density of 25 mA cm^{-2} for

a) 10 seconds, b) 100 seconds and c) 1000 seconds.

The figure clearly shows that, like alloy E, using a current density of 25 mA cm^{-2}, the current efficiency for the ferrate (VI) reaction falls with increasing charge passed on

the conditioning phase. The reduction peak heights are smaller than those seen on alloy E. This was expected. The other alloys all followed this trend. Repeating the experiments with the same applied current densities used with alloy E it was found that, with 1 mA cm^{-2} being used to condition the electrode as well as generate the ferrate (VI) low values were obtained for the reduction peak current density. However, in all cases increasing the conditioning time caused the reduction peaks to increase. At the higher applied current densities there was always a drop in current efficiency for the formation of ferrate (VI) with increased conditioning time. Also the reduction peak potential for ferrate (VI) moved slightly to more positive potentials as the conditioning time was increased. The reasons for the variations with applied current are not clear.

These results show that, for current densities greater than 1 mA cm^{-2}, as the charge used in the electrolyses is increased the corrosion film on the anode is altered in such a way as to lower the current efficiency of the ferrate (VI) reaction. At low applied currents the rate at which the oxide film is formed and the rate at which it undergoes change is slow and this facilitates the production of ferrate (VI). Increasing the applied current causes the surface film to form faster. The film formed when a charge, equivalent to 5 mA cm^{-2} for 100 seconds, is passed produces a surface which allows ferrate (VI) to be formed in with the highest current efficiency. However, increasing the charge on the conditioning phase, results in the formation of the oxide species whose presence on the anode results in a lowering of the current efficiency.

5.6 Effect of temperature on ferrate (VI) formation on iron alloy anodes.

(I) Alloy C.

In the flow cell experiments it was shown that working at elevated temperatures was not beneficial to the production of ferrate (VI). The pulse ramp experiments described in previous sections have proved to be helpful in the estimating of the amount of ferrate (VI) generated under constant current conditions. It was decided to use this technique to examine the effect that increasing the temperature would have at short times on the electrogeneration of ferrate (VI)

Using alloy C a set of voltammograms were recorded between +0.6 V and -0.7 V vs Hg/HgO at a sweep rate of 250 mV s^{-1}, in 10 M NaOH at 333 K, after a constant current pulse, (5 mA cm^{-2}) was applied for 20 seconds. Immediately prior to the experiment the electrode was conditioned by applying a constant current density of 5 mA cm^{-2} for 10, 100, 400 and 1000 seconds. The electrode was polished after each voltammogram was recorded.

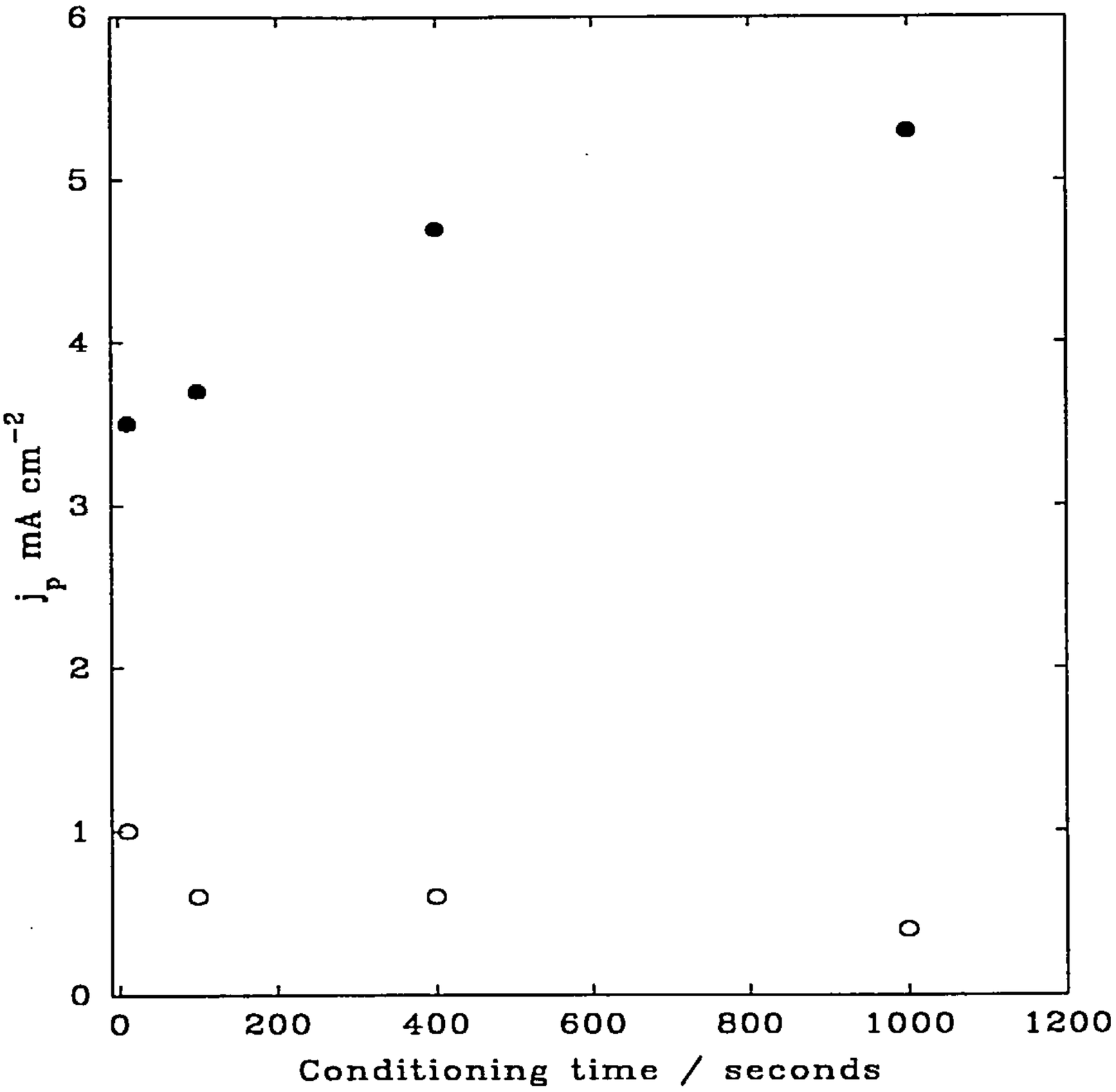

Figure 5.10

Plot of ferrate (VI) reduction peak current density vs time in 10 M NaOH. The ferrate (VI) was generated on alloy C by application of a constant current pulse of 5 mA cm^{-2} for 20 seconds. Immediately prior to this, the surface of the electrode was conditioned by applying the same current density for 10, 100, 400 and 1000 seconds. The scan rate was 250 mV s^{-1}.

O $T = 298\ K$ ● $T = 333\ K$

After 100 seconds the electrode had a black oxide film on the surface of the disc. As the conditioning time increased the film began to change in colour from black to a dark brown. It was also noted that a considerable quantity of ferrate (VI) was being generated during the longer conditioning times and the electrolyte needed to be changed for a fresh solution after each voltammogram was recorded. The potential where the ferrate (VI) reduction occurred shifted considerably from -0.25 V vs Hg/HgO after 10 seconds conditioning to -1.6 V vs Hg/HgO after 1000 seconds conditioning. Figure 5.10 shows a comparison of reduction peak current density vs conditioning time recorded at 298 K and 333 K.

Applied current density / mA cm^{-2}	Conditioning time / s	Reduction peak current density at 298 K / mA cm^{-2}	Reduction peak current density at 333 K / mA cm^{-2}
1	10	0.40	0.81
1	100	0.60	0.81
1	1000	0.91	1.01
25	10	1.12	6.9
25	100	1.01	8.5
25	1000	0.81	17.3

Table 5.2

Summary of results obtained from linear sweep voltammograms recorded on electrode C after ferrate (VI) was generated using a constant current pulse of (1 mA cm^{-2} and 25 mA cm^{-2}) for 20 seconds. Prior to the electrogeneration the electrode was conditioned by applying the same current density used to form ferrate (VI) for 10, 100 and 1000 seconds. Temperature 333 K.

From the plot it is clear that more ferrate (VI) is being generated at 333 K when compared to the corresponding experiment at 298 K. As was shown in section 5.5, at room temperature, the peak current for the reduction of ferrate (VI) decreases with increased conditioning time. At 333 K however, this does not seem to be the case as the

reduction peak current density actually improves with conditioning. The oxide colour seen in this experiment was a different colour to that seen on the iron wool anode used in the flow cell experiments, but this may have been due to the size of the oxide particles or thickness of the layer.

The electrolysis was repeated at 1 mA cm^{-2} and 25 mA cm^{-2} and the results of the voltammetry are shown in table 5.2. The table shows that there is very little difference between the 298 K and 333 K experiments when 1 mA cm^{-2} was used as the pulse current density. Only a slight shift in E_p towards positive potentials was observed as the conditioning time, increased. However, when the applied current density was increased to 25 mA cm^{-2} the peak current density for the ferrate (VI) reduction increases markedly with conditioning time giving values much higher than the corresponding 298 K experiment. As with the previous set of experiments there was a considerable shift towards positive potentials with increasing conditioning time. During the experiments it was noted that at 1 mA cm^{-2} the electrode only became coated in a black/brown oxide after 800 seconds, whereas at 25 mA cm^{-2} the brown oxide was present after 100 seconds. When a cyclic voltammogram was recorded on the oxide coated electrode there were no additional oxidation peaks observed, and it had the same form as that shown in figure 3.18.

From the results, it can be seen that more ferrate (VI) is generated when the temperature is increased from 298 K to 333 K. It would seem from the data collected that the nature of the oxide plays an important role in the electrolyses. The brown oxide formed in these experiments seems to behaves in a different manner to what is expected and actually increases the current efficiency for the ferrate (VI) reaction instead of reducing it.

To see if the same was true for the other iron alloys, the experiment was repeated with alloys B and E using 1, 5 and 25 mA cm^{-2} current densities to generate the ferrate (VI) and condition the electrode. Conditioning times of 10, 100, 400, 800 and 1000 seconds were used. For both electrodes, at all applied current densities a black oxide was formed on the surface of the anode after being conditioned for 100 seconds. This oxide film was the same colour as the one seen on the iron wool anode used in the

flow cell experiments. With both electrodes there was a shift in E_p towards more positive potentials with increased conditioning time.

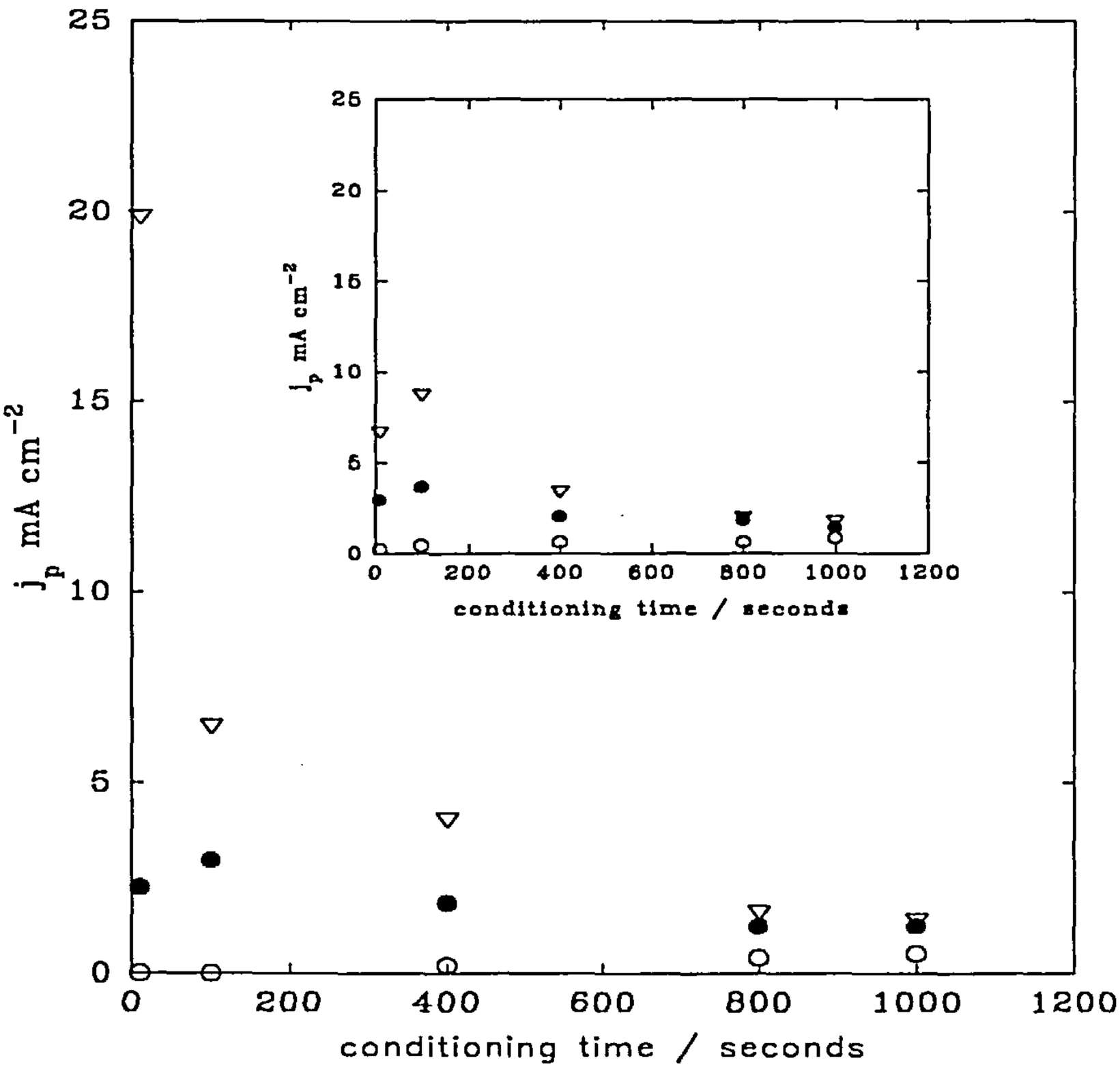

Figure 5.11

Plots of peak current density for the reduction of ferrate (VI) vs time at 333 K in 10 M NaOH. The ferrate (VI) was generated by applying a constant current density for 20 seconds. Immediately prior to this the electrode was conditioned for 10, 100, 400, 800 and 1000 seconds by applying the same current density. The main plot was recorded on alloy E and the inset was recorded on alloy B. The current densities used in the experiment were.

○ 1 mA cm^{-2} ● 5 mA cm^{-2} ∇ 25 mA cm^{-2}.

Figure 5.11 is a plot of ferrate (VI) reduction peak current density vs conditioning time for both alloys B and E. It is evident from the plots that conditioning the electrodes causes the reduction peak current density to drop to a value that is

comparable to that seen in the 298 K electrolyses. This fall in peak current density with conditioning time translates into a very large drop in current efficiency for the ferrate (VI) reaction and hence on these electrodes operating at elevated temperatures offers no positive advantages. It seems that the oxide species formed during the conditioning phase is inhibiting the formation of the ferrate (VI) or catalysing oxygen evolution.

Figure 5.12 shows a cyclic voltammogram of alloy E, still with the black oxide coating the surface, recorded between 0.6 V vs Hg/HgO and -1.35 V vs Hg/HgO at a sweep rate of 250 mV s^{-1} in 10 M NaOH at 298 K.

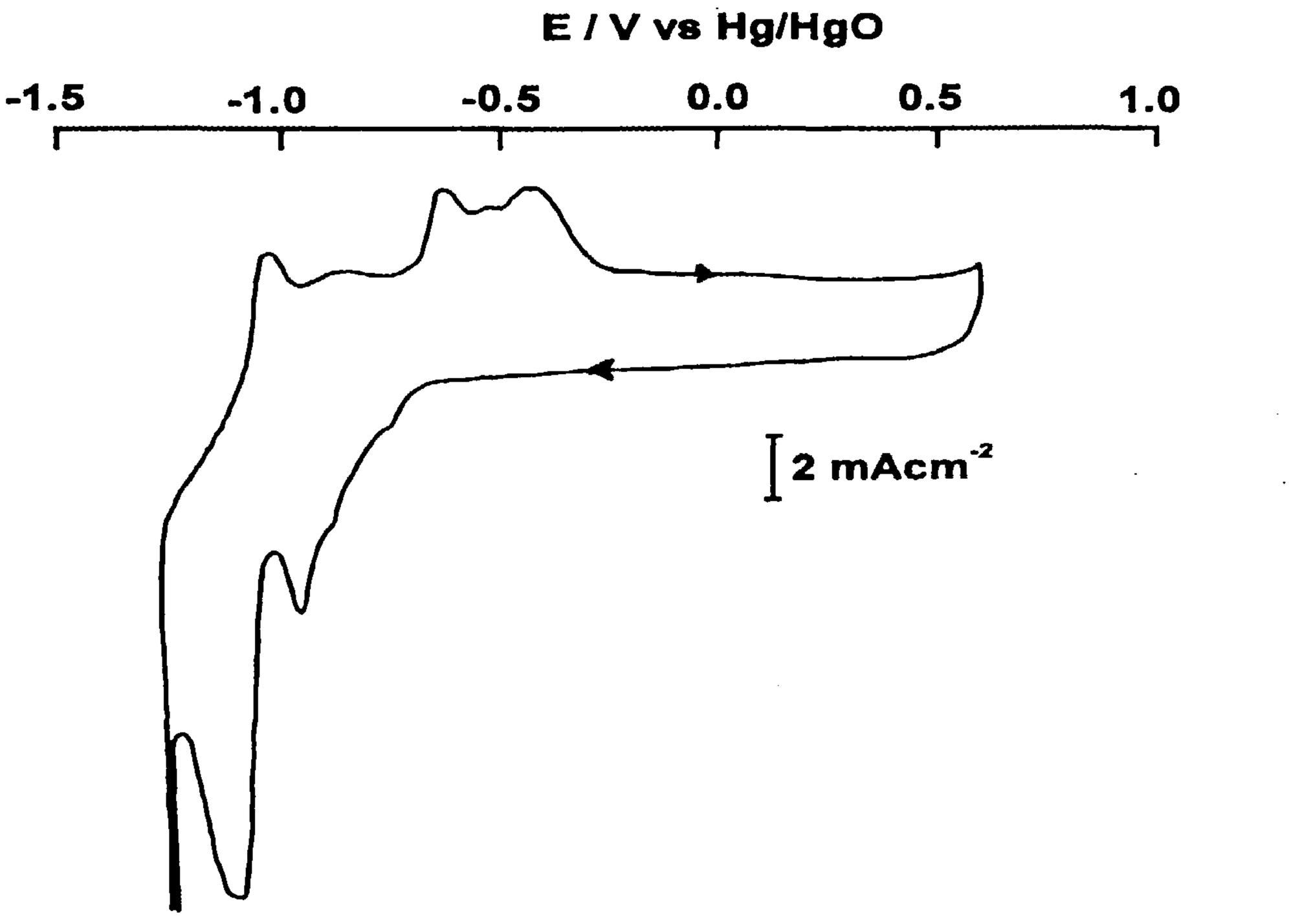

Figure 5.12

Current/potential curve recorded on alloy E after it had been conditioned for 1000 seconds in 10 M NaOH at 333 K. The potential sweep rate was 250 mV s^{-1}.

When compared to the voltammogram shown in figure 3.18 it can be seen that there are a number of additional oxidation peaks appearing in the potential region -1.1 V to -0.4 V vs Hg/HgO. There are also several small reduction peaks appearing on the

shoulder of the large reduction peak at -0.8 V vs Hg/HgO. These additional peaks were not observed when a voltammogram of alloy C was recorded.

It is tempting to suggest that, not only does the composition of the iron alloy effect the amount of ferrate (VI) formed in a constant current electrolysis, but it may also produce different oxide species on the surface when the electrode is conditioned.

From the data collected in these experiments, it seems that the oxide species formed on alloy C is different to the oxide formed on alloy E and B at 333 K. The surface film produced on alloy C under these conditions increases the current efficiency for the ferrate (VI) reaction, whereas the oxide films formed on alloy E and B reduces it. It is obvious from the results of the pulse ramp experiments, as well as the flow cell experiments, that the surface oxide/hydroxide species formed on the anode material during the transpassive dissolution undergoes complex changes in structure, composition or thickness which determines the ferrate (VI):oxygen ratio.

5.7 Summary of conclusions.

From the experiments reported in this chapter it has been shown that increasing the carbon content of the alloy used as the anode, increases the amount of ferrate (VI) formed by transpassive dissolution. Constant current electrolyses on flat plate anodes showed, the cell was operating at the best current efficiency, when a current density of 1 mA cm^{-2} was used to generate the ferrate (VI). Increasing the rate at which the ferrate (VI) was achieved by increasing the applied current resulted in low current efficiencies, (the higher the applied current, the lower the current efficiency). Running the cell at lower current densities produces less ferrate (VI) but in the initial stages of the reaction it the current efficiency increases to a value around 40 %. High carbon steels generate ferrate (VI) more efficiently because the iron is dissolving at a faster rate. This is probably due to the reaction of the carbon with the passivating layer on the electrode surface.

The pulse ramp technique developed to study the formation of ferrate (VI) and the effect of oxide formation proved to be an effective method for this purpose. From the experiments it has been shown that, the nature of the passivating oxide layer plays an important role when considering the transpassive dissolution of an iron containing alloy to form ferrate (VI). At 298 K the passage of a large charge results in the formation of an oxide species which lowers the ratio of ferrate (VI):oxygen produced in the reaction. However, when a small amount of charge has been passed (i.e. 5 mA cm^{-2} for 100 seconds), the condition of the surface film is one in which, the generation of ferrate (VI) occurs at improved efficiency.

When the temperature is increased to 333 K the oxide formed on alloy C seemed to improve the current efficiency for the ferrate (VI) reaction. Increasing the conditioning time resulted in the formation of more ferrate (VI).The oxide formed on electrode C was different to the one formed on alloy's B and E. Here the formation of the passive layer occurred quickly and the current efficiency for the ferrate (VI) reaction dropped to a value comparable to that seen at room temperature.

Chapter 6

Conclusions

A major objective of this programme was to seek conditions which gave an acceptable current efficiency for the electrosynthesis of ferrate (VI); this required a significant improvement on the conditions compared to those used by earlier workers. Two concepts, in particular, have been identified which demonstrate that current efficiencies can be improved.

The first concerns the advantage of using a cell with a three dimensional iron anodes. Using a "membrane" current density of 17 mA cm^{-2} and an anolyte which was 10 M NaOH, the cell with an iron wool anode gave a steady state current efficiency of ≈ 30%; this is both a higher current density and current efficiency than obtained with flat plate iron anodes. It is also possible to increase the rate of generation substantially by using current densities > 80 mA cm^{-2} although this is at a slight cost in current efficiency. The cell employed allows concentrations of ferrate (VI) > 20 mM to be formed in a couple of hours and hence it is a useful laboratory tool. Moreover, it is possible to envisage scale up of the cell to produce much higher concentrations and, hence, solid ferrate. It was shown that the half life of ferrate (VI) in 10 M NaOH is approximately 1 month, more than sufficient to allow several approaches to solid product isolation. As reported in the literature, the current efficiencies are initially even higher, but the ratio of oxygen evolution/ferrate (VI) formation increases due to a change in the oxide/hydroxide layer on the dissolving iron. Some preliminary experiments suggest that this decrease may be minimised using a current reversal regime while others have shown that ac electrolysis has the same advantageous effect. The use of large surface area electrodes also allows the formation of ferrate (VI) in systems where the conditions are normally considered very unfavourable. For example, the formation of ferrate (VI) in 1 M NaOH is not possible reaction using flat plate anodes because the rate of decomposition is higher than the rate of formation.

The second relates to the composition of the anode. The carbon content of the steel/iron alloy has been identified as a major factor influencing the ability of the anode to

dissolve as ferrate (VI) with a high current efficiency. Increasing the carbon content from 0.04 % to 0.90 % lead to a fivefold increase in the ferrate (VI) current efficiency and it has been confirmed that at fixed current density, it is the rate of iron dissolution which increases (rather than a decrease in O_2 evolution). It is thought that the increase in carbon content changes the structure of the metal (eg. increases the grain boundaries) or of the surface coating (eg. increases the number of pits).

The cell developed here opens up the possibility of producing ferrate (VI) from scrap iron/steel converted to a suitable high area form (eg. old piano strings or redundant car springs are a possible source of high carbon steel). It would now be valuable to investigate the performance of cells where the advantages of a high area anode are combined with careful selection of anode composition and/or an optimised current reversal or ac current regime.

The interest in ferrate (VI) was mainly as a water treatment chemical. In the introduction, three ways of using ferrate (VI) for water treatment was described. We believe that the formation of solid sodium ferrate may well be the preferred approach. This appears to be possible as does the generation of ferrate (VI) in concentrated NaOH for bleeding into an effluent stream. The current efficiency and the stability of ferrate (VI) decrease substantially if the medium contains < 5 M NaOH. This does not necessarily rule out the in situ generation of ferrate (VI) in say 1M NaOH and it would be interesting to monitor the concentration of organics during an electrolysis in 1 M NaOH containing organic. There is clear evidence that ferrate (VI) should react preferentially with the organic rather than with water.

More needs to be known about the reactions of ferrate (VI) with organic molecules. Some molecules appear to oxidise completely to CO_2 and this conclusion needs to confirmed by measurements of the total organic carbon. With others, substantial but only partial oxidation was confirmed. The contribution from adsorption onto the precipitating $Fe(OH)_3$ needs to be defined and more sophisticated analytical methods such as HPLC need to be developed to identify fragments that cannot be oxidised further. It would also be interesting and valuable to investigate the reaction of ferrate (VI) with larger organic molecules, particularly those which are toxic to biological treatment technology.

While the replacement of chlorine in water and effluent treatment remains a distant goal, ferrate (VI) has several advantages compared to other chemicals which are promoted as replacements for chlorine. Iron is benign or even welcome in the environment; in any case, most ferrate (VI) will end up as insoluble iron hydroxides (effective flocculants and adsorbers of organic materials) which are readily removed by filtration. Solid ferrate is easy to transport and this makes it attractive for use in remote sites. Overall, ferrate (VI) merits further study as a water treatment chemical and the search for more efficient electrosynthesis conditions should continue.

References.

[1] "*Fundamentals of Environmental Chemistry* ", 2nd edn., Stanley E. Manahan, Lewis, (1993), London.

[2] J. K. Fawell and D. G. Miller, *J. Inst. Wat. Environ. Man.*, **8**, (1994), 76.

[3] Committe Report, *J. Am.Wat.Work.Aass.*, **71**, (1979), 588.

[4] J. Bishop, *Environ. Sci. tech.*, **21**, (1987), 589.

[5] R. Appleton Jr. *43rd Purdue University Industrial Waste Conference Proceedings*, (1989), 375.

[6] " Industrial Electrochemistry ", D. Pletcher and F.Walsh, 2nd edn.., Chapman & Hall, (1990),London.

[7] "*Electrochemistry for a Cleaner Environment* ", Ed. D. J. Genders and N. L Weinberg, Electrosynthesis Company Inc., (1992), New York.

[8] "*Environmental Orientated Chemistry* ", Ed. C.A.C. Sequeira, Elsevier, (1994), Amsterdam

[9] I. R. Borrows, J. H. Entwise and J. A. Harrison, *J. Electroanal. Chem.*, **77**, (1977), 21.

[10] T. Arikado, C. Iwakura and H. Tamura, *Electrochim. Acta.*, **23**, (1978), 9.

[11] L. J. J. Janssen and L. M. C. Starmans *Electrochim. Acta.*, **22**, (1977), 1093.

[12] L. I. Krishtalik, *Electrochim. Acta.*, **26**, (1981), 329.

[13] P. Sonthimer, *Environ. Sci. Tech.*, **14**, 5, (1980), 510.

[14] N. Narkis, *Wat. Res.*, **29**, 1, (1995), 227.

[15] R. Muftikian, Q. Fernando, N. Korte, *Wat. Res.*, **29**, 10, (1995), 2434

[16] "*Kirk Othmer Encylopedia of Chemical Technology* ", 3rd edn. Vol 5, J. A. Woftowlcz, M. G. Noack, R. L. Doerr, Wiley Interscience Publications, (1979), New York.

[17] A. Katz and N. Narkis, *Wat. Res.*, **28**, 10, (1994), 2133.

[18] M. I. loupez, A. E. Croce and J. E. Sicre, *J. Chem. Soc. Faraday Trans.*, **90**, 22, (1994), 3391.

[19] F. Quentel and C. Elleoute, *Anal. Chim. Acta.*, **259**, (1994), 85.

[20] A. M. Couper, *Private Communication.*

[21] H. Zhou and D. W. Smith, *J. Environ. Eng.*, **120**, 4, (1994), 841.

[22] Y. Shuen Shen, Y. Ku and K. Chyr Lee, *Wat. Res.*, **29**, 3, (1995), 907.

[23] N. Takahashi and T. Nakai, *Wat. Res.*, **28**, 7, (1994), 1563.

[24] Sheng H. Lin and Wen. Y. Liu, *J, Environ. Eng.*, **120**, 2, (1994), 437.

[25] R. Andreozzi, V. Caprio and M.G. D'Amore, *Wat. Res.*, **29**, 1, (1995), 1.

[26] H. Galal-Gorchev and J. C. Morris, *Inorg. Chem.*, **4**, 6, (1965), 899.

[27] F. P. Bourgine, J. I. Chamman and H. Keria, J. G. Green, *J. Inst. Wat. Environ. Man.*, **7**, (1993), 571.

[28] G. Grguric, J. H. Trefry and J. J. Keaffaber, *Wat. Res.*, **28**, 5, (1994), 1087.

[29] S. Lubbecke and A. Volgelpohl, *Wat. Res.*, **29**, 3, (1995), 793.

[30] F. Jorand, F. Zartarian, F. Thomas, J. C. Block, J. Y. Bottero, G. Villemin, V. Urbain and J. Manem, *Wat.Res.*, **29**, 7, (1995), 1639.

[31] P. Svensson, *Chem. Tech.*, **2**, 1, (1995), 16.

[32] L. Jin, Z. Ding, M. A. Abraham, *Chem, Eng, Sci.*, **47**, 9, (1992), 2659.

[33] T. D. Thornton and P. E. Savage, *Ind. Eng. Chem. Res.*, **31**, (1992), 2451.

[34] S. B. Hawthorne, Y. Yang and D. J. Miller, *Anal. Chem.*, **66**, (1994), 2912.

[35] "*Instrumental Methods in Electrochemistry* ", Southampton Electrochemistry Group, Ellis Horwood, (1993), New York.

[36] "*Electrochemisry for Technologists* ", G. R Palin, 1st edn. Pergamon Press, (1969), London.

[37] "*Electrochemistry of Cleaner Enviroments* ", Edit. J O'M. Bockris, Plenum Press, New York, (1977).

[38] J. V. Flora and P. B. Masao, *Can. J. Chem. Eng.*, **61**, (1983), 568

[39] I. H. Yeo, D. C. Johnson, S. Kim and R. Jacobson, *J. Electrochem. Soc.*, **139**, (1989), 1395

[40] R. Kotz, S. Stucki and B. Carcer, *J. Appl. Electrochem.*, **21**, (1991), 14.

[41] R. Kotz, S. Stucki and B. Carcer, W. Suter, *J. Appl. Electrochem.*, **21**, (1991), 99.

[42] C. H. Comninellis and A. Nerini, *J. Appl. Electrochem.*, **25**, (1995), 23.

[43] C. H. Comninellis, *ICHEME Syposium Series*, No 127, (1992), 189.

[44] O. J. Murphy, G. D. Hitchens, L. Kaba and C. E. Verostko, *Wat. Res*, **26**, 4, (1992), 443.

[45] J. F. Rusling, B. J. Scheer, A. Owlia, T. T. Chou and J. M. Bobbitt, *J. Electroanal. Chem.*, **178,** (1994), 129.

[46] M. R. Deakin, P. M. Kovach, K. J. Stutts and R. M. Rightman, *Anal. Chem.*, **58**, (1986), 1474.

[47] C. Lamy, *Electrochim. Acta.*, **29**, 11, (1984), 1589.

[48] L. Kaba, G. D. Hitchens and J. O'M. Bockris, *J. Electrochem. Soc.*, **137**, 5, (1990), 1341.

[49] L. Szpyrkowich, J. Navmczyk and F. Zilio-Grandi, *Wat. Res.*, **29**, 5, (1195), 517.

[50] S. H. Lin and Chi F. Peng, *Wat. Res.*, **28**, 2, (1994), 277.

[51] G. Okada, V. Guruswemy and J. O'M. Bockris, *J. Electrochem Soc.*, **128**, 10, (1981), 2097.

[52] P. M. Dhooge, D. E. Stilwell and Su Moon Park, *J. Electrochem. Soc.*, **129**, 12, (1982), 1719.

[53] D. Pletcher and M. Fleischmann, *J. Appl. Electrochem.*, **1**, (1971), 1.

[54] F. Goodridge and E. O. Umeh, *Electrochem. Acta.*, **20**, (1975), 991.

[55] C. Zawodzinski, Proceedings of " *8th International Forum on Electrolysis in the Chemical Industry* ", Orlando, Nov. 1994.

[56] C. Ponce de Leon and D. Pletcher, *J. Appl. Electrochem.*, **25**, (1995), 307.

[57] P. C. Foller and T. Bombard, *J. Appl. Electrochem.*, **25**, (1995), 613.

[58] F. T. A. Vork and E. Barendrecht, *Electrochim. Acta.*, **35**, 2, (1990), 139.

[59] S. Zecevic, D. M. Drazic and S. Gojkovic, *Electrochim. Acta.*, **36**, 1, (1991), 5.

[60] " *A Frist Course in Electrochemical Engeenering* ", Frank, C. Walsh, The Electrochemical Consultancy (1991), Romsey.

[61] G. Kreysa, C. Reynuaan, *J. Appl. Electrochem.*, **12**, (1992), 241.

[62] "*A Comprehensive Theatise on Inorganic and Theoretical Chemistry*, Vol. VIII, J. W. Mellor, Longmans, (1942), London.

[63] H. J. Horstowski and A. B. Scott, *J. Chem. Phys.*, **18**, 1, (1950), 105.

[64] R. K. Murmann, M. L. Hoppe and E. O. Schlemper, *Acta. Cryst.*, B38, (1982), 2237.

[65] A. Carrington, D. Schonland and M. C. R. Symons, *J. Chem. Soc.*, (1957), 659.

[66] A. Carrington, D. Schonland and M. C. R. Symons, D. J. E. Ingram, (1956), 4710.

[67] W. Leavason and C. A. M^{c} Auliffe, *Coord. Chem. Rev.*, **12**, (1974), 151.

[68] R. H. Wood, *J. Am. Chem. Soc.*, **80**, (1958), 2038.

[69] H. J. Bielski and M. J. Thomas, *J. Am. Chem. Soc.*, **109**, (1987), 7761.

[70] J. Kalencinski, *Ann. Soc. Chim. Pol.*, **41**, (1967), 661.

[71] T. Ernst, M. Wawreenczky, M. Cyfert and M. Wronska, *Bull. Acad. Pol, Sci. Ser. SCI. Chem.*, **27**, 10, (1973), 733.

[72] R. K. Murmann and H. Goff, *J. Am. Chem. Soc.*, **93**, 23, (1971), 6058.

[73] R. J. Audette, J. W. Quail and P. J. Smith, *Tetrahedron Lett.*, **3**, (1971), 279.

[74] D. G. Lee and H. Gai, *Can. J. Chem.*, **17**, (1993), 1394.

[75] J. N. BeMiller, V. Ghanti and S. D. Darling, *Tetrahedron Letts.*, **40**, (1972), 4143.

[76] R. K. Murmann and P. Robinson, *Wat. Res.*, **8**, (1974), 543.

[77] M. Gilbert, *Masters Thesis University of Miama*, (1975).

[78] M. Gilbert, T. D. Waite and C. Hare, *J. Am. Wat. Work. Ass.*, **68**, (1976), 495.

[79] T. D. Waite and M. Gilbert, *Am. Wat. Work. Ass. Conference*, Allantic City, June (1978).

[80] T. D. Waite, *1st Annual Report to the National Science Foundation*, March (1978).

[81] J. Fagen and T. D. Waite, *Environ. Sci. Tech.*, **17**, (1983), 123.

[82] T. D. Waite and T. Schink, *Wat. Res.*, **14**, (1980), 1705.

[83] S. Farooq and A. Bari, *J. Environ. Eng.*, **122**, 2, (1986), 301.

[84] S. J. DeLuca and A. C. Chao, *J. Environ. Eng.*, **109**, 5, (1983), 1159.

[85] R. Bartzatt and D. Nagel, *Arch. Environ. Heal.*, **46**, 5, (1991), 313.

[86] J. D. Carr, P. B. Kelter and A. T. Ericson, *Environ. Sci. Tech.*, **15**, 2, (1981), 184.

[87] T. D. Waite and M. Glibert, *J. Wat. Poll.Control.Fed.*, March, (1978), 543.

[88] S. DeLuca and A. C. Chao, *J. Environ. Eng.*, **109**, 1, (1983), 36.

[89] R. K. Murmann, *Selected Water Resources Report PR 238 057*, (1971).

[90] T. D. Waite, *J. Environ. Eng. Div.*, **105**, 1, (1993), 1023.

[91] J. P. Deininger, L. K. Chatfield and D. R. Churchwell, *Proc. Symp. Waste. Manage.*, **90**, 1, (1990), 789.

[92] V. Voss, T. Votapka and C. Bricker, *Wat. Res.*, **14**, (1980), 921.

[93] B. B. Ezhov, O. G. Malandin, A. V. Vasev and A. A. Kamnev, G. V. Suchkova, *Sov. Electrochem.*, **23**, (1987), 524.

[94] A. A. Kamnev and B. B. Ezhov, *Sov. Electrochem.*, **24**, (1988), 1027

[95] A. A. Kamnev, B. B. Ezhov, O. G. Malandin and A. V. Vasev, *Sov. Electrochem.*, **23**, (1987), 946.

[96] V. V. Nechiporuk and I. L. Elgurt, *Electrokhimia.*, **28**, 2, (1992), 226.

[97] V. P. Lukovtev and A. D. Davydov, *Russ. J. Electrochem.*, **29**, 3, (1993), 261.

[98] A. D Davydov, *Electrokhimia.*, **27**, 8, (1990), 947.

[99] I. M. Dalrymple, Proceedings of "*9th International Forum on Electrolysis in the Chemical Industry* ", Clearwater Beach, (1995).

[100] P. Millington, Proceedings of "*Electrochemical Processing Inovations and Progress* ", April (1993), Glasgow.

[101] *Atlas of Electrochemical Equilibria in Aqueous Solution,* M. Porbaix, Pergamon Press, (1966), Oxford.

[102] "*Encyclopedia of Electrochemistry of the Elements* ", Part IX, a-2, Ed. A. J. Bard, Marcel Dekker Inc., (1973), New York.

[103] R.S. Scherbler Guzman, J. R. Vilche and A. J. Arvia, *Electrochim. Acta.*, **24**, (1979), 395.

[104] H. G. Silver and E. Lekas, *J. Electrochem. Soc.*, **117**, 1, (1970), 5.

[105] J. C. Ruban, *J. Chem. Soc, Faraday Trans.*, **85**, 12, (1989), 4247.

[106] M. Odziemkowski, J. Ellis and D. E. Irish, *Electrochim. Acta.*, **39**, (1994), 2225.

[107] D. W. Shoesmith, P. Taylor, M. G, Balley and I. Ikenda, *Electrochim. Acta.*, **23**, (1977), 903.

[108] R.S. Scherbler Guzman, J. R. Vilche and A. J. Arvia, *J. Appl. Electrochem.*, 11, (1981), 551.

[109] S. Asakura and K. Nobe, *J. Electrochem. Soc.*, **118**, 4, (1971), 536.

[110] Shenhao Chen and C. Wang, *Electrochim. Acta.*, **39**, (1994), 731.

[111] W. Tshinkel, H. Neugebauer and A. Neckel, *J. Electrochem. Soc.*, **137**, 5, (1990), 1475.

[112] N. Jayalahshmi and V. S. Muralipharan, *J. Pow. Sorc.*, **32**, (1990), 277.

[113] R. D. Armstrong and I. Baurhoo, *J. Electroanal. Chem.*, **34**, (1972), 41.

[114] R. D. Armstrong and I. Baurhoo, *J. Electroanal. Chem.*, **40**, (1972), 325.

[115] J. C. Poggendorf, *Ann. Chem.*, **54**, (1841), 372.

[116] R. E. Wilson, W. Grenville Horsch, M. A. Youtz, *Ind. Eng. Chem.*, **13**, 9, (1921), 763.

[117] O. V. Travin, *Bull. Soc. France,* (1951), 510.

[118] R. Knoedler and K. E. Heusler, *Electrochim. Acta.*, **17**, (1972), 197.

[119] F. Haber, *Z Elektrochem.*, **7**, (1901), 215.

[120] W. Pick, *Z. Electrochim.*, **7**, (1901), 713.

[121] G. Grube and H. Gmelin, *Z. Electrochim.*, **26**, (1920), 153.

[122] J. Tousek, *Collect. Czech. Chem. Commun.*, **27**, (1962), 908.

[123] J. Tousek, *Collect. Czech. Chem. Commun.*, **27**, (1962), 914.

[124 A. S. Venkatadri, W. F. Wagner and H. H. Bauer, *Anal. Chem.*, **43**, 8, (1971), 1115.

[125] *United States Patent 4,435,256*, P. Deininger, Olin Corporation, 6 Mar. (1984).

[126] *United States Patent 4,435,257*, P. Deininger and R. L. Dotson, Olin Corporation, 6 Mar. (1984).

[127] K. Bouzek and I. Rousar, *Electrochim. Acta.*, **38**, (1993), 1717.

[128] K. Bouzek and I. Rousar, *J. Appl. Electrochem.*, **23**, (1993), 1317.

[129] A. S. Venkatadri, H. H. Bauer and W. F. Wagner, *J. Electrochem. Soc.*, **121**, 2, (1974), 249.

[130] G. W. Thompson, L. T. Ockerman and J. M, Schreyer, *J. Am. Chem. Soc.*, **73**, (1951), 1379.

[131] F. Beck, R. Kaus and M. Oberst, *Electrochim. Acta.*, **30,** (1985), 173.

[132] "*Fundamentals of Analytical Chemistry* ", D. A. Skoog, D. M. West and F. J. Holler, 5th edn., Saunders College Publishing, (1988), Fort Worth.

[133] "*Handbook of Chemistry and Physics* ", 56th edn. CRC Press, (1975).

[134] " *Electrochemical Methods - Fundamentals and Applications* ", A. J. Bard and L. R. Faulkner, Wiley Publications, (1980) New York.

[135] " *Corrosion Engineering* ", M. G. Fontana, McGraw-Hill, (1987), New York.